“Modulation of estrogen receptor alpha function through dietary fatty acids”

Inaugural-Dissertation

To obtain the academic degree

Doctor rerum naturalium (Dr. rer. nat.)

Submitted to the Department of Biology, Chemistry and Pharmacy

of Freie Universität Berlin

by

ZSÒFIA BÀN

from Budapest

2017

Die Arbeit wurde unter der Leitung von Prof. Dr. med. Ulrich Kintscher

Von April 2013 bis Juni 2017 angefertigt.

1. Gutachter: Prof. Dr. med. Ulrich Kintscher
2. Gutachter: Prof. Dr. rer. nat. Matthias F. Melzig

Disputation am 25.10.2017

„In der Wissenschaft gleichen wir alle nur den Kindern, die am Rande des Wissens hier und da einen Kiesel aufheben, während sich der weite Ozean des Unbekannten vor unseren Augen erstreckt.“

(Sir Isaac Newton)

Content

Abbreviations

9-PAHSA	Palmitic acid 9-hydroxy-stearic acid
Adipoq	Adiponectin (gene)
AF-1, AF-2	Activation function 1, 2
AgRP	Agouti-related protein
Angptl4	Angiopoietin- like protein 4
ANOVA	Analysis of variance
aP2	Adipocyte protein 2
ARC	Arcuate nucleus
Arg-1	Arginase 1 (gene)
ArKO	Aromatase knock-out
ATGL	Adipose triglyceride lipase
ATM	Adipose tissue macrophage
ATP	Adenosine triphosphate
AVPV	Anteroventral periventricular nucleus
BAC	Bacterial artificial chromosome
BCA	Bicinchoninic acid assay
BMDM	Bone marrow-derived macrophage
bp	Base pairs
BPA	Bisphenol A

BSA	Bovine serum albumin
BW	Body weight
C16:0	Palmitic acid
C16:1	Palmitoleic acid
C18:0	Stearic acid
C18:1n9	Oleic acid
C20:4n6	Arachidonic acid
Cas 3 (8)	Caspase 3 (8)
CD	Control diet
cDNA	Complementary desoxy-ribonucleic acid
CMO	Carboxymethyloxim
CR	Caloric restriction
cs-FBS	Charcoal-stripped fetal bovine serum
CTSD	Cathepsin D (gene)
CV	Coefficient of variation
DAMP	Damage-associated molecular pattern
DAPI	4',6-diamidino-2-phenylindole
db	Diabetic
DBD	DNA binding domain
DC-SIGN	Dendritic cell-specific intercellular adhesion molecule-3-grabbing non-integrin (CD 209)
Dicer	Endoribonuclease dicer (gene)

DIO	Diet-induced obesity
DMEM	Dulbecco´s modified Eagle´s medium
DMSO	Dimethylsulfoxide
DNA	Desoxy-ribonucleic acid
dNTP	Deoxyribonucleotides
e.g.	For example
E1	Estrone
E2	17β-estradiol
E3	Estriol
EDTA	Ethylenediaminetetraacetic acid
EE	Energy expenditure
ELISA	Enzyme-linked immunosorbent assay
ERE	Estrogen response element
ERα	Estrogen receptor alpha
ERβ	Estrogen receptor beta
Esr1	Estrogen receptor 1 (gene)
F	Fat mass
FA	Fatty acid
Fabp4	Fatty acid binding protein 4 (gene)
$FADH_2$	Flavin adenine dinucleotide (hydroquinone form)
FAHFA	Fatty acid hydroxy-fatty acid

FBS	Fetal bovine serum
FSC	Forward scattered light
FSH	Follicle stimulating hormone
GAPDH	Glyceraldehyde 3-phosphate dehydrogenase
G-CSF	Granulocyte- colony stimulating factor
GLP1	Glucagon-like peptide
GLUT4	Glucose transporter type 4
GM-CSF	Granulocyte- and monocyte- colony stimulating factor
GPER1	G-protein coupled estrogen receptor 1
GPR30	G-protein coupled receptor 30
GTT	Glucose tolerance test
H&E	Hematoxylin and eosin
Hdac3	Histone deacetylase 3
HFD	High-fat diet
HPLC	High-performance liquid chromatography
HSL	Hormone-sensitive lipase
Hsp	Heat shock protein
Hypo	Hypothalamus
ICAM	Intercellular adhesion molecule
i.e.	“Id est” (that is)
IFNγ	Interferone gamma

IHC	Immunohistochemistry
IL	Interleukin
IP	Immunoprecipitation
IRE1α	Inositol-requiring enzyme 1 alpha
ITT	Insulin tolerance test
Jak-STAT	Janus kinase- signal transducer and activator of transcription
JNK	c-Jun N-terminal kinase
LBD	Ligand binding domain
LFD	Low-fat diet
LH	Luteinizing hormone
LM	Lean mass
LoxP	Locus of X-over in P1
LPL	Lipoprotein lipase
LPS	Lipopolysaccharide
Ltf	Lactotransferrin
MAPK	Mitogen-activated protein kinase
MC4	Melanocortin 4
MCK	Muscle creatine kinase
MFI	Mean fluorescence intensity
MIF	Macrophage migration inhibitory factor
MOER	Membrane only estrogen receptor

MRI	Magnet resonance imaging
mRNA	Messenger ribonucleic acid
MS	Mass spectrometry
MTC	Mitochondrial transport chain
NADH	Nicotinamide adenine dinucleotide (reduced form)
NET	Neutrophil extracellular trap
NFκB	Nuclear factor kappa-light-chain-enhancer of activated B cells
NK cell	Natural killer cell
NLRP3	NOD-like receptor family, Pyrin domain containing 3
NLS	Nuclear localization sequence
Nos2	NO-synthase 2 (gene)
NPY	Neuropeptide Y
ob	Obese
OVX	Ovariectomy/ ovariectomized
P4	Progesteron
PAI-1	Plasminogen activator inhibitor-1
PAMP	Pathogen-associated molecular pattern
PBS	Phosphate buffered saline
PCNA	Proliferating cell nuclear antigen
PDGF	Platelet-derived growth factor
PdgfRa	Platelet-derived growth factor receptor alpha

PMA	Phorbol-myristate acetate
POMC	Proopiomelanocortin
PPAR	Peroxisome proliferator-activated receptor
PS	Phosphatidylserine
PUFA	Polyunsaturated fatty acid
PVDF	Polyvinylidene fluoride
RER	Respiratory exchange ratio
Retn	Resistin (gene)
RPMI	Roswell Park Memorial Institute medium
RT-qPCR	Real-time quantitative polymerase chain reaction
SCD-1	Stearoyl-coenzyme A desaturase 1
SDS	Sodium dodecyl sulfate
SDS-PAGE	Sodium dodecyl sulfate- polyacrylamide gel electrophoresis
SEM	Standard error of the mean
SERM	Selective estrogen receptor modulator
SF-1	Steroidogenic factor 1
SM	Skeletal muscle
SRC	Steroid receptor co-activator
SSC	Side scattered light
T	Testosterone
T2DM	Type 2 diabetes mellitus

TCA	Tricarboxylic cycle
TGFβ	Transforming growth factor beta
T_H1 (2) cell	T-helper cell type 1 (2)
TLR 2 (4)	Toll-like receptor 2 (4)
TNF(α)	Tumor necrosis factor (alpha)
VCO_2	CO_2 production
VMH	Ventromedial hypothalamus
VO_2	O_2 consumption
WAT	White adipose tissue
WB	Western blot
Wnt4	Wingless-type MMTV integration site family member 4
WT	Wild type
αMSH	Alpha melanocyte stimulating hormone

Units of measurement

°C	Degree Celsius
µg	Microgram
µl	Mircoliter
µM	Micro molar
U	Units
kg	Kilogram

g	Gramm
min	Minute
cm	Centimetre
h	Hour
mg	Milligram
ml	Mililiter
nM	Nanomolar
IU	International units
kDa	Kilo dalton
kcal	Kilo calory
V	Volt
mM	Milimolar
M	Molar
ng	Nanogramm
rpm	Revolutions per minute
cnts	Counts
AU	Arbitrary units
d	Day

Figures and Tables

Figures

Tables

Abstract

In the present study, the impact of the deletion of adipose tissue ERα on metabolism was investigated *in-vivo* in both male and female mice (atERαKO). Besides a basal characterization on normal chow diet, a body weight dynamics protocol has been applied. The protocol included the induction of body weight gain through ad-libitum HFD-feeding and a phase of caloric restriction, performed with monitored LFD-feeding. The lack of specificity of the model for adipose tissue resulted in difficulties in discriminating central from peripheral ERα effects. Most importantly, hypothalamic depletion of ERα led to dysregulation of the negative feedback mechanism of estrogen plasma levels in females resulting in increased circulating E2 levels. Thereby, the model became more complex and challenging to interpret due to high E2 levels additionally to the central and adipose-tissue ERα depletion. Notably, HFD-feeding in female atERαKO mice resulted in a high mortality rate based on severe bacterial infections of the uterus. Due to the unexpected and severe reproductive phenotype caused by “simple” HFD-feeding, we focused on the entity and etiology of the inflammation process taking place in these animals. The current study demonstrates that HFD-feeding contents can impair the natural host defense mechanisms, leading to exaggerated inflammation in response to commensal bacteria. atERαKO mice fed a HFD, displayed markedly increased number of infiltrating neutrophils, likely provoking the damages seen in the uterine wall and leading to a state similar to sepsis. Stearic acid was identified as the fatty acid which was induced at the highest extent in plasma by HFD-consumption. Additional *in-vitro* analyses confirmed the link between high plasma levels of stearic acid and the depletion of anti-inflammatory macrophages (M2) required for the resolution of the inflammatory process. In particular, the fatty acid affected the polarization of macrophages towards M2, an anti-inflammatory phenotype known to be induced by E2. Further investigations outlined a novel mechanism of modulation of the estrogen receptor alpha by stearic acid. The fatty acid likely binds to the receptor through acylation and interferes with its transcriptional activity in macrophages. In summary, the present study demonstrates the ability of a dietary fatty acid to modulate the transcription activity of a nuclear receptor, i.e. ERα. This finding might open new perspectives for the treatment of ERα-related disorders.

Zusammenfassung

In dieser Studie wurde der Einfluss vom Adipozyten- Östrogen Rezeptor alpha (ERα) auf den Fettgewebs- und Gesamtstoffwechsel untersucht. Hierzu, wurde ein *in-vivo* knock-out Mausmodell (atERαKO) verwendet und anhand eines etablierten Gewichtsverlaufsprotokolls metabolisch charakterisiert. Neben der Phänotypisierung bei normaler Haltungsdiät, beinhaltete das besagte Protokoll eine Phase der Fütterung mit Hochfettdiät (HFD) mit dem Ziel einer Gewichtszunahme zu induzieren. In einer zweiten Phase, wurde die Futteraufnahme durch eine definierte fettarme Futtermenge eingeschränkt. Allerdings, erschwerte die mangelnde Spezifität des Modells für das Fettgewebe die Diskriminierung zwischen peripheren und zentralen Effekten von ERα. In atERαKO Mäuse, wurde eine reduzierte ERα-Expression im Hypothalamus nachgewiesen, die dazu führte das negative Rückkopplungssystem für die Regulation der Östrogen-Biosynthese zu unterbrechen. Bei weiblichen atERαKO Tieren äußerte sich dies in erhöhten zirkulierenden Östrogenspiegeln. Durch die Herunterregulation von ERα im Fettgewebe und im Hypothalamus zusätzlich zu den erhöhten Hormonspiegeln wurde das transgene Modell komplexer und stellte eine Herausforderung für die Interpretation der metabolischen Daten dar. Überraschenderweise, führte die HFD-Fütterung der weiblichen atERαKO Tiere zu einer erhöhten Mortalität. Diese konnte auf schwerwiegenden bakteriellen Infektionen des Reproduktionstraktes der Mäuse zurückverfolgt werden. Aufgrund des unerwarteten und ausgeprägten Phänotyps, fokussierten wir die weiteren Untersuchungen auf die Pathogenese der Inflammation und die zugrundeliegenden Mechanismen, die zur Mortalitätszunahme unter HFD führten. Die vorliegende Arbeit zeigt, dass Bestandteile der HFD in der Lage sind die physiologischen Prozesse der Immunabwehr negativ zu modulieren und damit zur Überreaktionen auf opportunistische Erreger zu führen. In den Uteri der HFD-gefütterten mutanten Mäuse, konnte eine erhöhte Anzahl an neutrophilen Granulozyten beobachtet werden, die schwere Schäden an der Uteruswand induzierten und die Tiere in einem der Sepsis ähnlichen Zustand versetzten. Stearinsäure wurde als Plasma-Fettsäure identifiziert, die durch die HFD am stärksten induziert wurde. Zusätzliche *in-vitro* Studien bewiesen eine Korrelation zwischen hohen Stearinsäurespiegeln und die Reduktion von anti-inflammatorischen Macrophagen, die mitunter die Aufgabe tragen, den Entzündungsprozess einzudämmen und neutrophile Granulozyten zu

phagozytieren. Insbesondere konnte gezeigt werden, dass die Fettsäure trotz hoher Östrogenspiegel, die sich normalerweise auf Makrophagen anti-inflammatorisch auswirken, die M2-Polarisation inhibierte. Zusammengefasst stellt die Arbeit eine zuvor unbekannte Interaktion zwischen ERα und Stearinsäure vor, bei der vermutlich das Prozess der Acylierung des Rezeptors zu einer Reduktion der transkriptionellen Aktivität des Rezeptors führt.

1. Introduction

1.1. Obesity and sexual dimorphism in fat distribution

Today, obesity is becoming pandemic and represents one of the most meaningful challenges for health, especially in the Western world as well as in economically arising countries as China and India. Worldwide, about 50% of the population is obese (Flegal et al., 2012) and approx. two-thirds of the male and half of the female German population are overweight (Robert-Koch-Institute, 2012). Not only the trend in adult individuals, but also the incidence of obesity in children is increasing and concerning (Ogden et al., 2014).

Obesity is defined as a state of exceeding fat accumulation, which leads to several adverse health problems and to a higher mortality rate (van der Klaauw and Farooqi, 2015). Indeed, it is associated with insulin resistance, type 2 diabetes (T2DM), as well as cardiovascular diseases and cancer (Calle and Kaaks, 2004; Morentin and Audicana, 2011; van der Klaauw and Farooqi, 2015). Obesity is a complex disorder which results from an imbalance between food consumption (and therefore energy intake) and energy expenditure. Factors influencing energy homeostasis include not only food intake and exercise, but also fetal nutrition, culture, psychosocial circumstances and gene susceptibility (Kopelman, 2000).

Several studies demonstrated that food intake, as one of the key parameters of body weight balance, is mainly regulated in the hypothalamus, including two specific regions, the arcuate nucleus (ARC) and the ventromedial hypothalamus (VMH) (Louis-Sylvestre, 1980; Smith, 2000). The ARC contains two important subsets of orexigenic neurons: activated Agouti related protein (AgRP)- and neuropeptide Y (NPY) neurons. Conversely, proopiomelanocortin (POMC) neurons of the ARC have anorexigenic effects, causing satiety (Kim et al., 2000). POMC neurons release alpha melanocyte-stimulating hormone (αMSH), while the orexigenic effects of NPY- and AgRP- neurons rely on melanocortin 4 (MC4). Both neuropeptides bind to the MC4 receptor antagonizing (αMSH) or activating (MC4) it (Kim et al., 2000). Notably, not only the regions of the hypothalamus participate in regulating energy homeostasis: activation of the mentioned neurons, as NPY and AgRP is also modulated by peripheral signals. These include increased ghrelin levels, dropping glucose plasma levels, lowered cholecystokinin and/or leptin levels. Leptin is secreted by adipocytes and its concentration correlates to the amount of fat tissue (Friedman and Halaas,

1998; Schwartz et al., 1996). Binding of leptin to the leptin receptor was shown to affect the Jak-STAT (Janus kinase- signal transducer and activator of transcription) and the MAPK (mitogen-activated protein kinase) signaling pathways (Myers et al., 2008; Sainz et al., 2015). This adipokine inhibits AgRP and NPY neurons and activates POMC neurons. In obese patients, leptin levels are exponentially increased due to higher fat tissue amounts (Considine et al., 1996). However, leptin fails to reduce appetite in obese individuals, as these individuals become leptin resistant, similarly to insulin resistance in T2DM patients (Sainz et al., 2015). Two mutant mouse strains corroborate the relevance of this adipokine, showing that homozygous mutation in the leptin gene (ob/ob mice) or of its receptor (db/db mice) cause hyperphagia and therefore obesity (Coleman, 2010). Leptin, as well as ghrelin and cholecystokinin demonstrate that peripheral organ crosstalk with the central nervous system plays a pivotal role in body weight regulation, affecting energy intake and expenditure. Besides the effects of leptin on the central regulation of food intake, adipose tissue is a putative regulator of energy homeostasis itself. Importantly, brown and “brite” or “beige” adipose tissue have been shown to influence energy expenditure (Cannon and Nedergaard, 2004).”Beige” or “brite” adipose tissue is white adipose tissue that mostly due to sympathetic stimuli displays “brown-like” features. While white adipose fat cells are mainly responsible for energy storage in form of lipids, brown or beige fat cells are assigned to heat production, especially during cold exposure. Compared to white adipocytes, brown and beige adipocytes present multilocular lipid droplets and most importantly a higher number of mitochondria. The process of white adipocytes turning into beige ones is referred to as “browning” or more correctly “beiging”. In the last years, several studies have investigated the factors and mechanisms which drive beiging, as brown/beige adipose tissue is linked to higher mitochondrial activity and thermogenesis (Fenzl and Kiefer, 2014; Stanford et al., 2015). The uncoupling of the mitochondrial oxidative chain, which produces adenosine triphosphate (ATP), in order to translate energy in non-shivering thermogenesis, increases energy expenditure and can lead to weight loss.

Beyond the necessity of life style intervention, e.g. exercise and dietary changes, major efforts have been included to develop pharmacological strategies to support weight loss. However, today we still rely on drugs to treat obesity that mainly address satiety (Jones and Bloom, 2015). These substances often cause adverse effects as hypertension and valve disease, which are the reason to disqualify the application of

these pharmacological agents (Cunningham and Wiviott, 2014). Notably, it is important to consider that all available therapies except for pursuing caloric restriction, exercise or a bariatric surgery do not prevent patients from body weight re-gain (Bouchard et al., 1993a; Kissler and Settmacher, 2013; Swift et al., 2014). After weight loss, several mechanisms implying hypothalamic regulation counteract successful weight reduction and maintenance. Among these mechanisms, upregulation of appetite-inducing hormones (e.g. ghrelin), decrease in leptin and changes in nutrient metabolism and energy homeostasis contribute to weight re-gain (Swift et al., 2014). Therefore, there is an increasing necessity of understanding the underlying mechanisms of body weight regulation in order to elucidate potential targets for more safe and effective drugs.

In this context, it has been observed that pre-menopausal women are less prone to overweight than men. Moreover, a healthier fat distribution, e.g. a higher proportion of gluteal/femoral rather than intra-abdominal adipose tissue, characterizes women until the onset of menopause (Bjorntorp, 1992; Bouchard et al., 1993b). In line with these findings, post-menopausal women are more susceptible to fat accumulation, especially intra-abdominally, after the decline of circulating estradiol (E2), while E2 replacement ameliorates this trend (Gambacciani et al., 1997; Haarbo et al., 1991). On account of these observations, several investigations, including the present study, focused on the effects of E2 and the estrogen receptors in the context of body weight regulation and metabolism.

1.2. Estrogen receptor alpha

The estrogen receptor alpha (ERα) belongs to the family of nuclear receptors, more precisely to the sex steroid receptors. Jensen and colleagues discovered the estrogen receptor in 1962 (Jensen, 1962). It was believed to be the only mediator of estrogenic actions, until another not identical but highly homologues target protein was cloned: the estrogen receptor beta (ERβ) (Kuiper et al., 1996; Mosselman et al., 1996). ERα and ERβ are ligand-activated transcription factors, able to bind the DNA at specific sequences in order to modulate gene transcription. Endogenous ligands present in mammals are estrone (E1), 17β-estradiol (E2) and estriol (E3) (Kamat et al., 2002). In females, estrogens are synthesized mainly in maturating follicles in the ovaries, while during pregnancy, high E2 levels are produced by the placenta. In men, the testes synthesize much lower concentrations of estrogens. In the follicles of

the ovaries, a “two-cell” or “two-compartments”-biosynthesis occurs (Hillier et al., 1994). The first step takes place in the theca cells of the growing follicles, where androgens (e.g. testosterone and androstenedione) are produced from cholesterol upon stimulation with luteinizing hormone (LH). In a second step, androgens diffuse into granulosa cells, where the conversion to estrogens is induced by the aromatase, an enzyme which is expressed selectively in granulosa cells upon stimulation by follicle-stimulating hormone (FSH).

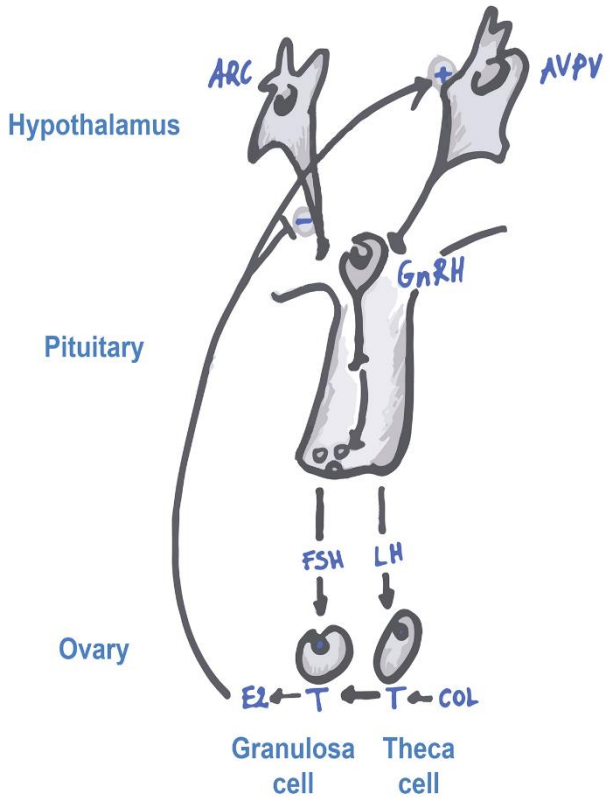

Figure 1: Hypothalamic-pituitary-gonadal axis regulating the biosynthesis of estrogens (adapted from Lopez and Tena-Sempere, 2015).

The hypothalamic-pituitary-gonadal axis regulates the biosynthesis of 17β-estradiol (E2) in the ovaries. The positive and negative feedback mechanism involves kisspeptin neurons in the arcuate nucleus (ARC) and anteroventral periventricular nucleus (AVPV), mediating respectively the negative and positive feedback. Stimulation of the pituitary through hypothalamic gonadotropin releasing hormone (GnRH) induces secretion of the gonadotropins luteinizing hormone (LH) and follicle stimulating hormone (FSH). LH stimulates the synthesis of androgens, as testosterone (T), from cholesterol in theca cells of the ovary. In a second step, T is converted to E2 by the aromatase, which is expressed in granulosa cells.

Estrogens are lipophilic molecules that diffuse through the cell membrane, binding to ERα and ERβ in the nucleus. After conformational modification and release from the heat-shock protein (hsp) complex (Baulieu et al., 1990; Pratt, 1993), the receptors

can dimerize. Homodimers of ERα can then bind to specific DNA sequences, called estrogen response elements (ERE), present in the promoter regions of target genes. Originally, ERE was recognized as a sequence containing a palindromic inverted element (5´GGTCAnnnTGACC3´) where the flanking nucleotides are responsible for the affinity to ERα (Gruber et al., 2004; Klinge, 2001; Klinge et al., 1997). However, different studies demonstrated that ERα can also act indirectly through interaction with other transcription factors, affecting non-ERE regions and therefore modulating transcription in an alternative manner (Jacq et al., 1994; Sadovsky et al., 1995). Nowadays, it is known that besides the classical action of ERs, estrogens can promote rapid signal transduction through extranuclear receptors, localized nearby the cellular membrane (Levin, 2009b). Furthermore, GPER1 (G-protein coupled estrogen receptor 1), or better known as GPR30 (G-protein coupled receptor 30), was controversially discussed as a mediator of rapid-acting estrogenic effects (Levin, 2009a). In general, estrogenic effects are correlated to various signaling pathways that can depend on the targeted tissue. Thus, it becomes obvious that hormonal regulation through ERα is highly complex and heterogeneous.

1.2.1. Structure and function

ERα is encoded by the *Esr1* gene containing eight exons and its mRNA can be subdivided into the five regions A/B, C, D, E and F as for all members of the nuclear receptor family. These regions form the following functional domains: the N-terminal activation domain (AF-1), the DNA binding domain (DBD), the ligand binding domain (LBD), the nuclear localization sequence (NLS) and the dimerization domain. The A/B region contains besides the AF-1 domain many phosphorylation and sumoylation sites. AF-1 is responsible for transactivation and was reported to act also ligand independently, binding directly or via co-factors to parts of the primary transcription machinery. The centrally located C region which encodes the DBD is highly conserved and includes two Zinc-finger structures (each Zn^{2+}-ion coordinating four cysteine residues) involved in DNA binding and dimerization. The amino acids of the C-terminal zinc-finger (*P*-box) are essential for the recognition of the ERE sequence (Danielsen et al., 1989; Mader et al., 1989; Umesono and Evans, 1989), while the *D*-box (N-terminal Zn-finger) is one of the important structures involved in DNA-dependent stabilization of the homodimer. While the hinge region and the NLS belong to the short D region, the large E region encodes for the LBD, a dimerization

interface, another NLS, the ligand-dependent activation function 2 (AF-2) and an interaction site for heat-shock proteins (hsp90 and hsp70). Transcriptional activity of ERα is dependent on the two transactivation domains AF-1 and AF-2. In the latter region two essential structures in terms of transcriptional activity have been identified. Belonging to this domain is the helix12, which was demonstrated to be indispensable for ligand dependent activation (Heery et al., 1997; McKenna et al., 1999). After conformational modification due to ligand binding, a hydrophobic pocket (nuclear receptor interaction domain (*NR*-box)) can enable the receptor to interact with LXXLL motifs, present, for example, on the members of the SRC (steroid receptor co-activator) family of co-activators and therefore recruit co-activators (Heery et al., 1997; Shiau et al., 1998). Furthermore, crystal structure analyses revealed that ERE preference can be modulated depending on the ligand bound to the receptor (Hall et al., 2002). Other studies also demonstrated that allosteric recruitment of various co-factors can alter the preference for divergent ERE sequences and therefore modulate transcription depending on the presence of specific co-factors (Hall et al., 2002). This is one of the mechanisms, underlying the selective regulation of ERα function in divergent tissues and cell types.

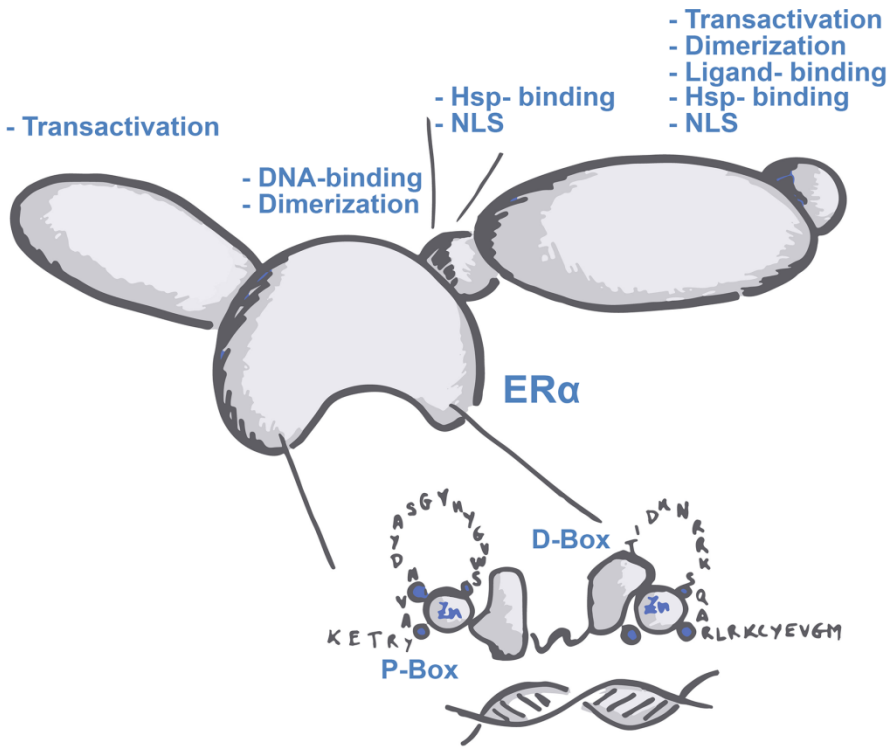

Figure 2: Schematic illustration of the functional and structural domains of the estrogen receptor alpha (adapted from Grandien et al., 1997)

The different domains of the receptor are responsible for transactivation, DNA-, heat shock protein- and ligand-binding. Nuclear localization structures (NLS) and dimerization domains are integrated for a fully functional receptor. The DNA-binding domain (DBD) contains two Zinc-finger structures, the P- and the D-Dox, which are involved in estrogen response element (ERE) recognition and DNA-dependent dimerization.

As sexual hormones, estrogens are essential for the development and proper function of the reproductive tract. Both ERα and ERβ are expressed in the myometrium (outer muscular layer of the uterus) as well as in the endometrium (functional layer of the uterus), fluctuating in their expression depending on the stage of the menstrual cycle and during life-time. The highest expression of ERα in stromal cells is reached during the proliferative phase and decreases during the secretory phase (Critchley and Saunders, 2009), whereas in the fallopian tube, mRNA levels of ERα remain constant, independently of the rise of progesterone levels after ovulation (Horne et al., 2009). ERβ but not ERα has been detected in other cell types essential for the remodeling of the uterine tissues throughout the menstrual cycle, as uterine endothelial cells and uterine-specific immune cells (Critchley et al., 2001; Henderson et al., 2003). In rodents, the whole body ERα knock-out (ERαKO) model has been

shown to lead to hypoplastic uteri, hemorrhagic ovaries and infertility (Couse et al., 1999). Lack of ovulation and erratic estrous has also been observed in theca-specific knock-out of ERα, while male mice lacking aromatase (ArKO mice) display a late onset of the testicular phenotype (Robertson et al., 2002). In summary, estrogenic effects are required for physiological development and function of both male and female reproductive tracts. Importantly, it has to be taken into account that gene-engineering affecting estrogen related genes might influence reproductive functions of transgenic mice and possibly the overall phenotype.

1.2.2. Relevance for body weight regulation and metabolism

Estrogens control via ERα many physiological processes regarding not only development and reproduction, but also energy homeostasis, including regulation of metabolism (Hevener et al., 2015). While ERα plays a pivotal role in body weight and energy homeostasis, knock-out of whole body ERβ did not affect body weight or fat distribution (Faulds et al., 2012; Foryst-Ludwig et al., 2008). However, HFD-feeding of ERβ knock-out mice lead to increased body weight, fat mass and interestingly to improved insulin sensitivity when compared with wild type controls (Foryst-Ludwig et al., 2008). Foryst-Ludwig and colleagues demonstrated that the observed phenotype relies on the repressive action of ERβ on the key regulator of adipogenesis PPARγ (Foryst-Ludwig et al., 2008).

Pre-menopausal women display a different fat distribution than men, having higher amount of femoral/gluteal adipose tissue rather than accumulating fat intra-abdominally. This has been shown to be less pathogenic, while intra-abdominal fat accumulation has been correlated to higher risk for diabetes and atherosclerosis (Wajchenberg, 2000). After the onset of menopause, the decline of E2 plasma concentrations leads to fat re-distribution to a “male-like” pattern, an increase in metabolic disorders (Gambacciani et al., 1997) and cardiovascular diseases in women (Regitz-Zagrosek and Kararigas, 2017).

In rodent models, the homozygous deletion of whole body ERα (ERαKO) in both sexes is correlated to adiposity, insulin resistance, impaired glucose tolerance and higher susceptibility to high-fat diet (HFD) (Heine et al., 2000; Ribas et al., 2010). While ERαKO mice are affected by obesity and related metabolic disorders (Heine et al., 2000), the whole body knock-out of ERβ (ERβKO) does not alter fat distribution

when compared to wild-type controls (WT) (Ogawa et al., 1999). Importantly, the replacement of E2 in ovariectomized (OVX) WT mice in physiological concentrations, rescues enhanced food intake (Clegg et al., 2006) and prevents adiposity (Geary et al., 2001). Further investigations revealed a putative role of ERα in central regulation of energy expenditure and food intake (Lopez and Tena-Sempere, 2015). As mentioned before, the hypothalamic nuclei VMH and the ARC have been known for a long time to control energy balance. In pro-opiomelanocortin (POMC) neurons of the ARC, highly expressed ERα (and not ERβ) has been demonstrated to modulate energy expenditure, appetite and reproduction (Xu et al., 2011). Murine deletion of ERα in these cells resulted in hyperphagia, while ablation of ERα in SF-1 (steroidogenic factor 1) cells of the VMH caused decreased energy expenditure and visceral fat accumulation without affecting food intake (Xu et al., 2011). Moreover, ERα is able to modulate the function of leptin, a potent catabolic hormone secreted by adipocytes. Administration of exogenous E2 was demonstrated to regulate the mRNA expression of the leptin receptor via ERα (Bennett et al., 1999) and leptin sensitivity could be restored in OVX female mice as well as improved in males by E2 supplementation (Clegg et al., 2006). Other metabolically relevant tissues express high levels of ERα and are affected by modulation through estrogens. In mice, knock-out of ERα in skeletal muscle results in insulin-resistance and lower muscular glucose disposal (Riant et al., 2009; Ribas et al., 2016). These investigations could not prove the causality between tissue specific deletion of ERα and the depletion of GLUT4 (glucose transporter type 4) mRNA expression. However, further studies demonstrating the concomitant induction of both ERα and GLUT4 in exercised muscle (Dela et al., 1994; Fu et al., 2009) suggest a putative role in the regulation of myocyte glucose metabolism, probably modulating the insulin signaling pathway (Ordonez et al., 2008; Riant et al., 2009). ERα was demonstrated to positively affect fatty acid oxidation through mechanisms involving the intracellular uptake of fatty acids, shifting substrate utilization and regulation of mitochondrial function (Hevener et al., 2015). Adipose tissue is another putative metabolic tissue, which is affected by estrogen action. As already described, ERα is highly expressed in adipose tissue and seems to be a key regulator of the sexual dimorphism in fat distribution between females and males. These observations outline the relevance of adipose tissue ERα, but are not sufficient to elucidate the mechanisms responsible for the phenotype of ERαKO mice. Therefore, tissue or cell type specific models are required in order to

outline tissue-specific ERα action in the context of glucose- and fatty acid metabolism.

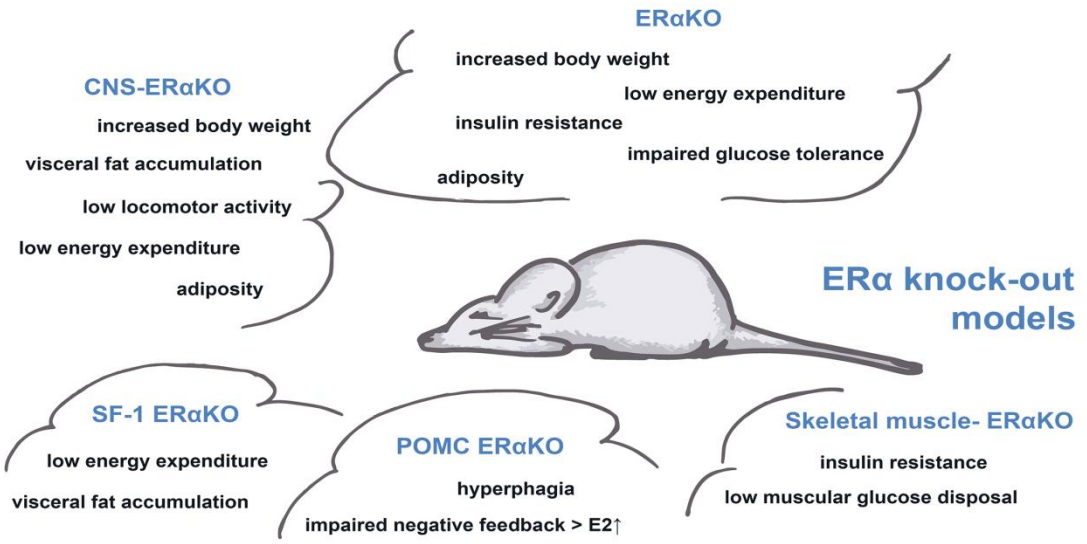

Figure 3: Summary of the phenotype of different estrogen receptor alpha (ERα) models.

ERαKO: whole body ERα knock-out; CNS- ERαKO: central nervous system- knock-out model; SF-1 ERαKO: ERαKO in steroidogenic factor 1-positive neurons (ventromedial hypothalamus); POMC ERαKO: ERαKO proopiomelanocortin neurons (arcuate nucleus of the hypothalamus); skeletal muscle ERαKO: knock-out model for skeletal muscle ERα driven by muscle creatine kinase (MCK-Cre)-dependent Cre-recombinase.

1.2.3. Effects on the immune response

There is a growing body of evidence that immune cells, in particular macrophages, play a crucial role in the regulation of whole body metabolism (Chawla et al., 2011; Olefsky and Glass, 2010). Adipose tissue inflammation is observed in obese patients and is correlated to glucose intolerance and decreased insulin sensitivity. In lean individuals, a low percentage of adipose tissue macrophages (ATM) is resident and displays an anti-inflammatory phenotype (M2 polarized), which is maintained by eosinophils via secretion of interleukin 4 (IL-4) (Wu et al., 2011). In this state, ATMs produce and secrete interleukin 10 (IL-10), which was shown to preserve glucose homeostasis in adipocytes (paracrine effect) as well as in other metabolic tissues (systemic effect), for example in muscle (Dagdeviren et al., 2016; Exley et al., 2014). The anti-inflammatory properties of ATMs are also maintained by adipocytes themselves, which secrete adiponectin, a hormone shown to act in a synergistic manner with IL-4 (Kumada et al., 2004). On the contrary, it has been shown that in

obese individuals a huge number of monocytes infiltrate the adipose tissue, subsequently differentiating to ATMs (Kanda et al., 2006; Weisberg et al., 2003). Due to obesity related excess of nutrients, enlarged adipocytes undergo cellular stress and partly apoptosis, releasing cytokines that create a pro-inflammatory milieu (Cinti et al., 2005; Sun et al., 2011). Local increase of pro-inflammatory signals as interleukin 6 (IL-6) and tumor necrosis factor alpha (TNFα) are major signals for the recruitment of monocytes to the inflamed adipose tissue, where ATMs turn into a pro-inflammatory M1-phenotype.

Ribas et al. found that deletion of ERα in myeloid cells in a rodent model leads to the typical metabolic disorders observed in ERαKO mice, e.g. glucose intolerance, insulin resistance, increased fat mass and lowered levels of adiponectin (Ribas et al., 2011). This study also evidenced the importance of macrophage ERα, which represses inflammation but is at the same time indispensable for the full capacity of phagocytosis as response to lipopolysaccharide (LPS) (Ribas et al., 2011). Accordingly, Calippe et al. have shown that E2 supplementation enhances the immune response of macrophages to intraperitoneal injection of thioglycollate and simultaneously limits the number of macrophages recruited to the peritoneum, likely repressing an exaggeration of the inflammatory process (Calippe et al., 2010). In conclusion, ERα seems to be a key regulator of macrophage function and is therefore relevant for the functional interplay of immune cells during the inflammatory process.

1.2.4. Selective estrogen receptor modulators (SERMs) in pharmacology: therapeutic usage and challenges

As previously emphasized, estrogens act via ERs in different tissues impacting several regulatory processes as metabolism, growth and proliferation and immune response. The multiple positive effects of ERα activation suggest that this receptor is a promising target for novel therapeutics for the treatment of obesity, type-2 diabetes and osteoporosis, at least in women. However, the narrow therapeutic window and the physiologically cycling levels of estrogens represent main challenges for the administration. More importantly, the lack of estrogen selectivity for specific tissues and the consequent side effects, for example higher risk for breast cancer, coronary heart disease and pulmonary embolism, are major concerns regarding the supplementation with estradiol.

The development of selective estrogen receptor modulators (SERMs) opened a new perspective of ER action. Small structural modifications in the molecules can deeply impact ER activation. SERMs can activate and repress ER(s) at the same time depending on the tissue or cell type. The first non-steroidal estrogenic modulator Clomiphene, a mixture of the two isomers zuclomiphene and enclomiphene, was initially developed as a potential birth control agent. However, first investigations in humans showed opposite effects and the drug was further tested and developed to induce ovulation for the treatment of infertility (Greenblatt et al., 1962). Similarly, tamoxifen, a failed contraceptive compound, was re-evaluated after testing as adjuvant for the therapy of estrogen positive breast cancer (Cole et al., 1971). In addition to these two SERMS, further studies and developmental effort led to the second generation of SERMS. The most popular and applied compound is raloxifene, which under the name ketoxifene was originally designed for breast cancer therapy. However, it was less efficient than tamoxifen. Raloxifen increases bone density and reduces the incidence of vertebral fractures in postmenopausal women (Ettinger et al., 1999; Maximov et al., 2013). Compared to tamoxifen, raloxifen has the advantage of not affecting the uterus, avoiding the risk of endometrial cancer (Jordan, 1988; Jordan et al., 1987). SERMs represent a challenging group of compounds, not only in terms of activating/inhibiting ERs in different tissues and subsequent adverse effects (higher risk of endometrial cancer, stroke and venous thromboembolism, hot flashes), but also due to pharmacokinetic issues. The attempt to improve the relatively short half-life of raloxifen, did not lead to success, as alteration of the structure resulted in loss of efficacy (Maximov et al., 2013). However, the idea of creating a “perfect SERM” is still attractive, since they could be applied for the treatment and prevention of breast cancer, osteoporosis and atherosclerosis in postmenopausal women at the same time. The compounds ospemifene, arzoxifene, lasoxifene and bazedoxofene belong to the “new SERMs” which reached phase III of clinical trials (Maximov et al., 2013). Notably, the risk/benefit ratio of these drugs has to be carefully evaluated in order to advance women´s health. The selective modulation of ERs represents an attractive but also challenging strategy to cure and prevent both breast cancer and osteoporosis, and it might additionally be considered for the application in metabolic diseases.

A completely new and promising strategy for the treatment of obesity and obesity-related diseases is the targeted delivery of estrogen into metabolic relevant tissues

by the covalent coupling of estradiol to a peptide. Tschöp and colleagues designed a molecule which is a hybrid of glucagon-like peptide (GLP-1) and estradiol connected by a hinge region. This region enables the uncoupling of estradiol only intracellularly, i.e. after binding of the peptide to the GLP-1 receptor and internalization of the whole complex (Finan et al., 2012). By this mechanism, it is possible to activate ER(s) only in metabolic relevant, e.g. GLP-1 receptor expressing cells, without affecting reproductive tissues and limiting side effects. Notably, the effects of chronic application of estrogens in metabolic tissues needs to be further explored, in order to better estimate potential consequences and side effects.

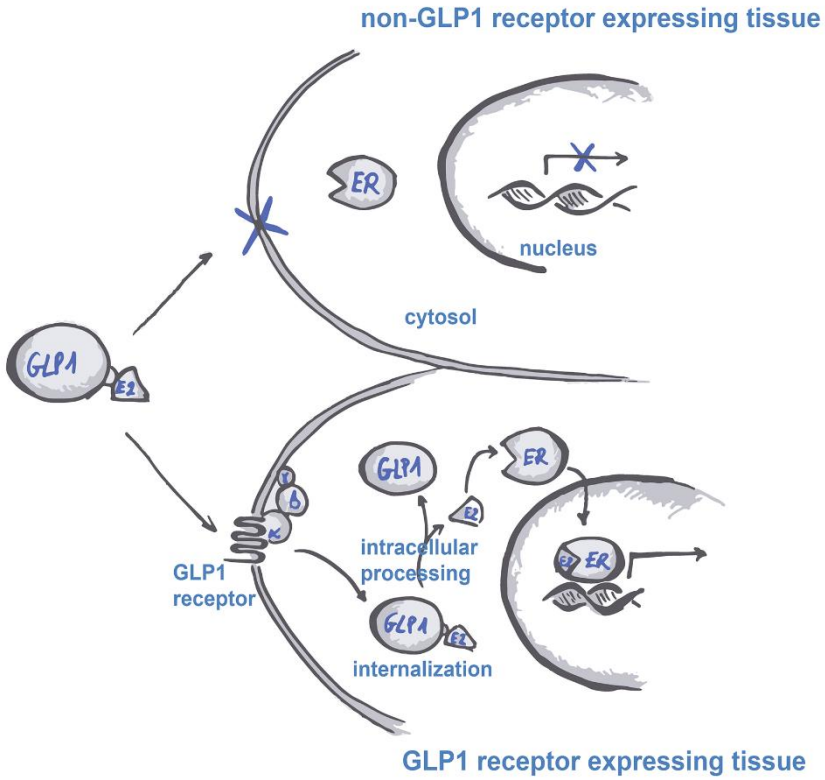

Figure 4: Schematic illustration of the mechanism of action of the GLP-1-estrogen-conjugate, described by Finan et al., 2012.

The stable glucagon-like peptide (GLP-1)-estrogen conjugate, delivers selectively estrogen to metabolic tissues, which express GLP-1 receptors. In absence of the transmembrane receptor, e.g. in reproductive tissue as breast and uterus, estrogen is unable to cross the membrane and induce transcription. Only after internalization and following intracellular processing, estradiol (E2) is released from the conjugate and can bind to the estrogen receptor (ER). The targeted delivery strategy is a novel approach in order to use estrogens for the therapy of metabolic disorders, without impacting reproductive organs.

1.3. Tissue-specific *in-vivo* knock-out models for studying the impact of adipose tissue estrogen receptor alpha on metabolism

As mentioned before, the deletion of ERα in mice results in several metabolic issues and obviously affects adipose tissue biology. Heine et al. described the ERαKO mice as obese, accumulating fat especially in visceral depots (Heine et al., 2000). Estrogen action in metabolic tissues is very complex and crosstalk between several organs leaves many questions unanswered concerning the adipose phenotype of ERαKO. Is obesity the result of the specific deletion of ERα in adipocytes, or rather a secondary effect arising from the deletion of estrogenic actions in liver, skeletal muscle, or even in immune cells? Alternatively, increased adiposity might be a simple consequence of the lack of ERα in single brain regions?

To further elucidate these questions *in-vivo*, tissue-selective knock-out models are indispensable for evaluating adipose tissue relevant mechanisms, as done for brain-specific or skeletal muscle-specific ERα knock-out models (Ribas et al., 2010; Xu et al., 2011). An elegant methodology to create suitable models is the “Cre LoxP system” which enables site selective DNA recombination of the gene of interest in a certain cell type or tissue. This technique requires the combination of two genetically modified mouse strains. A “floxed” strain can be created by the insertion of two 34 base pairs (bp) sequences, called LoxP flanks (locus of X-over in P1), including the DNA sequence that should be recombined (floxed gene). The LoxP flanks are necessary for recognition through an enzyme called Cre-recombinase, in order to localize the targeted DNA sequence. This enzyme is usually introduced in a second mouse strain and the knock-out model can be generated by mating these animals with the floxed strain. The Cre-recombinase is an enzyme derived from the bacteriophage P1, which is able to excide or reverse the DNA regions flanked by the LoxP flanks, depending on the orientation of the LoxP sequences (Stricklett et al., 1999). The accurate selection of a promoter driving the Cre-expression allows targeted deletion of the floxed gene in a specific cell type or tissue. As some genes are indispensable for development in earlier stages of the animal´s life, deletions through the Cre LoxP system can result in lethal phenotypes (Li et al., 1994). For these cases, investigators developed an inducible Cre-recombinase strategy in order to control the time point for the targeted deletion. For example, the expression of the enzyme can be regulated by coupling the Cre-recombinase to a modified LBD of the

estrogen receptor. The following administration of an exogenous estrogen as tamoxifen would then activate the recombinase and induce the intended DNA recombination (Feil et al., 1997).

The achievement of Gustafsson and others (Antonson et al., 2012; Chen et al., 2009) to engineer a mouse with a floxed ERα including the exon 3 (Antonson et al., 2012) allowed the generation of tissue-specific ERα knock-out models, by crossing it with different Cre-recombinase strains. For targeting adipose tissue the most widely used cassette is the promoter of the fatty acid binding protein 4 (Fabp4) gene. Fabp4 encodes the adipocyte protein 2 (aP2), a transport protein for fatty acids highly expressed in adipocytes. Alternatives have been developed in the last years, using cassettes like adiponectin or the platelet-derived growth factor receptor alpha (PdgfRa). Strengths and disadvantages of the described Cre-strains will be elucidated in chapter 6 “Discussion”. Besides the correct choice of a suitable promoter driving the Cre-recombinase expression, the deletion strategy of specific regions of the gene are crucial to avoid translation of truncated proteins with remaining activity. Unfortunately, this was the case for the first ERα knock-out mice, as the neo-ERαKO expressed a protein with estrogen-dependent transactivation of 35% (Couse et al., 1995). However, the floxed ERα mouse generated in the Gustafsson lab targets exon 3 of the ERα gene, which encodes the important structure of the Zinc-finger of the DBD, inducing a stop codon in the exon 4. Therefore, the predicted protein would lack both the DBD and the LBD, resulting in a protein without ERα activity (Antonson et al., 2012).

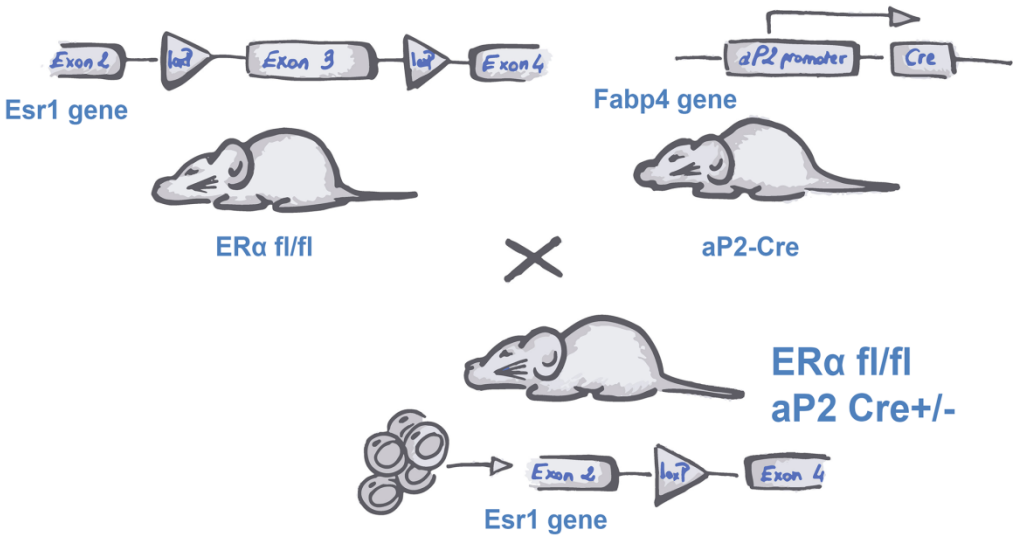

Figure 5: The Cre-LoxP system (adapted from Stricklett et al., 1999)

The generation of a floxed mouse of the targeted gene (e.g. ERα fl/fl) and of a transgenic mouse expressing the enzyme Cre-recombinase (Cre) dependently on the expression of a tissue/cell specific gene (e.g. Fabp4-gene), allows targeted deletion of the gene of interest. In the illustrated example, recombination of the estrogen receptor alpha gene (Esr1) is induced upon Cre expression in adipocyte protein 2 (aP2)-positive cells.

1.4. Obesity and inflammation

Cell-specific knock-out models are pivotal for the understanding of adipocyte biology in the context of obesity. This approach allows not only a selective analysis of fat cell-specific effects, but also a better understanding of the interplay between different cell types within the organ. As mentioned before, studies in rodents as well as in humans demonstrate a correlation between adipose tissue inflammation and obesity (Weisberg et al., 2003), while the causality between the two phenomena is not fully understood. However, inflammatory processes including changes in macrophage polarization are clear features of unhealthy adipose tissue (Kratz et al., 2014) and have to be considered in the context of obesity.

1.4.1. Macrophage polarization

Macrophages are immune cells belonging to the innate immune system, capable of engulfing particles, microbes and apoptotic cells in a process called phagocytosis. Furthermore, they play a crucial role in the initiation, regulation and termination of inflammatory processes of the innate and adaptive immune defense, including chemotaxis and antigen presentation. In contrast to neutrophils, macrophages have a longer half-life, surviving up to few months. Macrophages are derived from monocytes that are recruited due to chemotaxis from the bloodstream towards inflammation sites (extravasation). This type of macrophages, are often referred to as helper macrophages. Moreover, a high number of macrophages reside in different tissues, which are referred to as “resident” or “sentinel” macrophages (Lavin et al., 2015; Schiwon et al., 2014). These phagocytes are considered as being critical for the regulation of the microenvironment of several tissues, as discussed before for adipose tissue. Reciprocally, the microenvironment itself is influencing the phenotype of macrophages. Different factors characterize the local tissue microenvironment, for example cytokines, oxygen tension, metabolites, osmolality and acidification (El Kasmi and Stenmark, 2015). Macrophages are very sensitive to alterations of any of these conditions, responding in changes of their own cellular metabolism (El Kasmi and Stenmark, 2015). Therefore, macrophages are sensitive indicators of tissue homeostasis (Shalova et al., 2015) and have very heterogeneous phenotypes (Galvan-Pena and O'Neill, 2014; Murray and Wynn, 2011). Besides their localization and consequent subdivision into sentinel and helper macrophages, investigators tried to categorize subpopulations depending on their inflammatory features. A well-accepted classification is the macrophage polarization into M1 and M2. Macrophage polarization is a process of further differentiation conferring these cells a specific role in the multifactorial interplay of immune cells during inflammatory processes. The classically activated (M1) macrophages are cells that promote the inflammatory process. These phagocytes are activated by type 1 T helper cells (Th1 cells) (Mosser and Edwards, 2008; Stout and Suttles, 2004). Upon activation, M1 macrophages mainly produce pro-inflammatory cytokines and reactive nitrogen and oxygen intermediates, which increase the effectiveness of host defense. At the same time, M1 subsets play a pivotal role in antitumor immunity (Murray and Wynn, 2011; Ruffell et al., 2012). However, exaggerated activation of macrophages leads to enhanced tissue damage which can increase the risk for further infections. As a counterpart,

alternatively activated M2 macrophages play an important role during the resolution of inflammation and wound healing. The anti-inflammatory cytokines secreted by M2 macrophages antagonize the enhancement of the inflammatory process. At the same time, M2 macrophages are known to be more efficient than M1 macrophages in phagocytosis. Thereby they promote tissue clearance from debris, pathogens and apoptotic cells (Murray and Wynn, 2011). Further division in M2a, -b and –c macrophages has been also proposed for a more precise characterization (Kambara et al., 2015; Lefevre et al., 2010; Murray et al., 2014) of anti-inflammatory macrophages. The polarization process mainly depends on the microenvironment of the tissue where the macrophages are residing and the states of M1 and M2 are just the extremes of a heterogeneous spectrum of activation states of macrophages (Mosser and Edwards, 2008). Typical stimuli inducing a classical activation of macrophages are interferon γ (IFNγ) released from lymphocytes and the toll-like receptor (TLR) ligand lipopolysaccharide (LPS) present on the surface of bacterial cell membranes. The main triggers for M2 activation are interleukin 4 (IL4), secreted mainly by type 2 T helper cells (Th2), and other interleukins such as IL10 and IL13 (Kambara et al., 2015; Murray and Wynn, 2011). These stimuli induce intracellular signaling pathways regulating gene expression programs modulating the cytokine and/or growth factor production in macrophages (tumor necrosis factor α (TNFα), IL1β, IL6 for M1 type and IL10, transforming growth factor β (TGFβ), platelet-derived growth factor (PDGF) for M2 polarized cells) (Murray and Wynn, 2011). Notably, imbalances or inhibitory agents on polarization might lead to severe consequences for the immune system. In summary, macrophages are very heterogeneous cells and several mechanisms impacting their polarization have to be further elucidated.

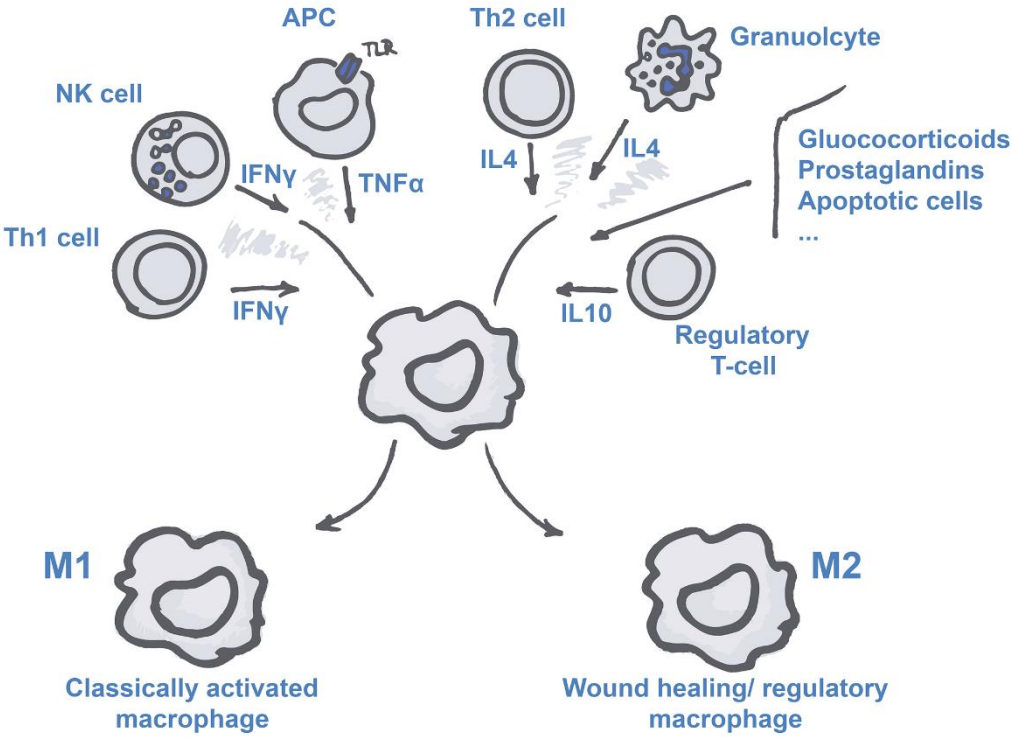

Figure 6: Schematic summary of known stimuli inducing macrophage polarization (adapted from Mosser and Edwards, 2008).

T-helper cells type 1 (T_h1 cells), natural killer cells (NK cells) and antigen-presenting cells (APC), release pro-inflammatory stimuli as interferon gamma (IFNγ) and tumor necrosis factor alpha (TNFα) and induce M1 polarization in macrophages. On the other hand, T-helper cells type 2 (T_h2 cells), granulocytes and regulatory T-cells promote a M2 phenotype of macrophages upon secretion of anti-inflammatory cytokines as interleukin 4 and 10 (IL4, IL10). Moreover, glucocorticoids, several prostaglandins and apoptotic cells are further stimuli inducing a M2 phenotype.

1.4.2. Physiological activation of the acute inflammation process

Clearly, not only macrophages are involved in the tight regulation of inflammatory processes, as the physiological immune defense is the result of a complex interplay between different immune cells and epithelial cells. A detailed description of all the known processes ongoing during infectious diseases would go beyond the scope of this introduction. However, the mechanism behind the regulatory effects of macrophages and neutrophils in regard to pathogen defense as part of the innate immune response are relevant for the understanding of how immune defects can lead to inflammatory diseases. Infiltrating microorganisms and damaged endogenous structures by pathogens are recognized as foreign by respectively pathogen-associated molecular patterns (PAMPS) and damage-associated molecular patterns

(DAMPS). These antigens bind to specific receptors expressed on tissue resident macrophages, dendritic cells, Kupffer cells and mast cells. After activation of these cells, they recruit leukocytes, mainly neutrophils and monocytes, from the blood stream to the inflammation site through release of cytokines as TNFα, lL17 and IL1β and activation of endothelial cells. In order to facilitate the extravasation and to attract leukocytes to the correct spot, activated endothelial cells express surface proteins such as P- and E-selectin and different integrins (ICAMs) on the luminal cell membrane. Upon random contact with the vessel wall, neutrophils and monocytes recognize the inflamed epithelial tissue, which induces the “rolling” of these cells along the endothelium (Borregaard, 2010). Further contact mediated by proteins of the β2 integrin family along the inflammatory gradient leads to firm adhesion to endothelial cells and follows transmural migration into the tissue (Amulic et al., 2012; Wong et al., 2010). Once the leukocytes overcome the endothelial barrier, they follow the gradient of chemoattractants and cytokines in order to reach microbes and damaged host tissue. The main neutrophil recruiting and activating chemokine is IL8, which in lower concentrations promotes the expression of β2 integrins, while in higher concentrations IL8 induces oxidative burst and degranulation of neutrophils (Ley, 2002). Importantly, activation of neutrophils is required for effective elimination of microbes and engages different mechanisms in order to exploit any vulnerable target of the pathogen microbe. Degranulation of several granula causes release of oxygen reactive species, metal chelator agents and antimicrobial proteins, as well as proteolytic enzymes. Furthermore, neutrophil activation can lead to phagocytosis and “NETosis”. The latter involves the secretion of neutrophil extracellular traps (NET), which encompasses an active cell death program with externalization of decondensed chromatin and exposure of antimicrobial agents in the extracellular matrix (Amulic et al., 2012; Brinkmann et al., 2004). Neutrophils contain a destructive cargo that is very effective and they are pivotal players of the immune response especially during bacterial infections. However, tight regulation of their deployment after successful antimicrobial action is required in order to limit host damage. Importantly, inflammation is pivotal for host defense and has to be tightly regulated. However, chronic inflammation as observed in adipose tissue of obese patients and/or failure of resolution of inflammation are severe complications. The process of inactivation is mainly orchestrated by macrophages and neutrophils themselves and will be further described in the next section.

1.4.3. Neutrophil clearance and resolution of inflammation

As mentioned before, neutrophil inactivation and clearance has to be tightly controlled in order to resolve inflammation and diminish harmful effects on host cells. Resolution of inflammation is an active process encompassing inhibition of further leukocyte recruitment, withdrawal of pro-inflammatory signals and removal of debris and apoptotic cells in order to restore tissue homeostasis. On the one hand, neutrophil apoptosis itself produces stimuli that inhibit the recruitment of further neutrophils. Through so called “find me” signals, at the early stages of apoptosis, they attract phagocytes, mainly resident and monocyte-derived macrophages. At later stages of apoptosis, neutrophils externalize intracellular proteins and structures such as phoshatidylserin (PS) and cardiolipin in order to induce engulfment by the already attracted macrophages in a process called efferocytosis. These signals are described as “eat me” signals, opposed by “don´t eat me” signals as plasminogen activator inhibitor-1 (PAI-1), CD31 and CD47, which inhibit efferocytosis (Bratton and Henson, 2011). Phagocytosis of apoptotic neutrophils by macrophages induces the expression of anti-inflammatory signals that promote M2 polarization, as transforming growth factor beta (TGFβ) and IL10 (Kennedy and DeLeo, 2009). On the other hand, there are mechanisms that prolong neutrophil survival by upregulating the expression of survivin protein (upregulated by LPS, granulocyte colony stimulating factor (G-CSF) and granulocyte and monocyte colony stimulating factor (GM-CSF)) or by inhibition of neutrophil caspases (Cas). Cas 3 and Cas 8 are known to be associated with proliferating cell nuclear antigen (PCNA) in the cytosol and are activated due to induced apoptosis by proteosomal degradation of PCNA (Witko-Sarsat et al., 2010). In diseases as sepsis and Wegener´s granulomatitis investigators demonstrated a stabilization of PCNA, leading to defects in the resolution of inflammation correlated to lower Cas3 and Cas8 activity (Witko-Sarsat et al., 2010). Aside from neutrophil properties, the macrophage phenotype influences the efferocytic capacity as well. It has been demonstrated that M2 macrophages are more efficient in efferocytosis, while M1 polarization has been associated to several chronic autoimmune diseases such as system lupus erythematosus, cystic fibrosis or chronic obstructive pulmonary disease (Elliott and Ravichandran, 2010; Krysko et al., 2010; Munoz et al., 2010). One of the key properties that allows functional engulfment of apoptotic neutrophils is the expression of bridge molecules on the extracellular macrophage membrane (Bratton and Henson, 2011). Furthermore, the presence of lipoxins, resolvins,

annexin I and adiponectin has been shown to facilitate phagocytic effectiveness (Serhan et al., 2011; Takemura et al., 2007). Notably, multiple mechanisms are involved in the tight regulation of inflammatory processes. The balance between anti- and pro-inflammatory signals is pivotal in order to neither suppress the necessary immune host defense nor to damage redundantly host tissue. In both scenarios, defects can lead to severe and chronic disorders (Amulic et al., 2012). Chronic inflammation is, as mentioned before, also one cause of obesity related disorders as insulin resistance. In this context, the main agents that induce inflammation are excessive amounts of dietary lipids and the resulting fatty acids that the body fails to store in adipocytes.

1.5. Fatty acids and obesity

In obesity, a crucial cause for the development of adiposity and adipose tissue inflammation is often the uncontrolled intake of high amounts of dietary lipids and fatty acids (FA), increasing the storage in adipose tissue. As previously mentioned, the exhausted storage capacity of fat cells results in tissue inflammation.

Fatty acids are carboxylic acids with a long aliphatic chain and can be subdivided into short-, medium- and long-chain fatty acids. In the organism, most of the FAs are bound to a backbone structure. Depending on the type of backbone structure, FAs are components of triglycerides, phospholipids, sphingolipids, etc. In addition, FAs can be categorized by the presence of double-bounds. In contrast to saturated fatty acids, lacking any double-bound, unsaturated FAs display one or more double-bounds that allow increased physicochemical flexibility of the molecule. In vegetal lipids, the ratio of unsaturated to saturated FAs is much higher than in lipids of animal origin. Besides glucose and amino acids, FAs are metabolized in order to produce energy mainly in form of adenosine triphosphate (ATP). Through a process called β-oxidation, FAs are broken down to acetyl-CoA or other intermediates of the tricarboxylic cycle (TCA), which further produce NADH (nicotinamide adenine dinucleotide) and $FADH_2$ (flavin adenine dinucleotide). These reduction equivalents drive the proton gradient and therefore the mitochondrial transport chain (MTC) that sustains ATP production. One molecule of palmitic acid (C16:0) yields 106 molecules of ATP and is more efficient than the breakdown of glucose, which delivers only 32 ATP molecules. Although lipids are vital nutrients, differences in the composition of FAs especially in terms of saturation, have been associated with obesity and other

related metabolic disorders. There is a general acceptance of the theory that saturated FAs have a negative impact on body weight, triglycerides and total cholesterol levels (Lottenberg et al., 2012; Mazidi and Kengne, 2017), whereas unsaturated FAs have been correlated to lower cholesterol plasma levels, lower atherosclerotic risk and protective effects in regard to obesity and metabolic syndrome (Lottenberg et al., 2012; Mukwevho and Joseph, 2014). However, controversial data was derived from rodent experiments on the role of different FA categories and on the supplementation with dietary oils. For example, in a HFD mouse model the supplementation of extra virgin olive oils prevented the development of hepatic steatosis and improved the oxidative stress-status in hepatic tissue and plasma (Rincon-Cervera et al., 2016). In another study, Yang et al. have shown protective effects of 3-omega FAs and long-chain mono-unsaturated FAs in regard to HFD-induced metabolic syndrome (Yang et al., 2015). However, omega-3 FAs are conversely discussed concerning their impact on metabolic health due to their propensity for lipid peroxidation, causing oxidative stress (Maehre et al., 2015).
Importantly, FAs are not only necessary as fuel for energy supply of the organism, but are implicated in several functions as cell membrane structure, vehicle for the resorption of lipophilic vitamins, precursors for the synthesis of mediators and hormones, modulation of intracellular signaling pathways including regulation of transcription factors such as peroxisome proliferator-activated receptors (PPARs).

1.5.1. Fatty acids as lipokines

In the last years, an increasing body of evidence demonstrates functional and regulatory effects of different FAs, influencing cell signaling. Docosahexaonic acid (DHA) and other poly-unsaturated fatty acids (PUFAs) were recognized as endogenous PPAR ligands modulating transcription in metabolic tissues as adipose tissue and liver (de Souza et al., 2017; Miller et al., 2008). The different FA classes are also known to be responsible for modifications in the fluidity and flexibility of cell membrane, facilitating or inhibiting the formation for example of lipid rafts and caveolae (Yao et al., 2009). Along this line, macrophage ability of phagocytosis has been shown to be influenced by lipid composition of the plasma membrane (Schumann, 2016). Furthermore, palmitoleic acid (C16:1), a mono-unsaturated FA, was demonstrated to be released from adipose tissue modulating metabolic function in the muscle and suppressing hepatic steatosis in the liver (Cao et al., 2008). The

study of Cao et al (2008), was one of the first evidence that adipose tissue communicates with other organs in order to regulate systemic metabolic functions (Cao et al., 2008). The name lipokine originates from the discovery that single FAs released from fat cells can act as hormones. Our group investigated the impact of C16:1 on cardiac tissue, showing that this lipokine is a mediator of cardiac adaptation in response to exercise, resulting in physiological cardiac hypertrophy (Foryst-Ludwig et al., 2015). A further prominent discovery is the novel identification of a new class of lipids, fatty acid esters of hydroxy-fatty acids (FAHFAs) (Yore et al., 2014). Palmitic-acid-9-hydroxy-stearic acid (9-PAHSA) plasma levels were correlated with high insulin sensitivity, preventing metabolic complications related to HFD consumption. Yore et al. demonstrated that the action of PAHSA is mediated by the activation of the G-protein coupled receptor GPR120 (Yore et al., 2014). Interestingly, further studies proposed that intracellular FAs are able to modulate protein function by covalent binding of the lipid to the protein by acylation, altering the conformation of the protein itself. Similarly to other post-translational modifications like acetylation, phosphorylation or sumoylation, FA-protein binding can impact cell signaling. This process of acylation was first observed for C16:0 and was named “palmitoylation” (Bijlmakers and Marsh, 2003). There is growing evidence that FAs influence cell function by various pathways, and further investigations are clearly needed to understand how dietary lipids impact the FA composition in plasma, cell membrane and other compartments.

2. Objectives of the study

In previous studies performed by our group and others, ERα was identified as a key regulator of sexual dimorphism in fat distribution and metabolism (Benz et al., 2012). Moreover, investigations demonstrated impaired lipolytic activity in adipose tissue lacking ERα. This finding led to the assumption that adipose tissue ERα is necessary for the regulation of lipolysis especially during negative energy balance. The present investigations should provide the proof of concept, exploring metabolic changes and eventual alterations of the observed sexual dimorphism due to specific adipose tissue ERα deletion. Thus, the study should provide discrimination between central and adipose tissue ERα effects.

The initial aim of this study was to elucidate the role of adipocyte ERα in an *in-vivo* model concerning body weight dynamics and metabolic processes in obesity, focusing on adipose tissue related processes.

During the course of our experiments additional aims were added. As the unexpected and fatal phenotype emerged in female atERαKO mice, we focused on the pathogenesis of the inflammatory processes induced by HFD-feeding. With this, we further concentrated our investigations on the role of dietary FAs as non-classical modulators of ERα with respect to the impact on the immune response during bacterial infections. Following questions led us to the planning and execution of the experiments described in the result section:

1. Is HFD-feeding responsible for the development of the uterine inflammation in female atERαKO mice?

2. Which fatty acids present in the HFD might be the main trigger for inflammatory processes?

3. Which immune cells are affected by the HFD?

4. Which effects has stearic acid (C18:0) on macrophages?

5. How can C18:0 lead to a depletion of anti-inflammatory macrophages despite high 17β-estradiol levels in female atERαKO mice?

6. How can C18:0 influence ERα-signaling in macrophages?

3. Material

3.1. Animals, cell culture and bacteria

Animals

Adipose tissue-specific mice were generated by crossing B6.Cg-Tg(Fabp4-cre)1Rev/J mice (purchased by Jackson Laboratory, Bar Harbor, USA) with B6.129X1-Esr1tm1Gust (ERαfl/fl) mice, kindly provided by J.-A. Gustafsson (University of Houston, TX, USA). Female and male ERαfl/fl/ aP2-Cre-/+ (atERαKO) and, as control, ERαfl/fl/ aP2-Cre-/- (WT) littermates were used for all experiments.

Cell lines

Name	*Origin*	*Characteristics*	*Manufacturer*
THP-1 cells	Human, peripheral blood (acute monocytic leukemia)	Suspension cells, monocytes	ATTC, Wesel (GER)
HeLa cells	Human, cervix adenocarcinoma	Adherent cells, epithelial cells	ATTC, Wesel (GER)
L929 cells	Mouse, adipose tissue	Adherent cells, fibroblasts	Kindly provided by Antje Ludwig (AG. Stangl)

Bacteria

Name	*Genotype*	*Competence*
Escheria coli Top10	FmcrAΔ(mrrhsdRMS-mcrBC)φ80lacZΔM15 ΔlacX74 recA1 araD139 Δ(araleu)7697 galU galK rpsL (StrR) endA1 nupG	Chemically competent

3.2. Reagents and kits

3.2.1. Antibodies and enzymes

Antibodies

Name	*Antigen*	*Application*	*Manufacturer*
ERα (D8H8) Rabbit mAb	Monoclonal, C-terminus of human estrogen receptor alpha	IP, WB	Cell Signaling, Frankfurt a.M. (GER)
ERα (F-10): sc-8002 Mouse mAb	Monoclonal, C-Terminus of human estrogen receptor alpha	WB	Santa Cruz Biotechnology, Heidelberg (GER)
ERα (MC-20): sc-542 Rabbit pAb	Polyclonal, C-terminus of mouse estrogen receptor alpha	WB	Santa Cruz Biotechnology, Heidelberg (GER)
GAPDH (ab9484) Mouse mAb	Monoclonal, human protein	WB	Abcam, Cambridge (UK)
PE anti-human CD209, mouse	Extracellular domain of human CD209	FC, IHC	Biolegend, San Diego (USA)
PE anti-human CD11b, mouse	Human CD11b	FC	Biolegend, San Diego (USA)
PerCP/Cy5.5 anti-mouse F4/80, rat	Murine macrophages	FC	Biolegend, San Diego (USA)
Anti-mouse Ly-6G (Gr-1) PE	Monoclonal, mouse Ly-6G	FC	eBioscience, San Diego (USA)
Rat anti-mouse Mac3 antibody (clone M3/84)	Monoclonal, mouse Mac3	IHC	BD Pharmingen, San Diego (USA)
Rat anti-mouse Ly6G antibody (clone 1A8)	Monoclonal, mouse Ly-6G	IHC	Biolegend, San Diego (USA)

Donkey anti-rabbit HRP	Rabbit IgG (secondary Ab)	WB	Dianova, Hamburg (GER)
Rabbit anti-mouse HRP	Mouse IgG (secondary Ab)	WB	Dako, Glostrup (DEN)

Enzymes

Name	*Application*	*Manufacturer*
DNAse	RNA isolation	Qiagen, Hilden (GER)
M-MLV Reverse Transkriptase	CDNA synthesis	Promega, Mannheim (GER)
Proteinase K	DNA isolation	Qiagen, Hilden (GER)
RNAsin	CDNA synthesis	Promega, Mannheim (GER)
Taq Polymerase	PCR	PAN, Aidenbach (GER)
Trypsin/EDTA	Cell culture	Roche Diagnostics, Mannheim (GER)

3.2.2. Buffers, reagents and media

Name	*Application*	*Manufacturer/ composition*
LB Agar	Bacteria culture	Carl Roth, Karlsruhe (GER)
LB Medium (Lennox)	Bacteria culture	Carl Roth, Karlsruhe (GER)
dNTPs	cDNA synthesis, PCR	Promega, Mannheim (GER)
M-MLV RT 5x Buffer	cDNA synthesis	Promega, Mannheim (GER)
Random Primer	cDNA synthesis	Promega, Mannheim (GER)
Dulbecco´s modified eagle medium (DMEM)	Cell culture	Gibco by Life technologies, Karlsruhe (GER)

DMEM phenol red free	Cell culture	Gibco by Life technologies, Karlsruhe (GER)
DMSO	Cell culture	Sigma-Aldrich Chemie GmbH, Steinheim (GER)
Fetal bovine serum (FBS)	Cell culture	Life technologies, Karlsruhe (GER)
FBS, charcoal stripped	Cell culture	Sigma-Aldrich Chemie GmbH, Steinheim (GER)
Hepes	Cell culture	Gibco by Life technologies, Karlsruhe (GER)
Opti-MEM	Cell culture	Gibco by Life technologies, Karlsruhe (GER)
Penicillin/Streptomycin (Pen/Strep)	Cell culture	Biochrom AG, Berlin (GER)
Phosphate buffered saline (PBS)	Cell culture, IHC, IP	Gibco by Life technologies, Karlsruhe (GER)
Roswell Park Memorial Institute (RPMI) medium, phenolred free	Cell culture	Biochrom AG, Berlin (GER)
RPMI-1640	Cell culture	Gibco by Life technologies, Karlsruhe (GER)
Lipofectamin 2000	IP, WB	Invitrogen, Karlsruhe (GER)
Protein A Sepharose CL-4B	IP	GE Healthcare Europe GmbH, Little Chalfont (UK)
jetPEI macrophage	Luciferase gene-reporter assay	Polyplus transfection, Illkirch (FRA)
GeneRuler 100 bp DNA Ladder	PCR	Fermentas, St. Leon-Rot (GER)
Orange G	PCR	Merck, Darmstadt (GER)
1x TAE-Buffer	PCR, Nucleic acid electrophoresis	Tris 4.8 g EDTA2Na 0.74 g Acetic acid (100%) 1.14 ml

10x GenTherm buffer	PCR	Rapidozym GmbH, Berlin (GER)
Qiazol	RNA isolation	Qiagen, Hilden (GER)
Power SYBR Green PCR Master Mix	RT-qPCR	Applied Biosystems, Darmstadt (GER)
ECL™ Western blotting Detection Reagents	WB	Amersham, Buckinghamshire (UK)
G153A+B Developer	WB	AGFA, Köln (GER)
G354 Rapid Fixer	WB	AGFA, Köln (GER)
PageRuler™ Prestained Protein Ladder	WB	Fermentas, St. Leon-Rot (GER)
Restore™ Western blot Stripping Buffer	WB	Thermo Fisher Scientific, Langenselbold (GER)
1x TBS-T	WB, washing	10x TBS 100 ml Tween-20 1 ml ddH_2O ad 1000 ml
0.5 M stacking buffer	WB, Gel	Tris-Base 6.05g ddH_2O ad 100 ml ⇨ pH= 6.8
1.5 M separating buffer	WB, Gel	Tris-Base 18.15g ddH_2O ad 100 ml pH= 8.8
6x probe buffer for WB (6xPB)	WB	Tris-Base 1M, 7ml, pH 6,8 SDS 1 g Glycerol 3 ml Dithiothreitol 0,93 g Bromphenol blue (2%) 60µl

10x running buffer	WB, Gel-electrophoresis	Tris-Base 0.25 M Glycin 19.92 M SDS 10%
10x TBS buffer	WB, washing	Tris-Base 24.22 g NaCl 87.4 g ddH_2O ad 1000 ml ⇨ pH= 7.6
Blocking buffer	WB, blocking	5% BSA or milk powder in 1x TBS-T
Blotting buffer (Towbin buffer)	WB, blotting	Tris-Base 0.025 M Glycin 0.192 M SDS 0.05 % Methanol 20 % ddH_2O ad 1000 ml
RIPA-buffer	WB, protein lysates	Tris pH 7.5 50 mM NaCl 150 mM MgCl2 5 mM Nonidet P-40 1% Glycerol 2.5% EDTA 1 mM Na3VO4 1mM NaF 50 mM Na4P2O7 10 mM Phenylmethylsulfonylfluorid 100 µM protease inhibitor « Com. Mini » 1 tablet in 50 ml

3.2.3. Primer and Vectors

Primer

Name	*Forward sequence (5´>3´)*	*Reverse sequence (5´>3´)*
mm18S	CCTGAGAAACGGCTACCACAT	TTCCAATTACAGGGCCTCGA
mmB2M	CTGCTACGTAACACAGTTCCACCC	CATGATGCTTGATCACATGTCTCG
mmERα	GAACGAGCCCAGCGCCTACG	GCCTTCGCAGGACCAGACCC
mmIlr4a	TTCCACGTGTGAGTGGTTCC	TCGGACACATTGGTGTGGAG
mmCD47	CATCCCTTGCATCGTCCGTA	TGGCATCGCGCTTATCCATT
mmPAI-1	TCCACAAGTCTGATGGCAGC	TGGTAGGGCAGTTCCACAAC
mmLy6G	TTCCATCGCCGTGTATGGTG	TCGTACTGGCAGCAATCAGC
mmNos2	GTCTTGCTTGGGGTCCATCA	GCATTCCTCCAGGCCATCTT
mmArg1	CTCCAAGCCAAAGTCCTTAGAG	AGGAGCTGTCATTAGGGACATC
mmCTSD	AACGTGCTTCCGGTCTTTGA	GCTCCCCGTGGTAGTACTTG
mmWnt4	ATCTCTTCAGCAGGTGTGGC	ACCCGCATGTGTGTCAAGAT
mmLtf	CAGCAGGATGTGATAGCCACAA	CACTGATCACACTTGCGCTTCT
mmERα (genomic)	GGAATGAGACTTGTCTATCTTCGT	GACACATGCAGCAGAAGGTA
Cre (genomic)	GCATTACCGGTCGATGCAACGAGTG	GAACGCTAGAGCCTGTTTTGCACGTTC
hsB-actin	GGGTCAGAAGGATTCCTATG	GGTCTCAAACATGATCTGGG
hsCCR7	ATGGACCTGGGGAAACCAAT	ATAGGTCAACACGACCAGCC
hsCD206	CATATCGGGTTGAGCCACTT	GAGGGATCTCCTGTGTTCCA

Vectors

Name	*Origin*
pERE-TkGL3	kindly provided by P.J. Kushner, Metabolic Research Unit and Diabetes Center, University of California, San Francisco, USA
hERα-pSG5	kindly provided by P. Chambon, Institut Clinique de la Souris, Illkirch Cedex, France
pSG5	kindly provided by P. Chambon, Institut Clinique de la Souris, Illkirch Cedex, France
pRL-CMV	Promega, Mannheim (GER)
pcDNA flag (WT)ERα	kindly provided by F. Acconcia, University Roma Tre, Rome, Italy
pcDNA flag (C447A)ERα	kindly provided by F. Acconcia, University Roma Tre, Rome, Italy

3.2.4. Chemicals, compounds and kits

Chemicals and compounds

Name	*Manufacturer*
17β-estradiol	Sigma-Aldrich Chemie GmbH, Steinheim (GER)
β-Mercaptoethanol	Sigma-Aldrich Chemie GmbH, Steinheim (GER)
Acrylamid/Bis (30%)	Serva Electrophoresis GmbH, Heidelberg (GER)
Agarose	Biozym Scientific GmbH, Oldendorf (GER)
Ammoniumpersulfat (APS)	Sigma-Aldrich Chemie GmbH, Steinheim (GER)
Ampicillin	Sigma-Aldrich Chemie GmbH, Steinheim (GER)
BSA (bovine serum albumin)	Thermo Fisher Scientific, Langenselbold (GER)
BSA, fatty acid free	Carl Roth GmbH, Karlsruhe (GER)

Bromophenol blue	VWR, Darmstadt (GER)
Complete Protease Inhibitor Cocktail Tablets	Roche Diagnostics GmbH, Mannheim (GER)
4',6-diamidino-2-phenylindole (DAPI)	Sigma-Aldrich Chemie GmbH, Steinheim (GER)
Dimethylsulfoxid (DMSO)	Sigma-Aldrich Chemie GmbH, Steinheim (GER)
Ethylendiamintetraessigsäure (EDTA)	Sigma-Aldrich Chemie GmbH, Steinheim (GER)
Ethidiumbromid	Carl Roth GmbH, Karlsruhe (GER)
Formaldehyde 37%	Merck, Darmstadt (GER)
Glucose	Merck, Darmstadt (GER)
Glycin	Carl Roth GmbH, Karlsruhe (GER)
Heparin	Ratiopharm, Ulm (GER)
Hydrochloric acid (HCl)	Merck, Darmstadt (GER)
Insulin (Insuman rapid)	Aventis Pharma, Frankfurt a.M. (GER)
Kaliumchlorid (KCl)	Carl Roth GmbH, Karlsruhe (GER)
Lipopolysaccharide (LPS)	Sigma-Aldrich Chemie GmbH, Steinheim (GER)
Magnesiumchlorid (MgCl2)	Carl Roth GmbH, Karlsruhe (GER)
Methanol	Merck, Darmstadt (GER)
Methylene Blue	Merck, Darmstadt (GER)
Milk powder	Carl Roth GmbH, Karlsruhe (GER)
Mounting medium	Dako, Glostrup (DEN)
NaAsc	Sigma-Aldrich Chemie GmbH, Steinheim (GER)
NaCl	Merck, Darmstadt (GER)
NaOH	Merck, Darmstadt (GER)
Sodiumdodecylsulfat (SDS)	Serva Electrophoresis GmbH, Heidelberg (GER)

Sodiumfluorid (NaF)	Sigma-Aldrich Chemie GmbH, Steinheim (GER)
Sodiumorthovanadat (Na3VO4)	Sigma-Aldrich Chemie GmbH, Steinheim (GER)
Sodiumpyrophosphat (Na4P2O7)	Sigma-Aldrich Chemie GmbH, Steinheim (GER)
Nonidet P-40 substitute (NP-40)	Sigma-Aldrich Chemie GmbH, Steinheim (GER)
Neo-Clear®(xylene substitute)	Merck, Darmstadt (GER)
Palmitoleic acid (C16:1)	Sigma-Aldrich Chemie GmbH, Steinheim (GER)
Phenylmethylsulfonylfluorid	Carl Roth GmbH, Karlsruhe (GER)
Phorbol-12-myristate-13-acetate (PMA)	Sigma-Aldrich Chemie GmbH, Steinheim (GER)
Stearic acid (C18:0)	Cayman Chemical Company, Michigan (USA)
Tris	Carl Roth GmbH, Karlsruhe (GER)
Tris-Base	Merck, Darmstadt (GER)
Tween 20	Carl Roth GmbH, Karlsruhe (GER)
Ultra-pure water	Biochrom AG, Berlin (GER)

Kits

Name	*Manufacturer*
BCA Protein Assay	Thermo Scientific, Rockford (USA)
Dual-Luciferase® Reporter Assay System	Promega, Mannheim (GER)
HR-NEFA	Wako Diagnostics, Neuss (GER)
Invisorb® Spin DNA Extraction Kit	Stratec Biomedical AG, Birkenfeld (GER)
Nucleo Bond® Extra Maxi	Macherey-Nagel, Düren (GER)
Phagocytosis Assay Kit (IgG FITC)	Cayman Chemical Company, Michigan (USA)
RNeasy® mini kit	Qiagen, Hilden (GER)

3.3. Instruments

3.3.1. Animal facility equipment

Name	*Manufacturer*
Blood glucose test equipment, Contour Next	Bayer Healthcare, Leverkusen (GER)
High-fat diet (HFD)	Research Diets Inc./ Brogaarden, Lynge (DEN)
Low-fat diet (LFD)	Research Diets Inc./ Brogaarden, Lynge (DEN)
MRI (Echo mouse MRI)	Echo Medical Systems, Houston (USA)
Metabolic cage system (TSE-Labmaster)	TSE- Systems GmbH, Bad Homburg (GER)
Rectal body temperature sensor (Vevo 770 system)	Visual Sonics, Toronto (CAN)

3.3.2. Laboratory equipment

Material

Name	*Manufacturer*
96-well PCR-plates	Sarstedt, Nümbrecht (GER)
96-well white bottom plates	VWR, Darmstadt (GER)
Cell culture flasks and plates	Sarstedt, Nümbrecht (GER)
Cell scraper	Sarstedt, Nümbrecht (GER)
Eppendorf tubes (0,2-2 ml)	Eppendorf, Hamburg (GER)
Falcons, pipettes and tips	BD, Sarstedt, VWR, Eppendorf
Glass covers, 12 mm	NeoLab Migge, Heidelberg (GER)
Hyperfilm ECL Chemiluminescence films	Amersham, Buckinghamshire (UK)
Microscope slides	Langenbrick, Emmendingen (GER)
Omnifix syringes	Braun Melsungen, Melsungen (GER)
Orion II microplate luminometer	Titertek Berthold, Pforzheim (GER)
Polyvinylidenfluorid-membrane (PVDF)	GE Healthcare, Solingen (GER)

Sterican cannulas	Braun Melsungen, Melsungen (GER)

Equipment

Name	*Manufacturer*
Bioruptor, Tissue ruptor	Diagenode, Liège (BEL)
Centrifuges	Eppendorf, Hamburg (GER)
CO2-Inkubator HeraCell 150	Heraeus, Hanau (GER)
Curix 60 Developer	Agfa, Köln (GER)
FACS Calibur flow cytometer	BD Biosciences, Heidelberg (GER)
Gel documentation system ChemiDoc	Bio-Rad, München (GER)
Laminar-Flow-Bench LaminAir 1.2	Heto-Holten, Allerod (DEN)
Mastercycler gradient	Eppendorf, Hamburg (GER)
Mikro 20 und 22R Centrifuge	Hettich, Hanau (GER)
Microscope (BZ-9000E)	Keyence Deutschland GmbH, Neu-Isenburg (GER)
Nanodrop® ND-1000 Spectrophotometer	PeqLab, Erlangen (GER)
pH-Meter pH211	Hanna Instruments, Kehl am Rhein (GER)
Real-time PCR-System Mx3000P	Stratagene, La Jolla (USA)
Rotor for tubes	Manufactured by Bettina Röder
Thermomixer	Eppendorf, Hamburg (GER)
Scale BL 1500S	Sartorius, Göttingen (GER)
Waterbath WB 14	Memmert, Schwabach (GER)
Western Blot equipment	Bio-Rad, München (GER)

3.4. Online tools and software

Name	*Application*
Chromas Lite software	DNA sequencing
EMBL-EBI Emboss Seqret	Sequence format converter
EndNote	Citations
GraphPad Prism	Statistical analysis and diagramms
Microsoft Office (Excel, PowerPoint)	Data analysis and figures
Stratagene MxPro	RT-qPCR data analysis
Photo Shop	Figures
Primer Blast NCBI	Primer design
PubMed	Literature
UCSC genome browser	Gene data bank

4. Methods

4.1. Animal experiments

4.1.1. Animal breeding and body weight dynamics-protocol

B6.Cg-Tg(Fabp4-cre)1Rev/J mice were crossed with B6.129X1-Esr1tm1Gust (ERαfl/fl) mice. For breeding, male ERαfl/fl/ aP2-Cre-/+ (atERαKO) were mated with female ERαfl/fl/ aP2-Cre-/- (WT), as female atERαKO were unfertile. All animals got ad-libitum access to “normal” control-diet (CD) and water and were housed with a 12h-light-dark cycle in a tempered (25°C) facility.

The phenotype of the first cohort of six weeks old female and male atERαKO and WT was characterized on CD. Phenotyping included body composition analysis by MRI measurement and assessment of metabolic parameters (respiratory exchange ratio (RER), energy expenditure (EE), locomotor activity, food intake and drinking) in metabolic cages (TSE-Labmaster system).

A second cohort underwent the same procedures as the first one at the age of fifteen weeks. Additionally, body temperature was measured as described below.

To study possible differences in body weight dynamics, a third cohort of animals, starting at the age of six weeks, was fed for 14 weeks a HFD ad libitum, in order to induce obesity. Body weight (BW) was assessed two times a week. Animals were characterized metabolically in the TSE-Labmaster and by MRI after four and after twelve weeks of HFD-feeding. Afterwards, both males and females were randomized into a DIO-group (diet-induced obese) and a CR-group (caloric restriction). The DIO-groups were fed a HFD until all final analyses (glucose and insulin tolerance test, blood sampling) were performed and sacrificed with cervical dislocation under isoflurane anesthesia for organ harvesting. The CR-groups were adapted to single-cage housing. After adaptation, the food-intake (HFD) was estimated daily. Caloric restriction was conducted with low-fat diet (LFD) in an amount corresponding 50% of the calories of average food intake during ad-libitum feeding until the animals lost 20% of BW (compared to the individual DIO-BW). BW was monitored daily directly before feeding, at 5:00 p.m. Analogously to the DIO-groups, caloric restricted animals were sacrificed after final metabolic analyses under isoflurane anesthesia and organs were harvested.

4.1.2. Determination of estrous cycle

Physiologically, female mice have an estrous cycle occurring over four to five days and it can be divided into three to four stages: proestrous, estrous, metestrous and eventually diestrous, which is a resting state that can be given, when females are housed without the presence of males for a longer period. During these phases the typical presence or regression of certain cell populations (epithelial cells with or without visible nucleus, leukocytes and cornified cells) allow us to determine which state currently occurs by analyzing the vaginal smear of the animals (Caligioni, 2009; Cora et al., 2015). Estrogen plasma levels are typically changing over the different stages of the cycle, starting to increase at the end of the metestrous and reaching the highest concentration directly before ovulation (proestrous). For analysis, vaginal smear was collected and evaluated histologically after staining for 20 min with 1% methylene blue solution.

As female atERαKO mice were unfertile, collection of vaginal smear was performed for four days in a row to proof whether they still cycle. Compared to control littermates no huge differences could be found in the cycle-status of atERαKO mice between the different time points, as shown in the figure below.

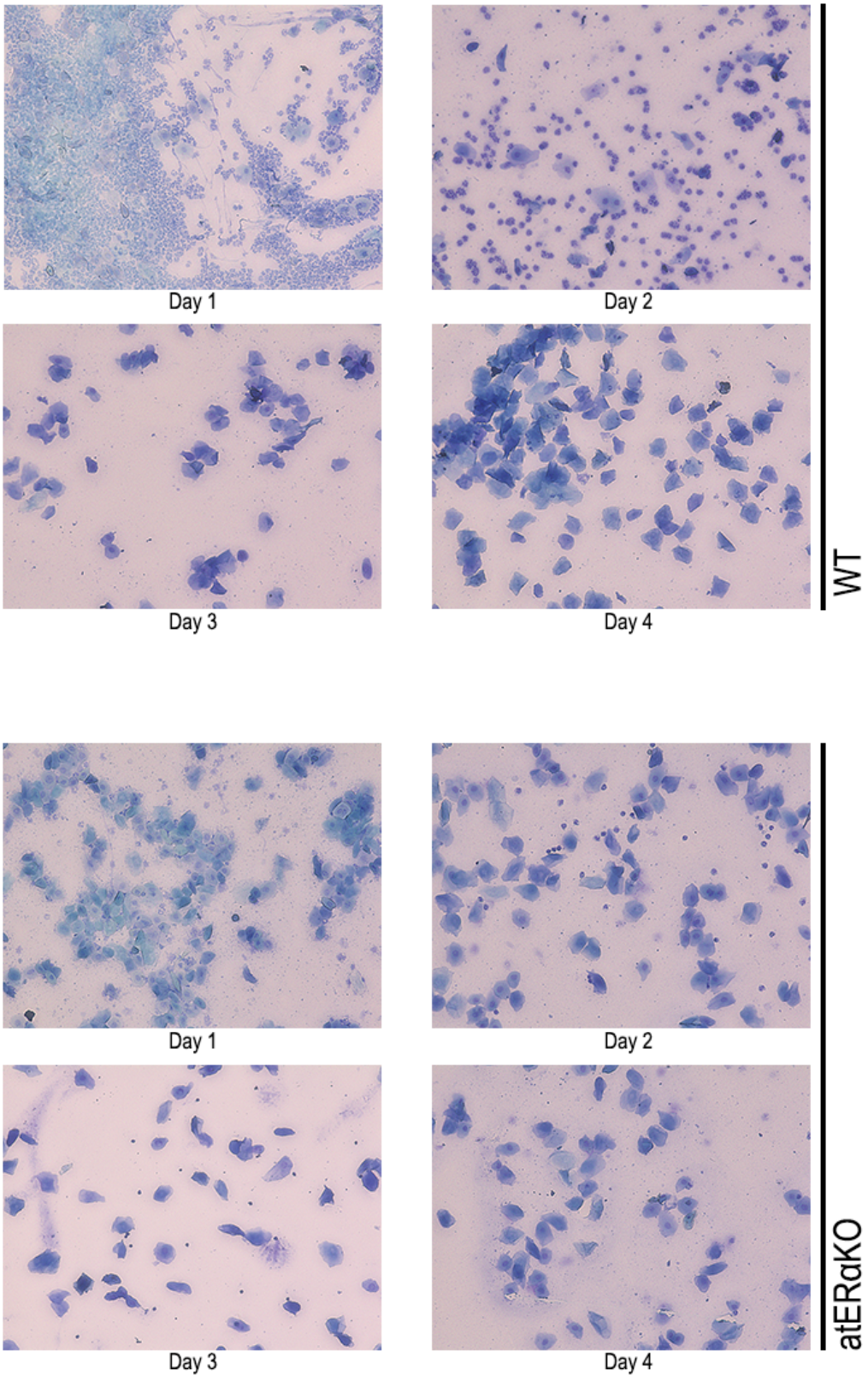

Figure 7: Representative vaginal smear of a WT and an atERαKO mouse, taken for four days in a row (published in Ban et al., 2017 *Sci Reports*)

In order to avoid confounding effects of oscillating estrogen levels in female animals during the different cycle states, estrous cycle was determined before sacrificing female animals. WT mice were sacrificed during estrous cycle-state, when estrogen levels are at the lowest, whereas female atERαKO mice, not having a regular estrous cycle, where sacrificed by exclusion of a state similar to proestrous.

4.1.3. Food monitoring and body temperature

Body temperature is one of the factors which contribute to whole energy expenditure together with activity and basal metabolic rate. Therefore body temperature was assessed rectally during basal phenotyping of the second cohort and after four (as time point of maximal weight gain) and fourteen weeks (stable DIO body weight) of HFD-feeding of the third cohort. The measurement was repeated for three to four days in a row to exclude eventual fluctuations caused by estrous cycle stages (females) and/or by stress levels of the animals (adaptation to the procedure compared to first measurement).

For the estimation of food intake, food monitoring occurred two times a week during HFD feeding, weighting the remaining food before and after addition of fresh HFD. Mean values were calculated per day for every cage, which contained three to five mice. A more detailed and individual analysis was performed during adaptation to single cages before caloric restriction. Also in this case, the amount of remaining and newly added HFD was assessed by weighting. Food intake was also monitored in the metabolic cages (see below), but for many mice, these values did not reflect the normal feeding behavior, probably due to insufficient adaptation to single cage/metabolic cage circumstances.

4.1.4. MRI – body composition analysis

Body composition was analyzed by nuclear magnetic resonance spectroscopy (MRI). Lean mass, fat tissue, free water and whole body water were measured. MRI analysis occurred during basal characterization for both (six and fifteen weeks old) cohorts and for the third cohort, after four and twelve weeks of HFD-feeding as well as after caloric restriction, when animals lost 20% of their DIO-weight.

4.1.5. Metabolic cages

At the same time points as for MRI analysis, animals underwent a measurement in metabolic cages (TSE LabMaster system) for a period of 23 h after one day of adaptation to single-cage housing. The respiratory exchange ratio (RER) and energy expenditure (EE) were assessed through indirect calorimetry, measuring the O_2 consumption (VO_2) and CO_2 production (VCO_2). EE was normalized to lean mass (LM), as different fat mass extension can be a confounding factor, as it leads to diverging BW. Locomotor activity was also assessed during the whole measurement through an infrared light beam system.

4.1.6. Intraperitoneal glucose and insulin tolerance test

For glucose and insulin tolerance test (GTT and ITT), animals were feasted overnight and blood glucose was measured after puncture of the lateral tail vein. Next, 1 g glucose/ kg BW (for GTT) or 0.25 IU insulin/ kg BW (for ITT) were injected intraperitoneally. After 15, 30, 60, 90, 120 and 150 minutes, blood glucose levels were assessed again as described before.

4.2. Ex-vivo experiments

4.2.1. Lipid profiling in mouse plasma samples

Final blood collection occurred through retro-orbital puncture under isoflurane anesthesia. 10 µl of heparin were added to 500-700 µl blood in order to inhibit coagulation. Next, samples were centrifuged for 5 min at 4,500 rpm and plasma was carefully pipetted into a new reaction tube. Plasma samples were frozen at -20°C until lipid profiling and 17β-estradiol measurement were performed. For fatty acid measurement, 100 µl were pooled out of three mouse plasma samples.

Lipid profiling was performed by Dr. Michael Rothe from Lipidomix GmbH (Berlin). A triplequad mass spectrometer coupled HLPC method, was used to separate and identify different fatty acids present in mouse plasma. First, samples were hydrolyzed and diluted 1:10 in a methanol solution, which contained internal standards. For separation, a reverse-phased column (Phenomenex Kinetex-C18 column 2.6 µm, 2.1 x 150 mm) was used and 5 µl of sample were eluted with a solvent gradient containing aqueous formic acid (0.1%) and acetonitrile. Fatty acid´s identity was

analyzed by an Agilent 6460 triplequad mass spectrometer with electrospray ionization.

4.2.2. 17β-estradiol measurement in mouse plasma samples

Measurement of estrogen levels in mice is a hugely challenging technique, where sample size and very low physiological hormone concentrations are limiting. Estimation of 17β-estradiol levels was performed by Prof. Dr. Gerhard Schuler (Justus-Liebig University, Gießen), who established in his group a sequential radioimmunoassay (Hoffmann et al., 1992).

As first step, 100µl of plasma sample, were extracted twice with toluene. Prior to immunoassay, the extracts were pooled and evaporated to dryness. After Re-dissolution in 0.1 ml BSA-phosphate buffer, an antiserum, directed against E2-6-carboximethyloxim (CMO)–BSA was added. Its cross-reactions were for estrone and estriol, respectively 1.3% and 0.7%. For all other tested non-phenolic steroids cross-reactivity was <0.01%. The minimum detectable concentration was 5 pg/ml; intra- and interassay coefficient of variation (CV) were 7.1 and 17.6%, respectively.

4.2.3. Histology

Histological sections, staining and pathological evaluation were performed by Prof. Dr. Robert Klopfleisch and Dr. Lars Mundhek from the veterinary pathology division of the FU Berlin.

After organ harvesting, ovaries and uteri of WT and atERαKO female mice were fixed in 10% formaldehyde solution for a minimum of 24 h. Next, organs were treated with different alcoholic and organic solutions for water deprivation and conservation, as shown in table 1. Finally, they were embedded in paraffin and 1 µm sections were cut, deparaffinised with xylene and rehydrated with a gradient of alcoholic solutions. For staining, citric acid was added and sections were heated for antigen retrieval. Next, slides were incubated with goat serum to avoid unspecific binding and then stained with hematoxylin and eosin (H&E), monoclonal rat anti-mouse Mac3 antibody (clone M3/84, BD Pharmingen, USA) and monoclonal rat anti-mouse Ly6G antibody (clone 1A8, Biolegend, USA). In uterine sections the grade of inflammation was estimated, as well as the Mac3 and Ly6G expression, with a semi-quantitative scoring system. Evaluation of histological stainings was performed blinded.

Step	*Duration*
1. 70% ethanol	1h
2. 80% ethanol	1h
3. 96%ethanol	1h
4. 100% ethanol	1h
5. 100% ethanol	1h
6. Neo-Clear®	40min
7. Neo-Clear®	40min
8. Paraffin 6	1h
9.Paraffin 9	1-24h

Table 1: Conservation procedure for organs after 24h fixation in formaldehyde

4.3. Cell culture

4.3.1. Secondary cell culture

Cultivation of THP-1 cells and differentiation to THP-1 macrophages

THP-1 cells are a monocyte-like cell lineage and were cultured in RPMI 1640 medium with addition of 10% charcoal stripped fetal bovine serum (cs-FBS) and 1% Pen/Strep. Cells are small and round and use to build loose agglomerates.

For experiments, cells were differentiated for 48h with 10 ng/ml phorbol-myristate-acetate (PMA, a proteinkinase C-activator) to macrophage-like cells. Through this procedure, cells turned to adherent cells, building again agglomerates/colonies. For luciferase gene-reporter assay, ca. 300,000 to 400,000 cells per well were seeded in 12well plates. For expression analysis and flow cytometry experiments, 700,000 to 900,000 cells were seeded in 6well plates, while for immunostaining and phagocytosis experiments, cells were seeded in 24well plates with a density of ca. 250,000 cells per well. Prior to the begin of experiments, a wash-out period of minimum 24 h with phenol red-free RPMI was needed to avoid estrogen mimicking effects of the indicator phenol red ($K_{d,\ \text{estrogen receptor}} = 2x10^{5}$ M) (Berthois et al., 1986). Prior to stimulation, cells were starved diminishing the FBS content to 2.5% for a maximum of 10h. Stimulation was performed with 10 nM 17β-estradiol (E2) and 50 µM stearic acid (C18:0) in 10% bovine serum albumin-solution and/or

lipopolysaccharide from *E. coli* (LPS, 100nM). As control for the fatty acid, sterile filtrated 10% BSA was used. Establishment of THP-1 differentiation into macrophages and FACS- and RT-qPCR experiments with THP-1 cells were carried out by Paul Maurischat (FU Berlin), during his internship as pharmacist.

Cultivation of HeLa cells

HeLa cells are an epithelial cell lineage derived from the cervical cancer cells of Henriette Lacks in 1951. Cells were cultivated in DMEM with the addition of 10% FBS and 1% Pens/Strep (Full DMEM) and splitted every 2 to 3 days avoiding layering of the cells. For detaching cells from the surface of the culture flask, 1ml Trypsin/EDTA was added to cells after washing with 10 ml PBS. After 2 min of incubation at 37°C, 9 ml of Full DMEM were added to inactivate trypsin. 0.5-1ml of the cell suspension was given into fresh Full DMEM.

For immunoprecipitation experiments, cells were plated into 10cm dishes and stimulated after transfection (see below) with E2, BSA or C18:0 as described for THP-1 macrophages.

4.3.2. Isolation of primary BMDM and differentiation to macrophages

Primary murine macrophages were obtained according to Weischenfeldt and Porse (Weischenfeldt and Porse, 2008), with some modifications of the protocol. After sacrificing WT female mice, tibia and femora of the animals were isolated, keeping the epiphyses closed. After disinfection in 70% alcoholic solution, bones were washed in PBS under the cell culture bench. Afterwards, epiphyses were opened carefully and bone marrow was flushed with a syringe with DMEM containing 1% Pen/Strep (starving DMEM). Cells were centrifuged, re-suspended with syringes and washed twice with starving DMEM.

For differentiation, ca. 4-10x 10^6 bone marrow cells were seeded in 10cm dishes with DMEM medium containing 10% conditioned medium from L929 cells (sterile filtrated supernatant of 100% confluent L929 cells, medium was left on cells for 7d), 10% cs-FBS and 1% Pen/strep (differentiation medium). Two days after isolation, differentiation medium was partly changed carefully, as differentiating cells were not yet adherent. After day 5, medium could be changed completely, eliminating all other cell species, which did not adhere. Again, on day 6, medium was changed to full DMEM (without addition of L929-conditioned medium). At this stage primary

macrophages were differentiated to adherent and in colonies organized cells. Figure 8 depicts the morphology of the cells throughout the different stages. On the next day, cells were stimulated for 6, 12 or 24h with E2 and C18:0 or BSA in the same concentrations as done with THP-1 macrophages. Due to higher sensitivity of the cells, wash-out with phenol red free medium, as well as deprivation of FBS was not possible.

For expression analysis, cells were washed with PBS after stimulation and harvested with RLT-buffer (supplied with the RNA isolation kit) for RNA and with ice-cold RIPA-buffer for protein isolation.

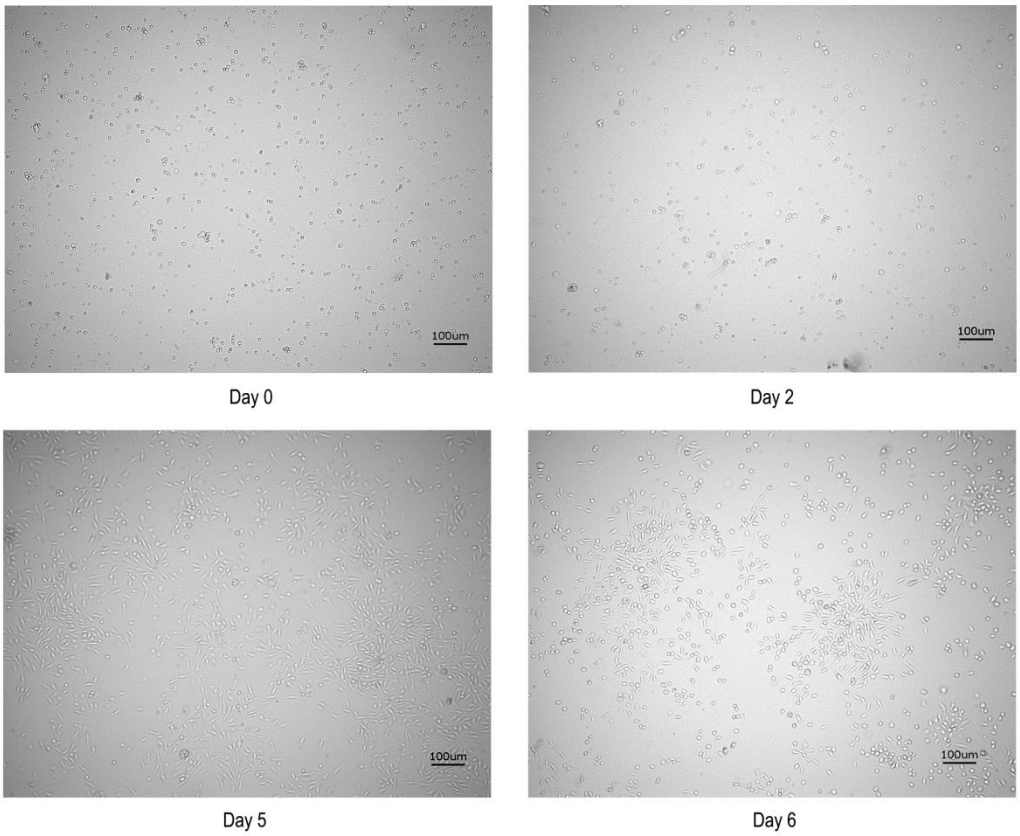

Figure 8: Morphology of differentiating bone marrow-derived macrophages (BMDM) throughout the days after isolation

4.4. Biomolecular methods

4.4.1. Genotyping of atERαKO mice

Genomic DNA of aP2-Cre ERα fl/fl animals was isolated from tail biopsies, using Proteinase K for digestion of the tissue and the Invisorb Spin DNA Extraction kit, accordingly to Stratec´s instructions. DNA was eluted from the columns with 50µl elution buffer.

Next, amplification of DNA was performed by polymerase chain reaction (PCR) using 4µl of isolated DNA, a primer pair for ERα (primer1= mmERα (genomic), 10µM), one for Cre (primer 2= Cre (genomic), 10µM) and the Taq-polymerase as enzyme:

Reagent	*Amount [µl]*	*Thermal profile*	
DNA	4	Step1: 95°C (initial denaturation)	5 min
10x buffer	5	Step2: 95°C (denaturation)	45 s
dNTPs	1	Step3: 56°C (annealing of primer)	45 s
Primer 1[for]	1	Step4: 72°C (elongation)	1 min
Primer 1[rev]	1	Step5: go to step2	34 cycles
Primer 2[for]	0.5	Step6: 72°C	7min
Primer 2[rev]	0.5	Step7: 4°C	forever
Taq polymerase	0.25		
H_2O	36.75		

Amplified PCR products were separated and analyzed by 2% agarose gel electrophoresis after addition of OrangeG as loading buffer and as marker for the DNA front. Agarose was diluted in TAE buffer and ethidium bromide (0.5µg/ml gel) was added. 10µl of the sample and 4.5µl of the ladder were pipetted into the wells of the gel and electrophoresis was performed at 150V for approximately 35 min. DNA bands were visualized and analyzed by a gel documentation system. As positive control (K), DNA from an B6.Cg-Tg(Fabp4-cre)1Rev/J mouse and, as negative control, H_2O were used.

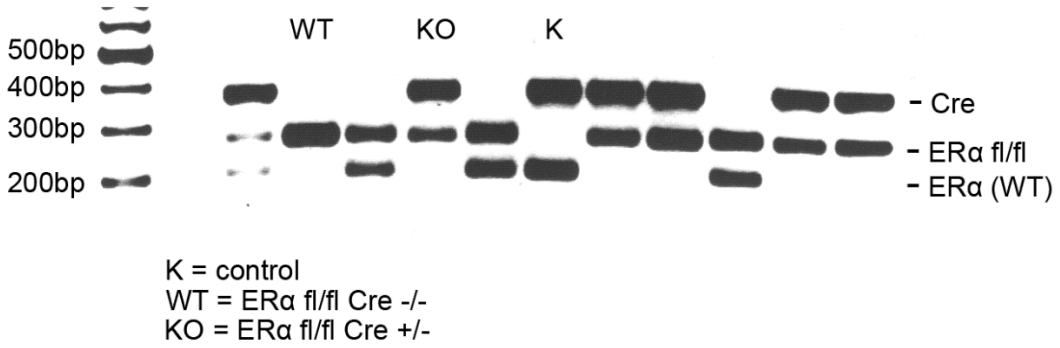

Figure 9: Documentation of representative gel electrophoresis from crossing B6.Cg-Tg(Fabp4-cre)1Rev/J and B6.129X1-Esr1tm1Gust (ERαfl/fl) mice. Bands display the genomic presence of the Cre, WT or floxed ERα. Further combinations beyond the indicated genotypes are the result of the breeding process.

4.4.2. Gene expression analysis

RNA isolation

Total RNA was isolated from animal tissues as well as from THP-1 macrophages and BMDM with Qiazol and Qiagen RNeasy mini kit accordingly to the manufacturer's instructions. RNA concentration was measured by UV-spectrometry (NanoDrop system).

cDNA synthesis

As complementary DNA (cDNA) is more stable than RNA, 1µg of isolated RNA was reverse transcribed to cDNA prior to real time PCR analysis (RT-qPCR). Therefore, following protocol was applied:

Reagent	*Amount*	*Procedure*	
DNA	1µg => X µl		
H_2O	37 µl- X µl		
Random Primer	1µl (100ng)	70°C (annealing to RNA)	5 min
Reverse transcriptase (or H_2O for negative control)	0.5µl		
RNasin	0.5µl		
5x M-MLV buffer	10µl		
dNTPs	1µl	37°C (transcription)	60 min

As negative controls two additional samples underwent the same procedure without the addition of the reverse transcriptase enzyme.

RT-qPCR analysis

For gene expression analysis, 5µl of cDNA (20 ng) were used in quantitative real time PCR (RT-qPCR) with the help of SybrGreen as fluorescent dye. Relative quantity of mRNA was calculated trough the 2^{-ddct} method after normalization to a house keeping gene (18S for animal tissues, β2-microglobulin for BMDMs and β-actin for THP-1 macrophages). All primer pairs were designed with the help of Primer Blast tool of NCBI and can be found listed in the material section.

4.4.3. Western Blot

Protein concentration of the lysates (with exception of protein lysates for immunoprecipitation) was estimated with the BCA assay kit, after sonication for 30s (40-50%). For protein expression analysis, 30 µg of protein lysate were incubated for 5 min at 95°C and separated for size through acrylamide (10-15%)-gel electrophoresis. SDS-PAGE was performed using a Bio-Rad equipment and electrophoresis buffer. Next, proteins were transferred to a PVDF (polyvinylidene fluoride) membrane (blotting step) after its activation in methanol for 1 min. Proteins were subjected to blotting at 100 V for 60 min in a tank blotting chamber with Towbin buffer. Afterwards, membranes were blocked for a minimum of 2h in 5% milk powder (for mouse antibodies) or 5% BSA (for rabbit antibodies) dissolved in 1xTBST. Membranes were incubated overnight at 4°C with the primary antibodies and washed four times with 1x TBST. For detection, membranes were incubated with the respective horseradish peroxidase-conjugated secondary antibodies for 1h at room temperature. Visualization occurred after another washing step (four times with 1xTBST) with enhanced chemiluminescence. For further analysis, membranes were stripped for 12 min with 16ml stripping buffer, blocked with the proper agent and incubated with the next primary antibody. If needed, loading control (housekeeper protein) was performed with GAPDH.

4.4.4. Plasmid replication

Transformation

Competent cells (*E.coli*) were transformed chemically with ca. 80 ng of the respective plasmids with the addition of 5M KCl buffer. Bacteria, buffer and plasmid were incubated for 20 min on ice and for another 10 min at room temperature. The cell suspension was then subjected to incubation in 1 ml LB medium for 1h at 180rpm and 37°C.

Selection of successfully transformed bacteria

For selection of successfully transformed bacteria from untransformed ones, 20µl and 200µl of the LB medium suspension were respectively given onto ampicillin agar-plates, making use of the expression of ampicillin resistance gene transferred from the plasmid. Untransformed cells were not able to grow and form colonies, as far as they did not exhibit antibiotic resistance.

Culture, amplification and plasmid isolation

One to three colonies from the agar-plates were picked with a pipette tip and given to 5 ml LB medium containing ampicillin (100µg/ml). Bacteria suspensions were incubated again at 37°C and 180 rpm for 8-9h. For further replications, 250-500µl of the now cloudy suspensions were pipetted into 150ml antibiotic containing LB medium and incubated overnight at the same conditions as described before.

Plasmids were isolated using the Nucleo Bond® Extra Maxi kit following the manufacturer´s instructions. Plasmid pellets were dissolved in 500µl ultra-pure water and concentration was estimated by UV-spectrometry (NanoDrop system).

4.4.5. Transfection of cells

HeLa cells were transfected for immunoprecipitation (IP) experiments with pSG5 (control vector), hERα-pSG5, pcDNA-wt ERα or pcDNA-C447 ERα plasmids with the help of Lipofectamine 2000 as transfection reagent and OptiMEM as transfection medium (serum deprived). 3µg of DNA/ 10cm dish were incubated with 6µl Lipofectamine at room temperature for 20 minutes and added drop by drop to the cells. Cells were incubated then for 3-4h with the transfection mix and medium was

afterwards changed to starving medium (DMEM with 1% Pens/strep and 2.5% cs-FBS).

Differentiated THP-1 cells, as macrophages, are difficult to transfect cells, that can easily phagocyte and digest the liposomes containing the plasmids. Therefore, the usage of a different transfection reagent was needed. JetPEI macrophage is a reagent that is able to complex with DNA and at the same time can be internalized by the cells through the binding of macrophage specific receptors expressed on the cell surface. For Luciferase experiments, 500 ng hERα-pSG5 or 250ng pcDNA flag ERα wt or pcDNA flag ERα C447A and 2 µg (or 1.4 µg for experiments with 250 ng ERα plasmids) pERE-TkGL3 and 5 ng pRL-CMV per well were incubated with 7µl transfection reagent at room temperature for 25min. Transfection mix was then added to the cells. Macrophages were incubated until medium was changed to starving medium.

4.4.6. Immunoprecipitation and lipid profiling of protein precipitates

For IP experiments, Sepharose A-beads were prepared on the day before cell harvesting. Therefore, beads were allowed to swell for 1h in PBS using a reaction tube-rotor. Next, beads were briefly centrifuged, supernatant was discarded and the same amount of fresh PBS as beads was added. 50µl of beads/PBS (1:1) per sample were added to 2µg rabbit anti-human ERα antibody and incubated overnight at 4°C under continuous rotation.

After transfection and stimulation, proteins of HeLa cells were harvested with RIPA buffer. After centrifugation of the protein lysates at 14,000rpm for 5 min, supernatant was added to 50µl of beads/PBS (1:1) without antibody to avoid unspecific binding of proteins to the beads. Therefore, samples were subjected to incubation for 1h at 4°C on the rotor. Next, Beads were centrifuged at 4°C and 1,200rpm for 1 min and supernatant was added to 50µl of beads-antibody mix (Ab-beads) and incubated overnight at 4°C for binding. On the next day, supernatant was frozen at -20°C and Ab-beads were washed six times for 5 min with RIPA buffer. After the last washing step, 30µl of 1x protein loading buffer (PLB) (5 parts RIPA and 1 part 6xPLB) were added to the now dry protein-Ab-beads complex. One IP sample per treatment was controlled by WB with mouse anti-human ERα antibody. All other IP samples were subjected to lipid profiling as described for mouse plasma samples. Before WB,

samples were incubated at 95°C for 5 min to allow separation of the proteins from the beads and were then centrifuged at 4°C and 14,000 rpm for 1min. As transfection control, 25µl of supernatant with addition of 5µl 6xPLB were analyzed as well by WB (rabbit anti-human ERα antibody).

4.4.7. Luciferase gene reporter assay

After transfection and stimulation for 24h, THP-1 macrophages were harvested with 150µl passive lysis buffer (provided with the kit Dual-Luciferase® Reporter Assay System) per well under vigorous shaking for 3 min. Duplicates of 40µl of the lysate of each sample were pipetted into a 96well flat bottom plate. Analysis was performed with Orion II microplate luminometer. For evaluation, firefly values were normalized to renilla and relative activation of the estrogen response element (ERE), e.g. E2+BSA (as 100%) versus E2+C18:0, was calculated.

4.4.8. Flow cytometry (FACS)

Flow cytometry is a technique, which allows cell counting and in parallel characterization of cells in regard to granularity, size and, if antibodies for specific cell types were added, also in regard to phenotype. Through reflection and diffraction of different light beams, cell granularity (analyzed as extent of side scattered light (SSC) and size (measured by the extent of forward scattered light (FSC)) can be assessed. With different fluorescent dye-labeled antibodies, further immunophenotyping of cell populations is possible.

Flow cytometry experiments (FACS) were used for characterization and evaluation of the differentiation of BMDMs with an antibody for a macrophage marker (F4/80) and an antibody for a marker for neutrophils (Ly6G), also expressed on macrophage precursors. For this purpose BMDMs were analyzed directly after isolation and after day 6 of differentiation. Dot plots of the two cell populations are depicted in figure 10.

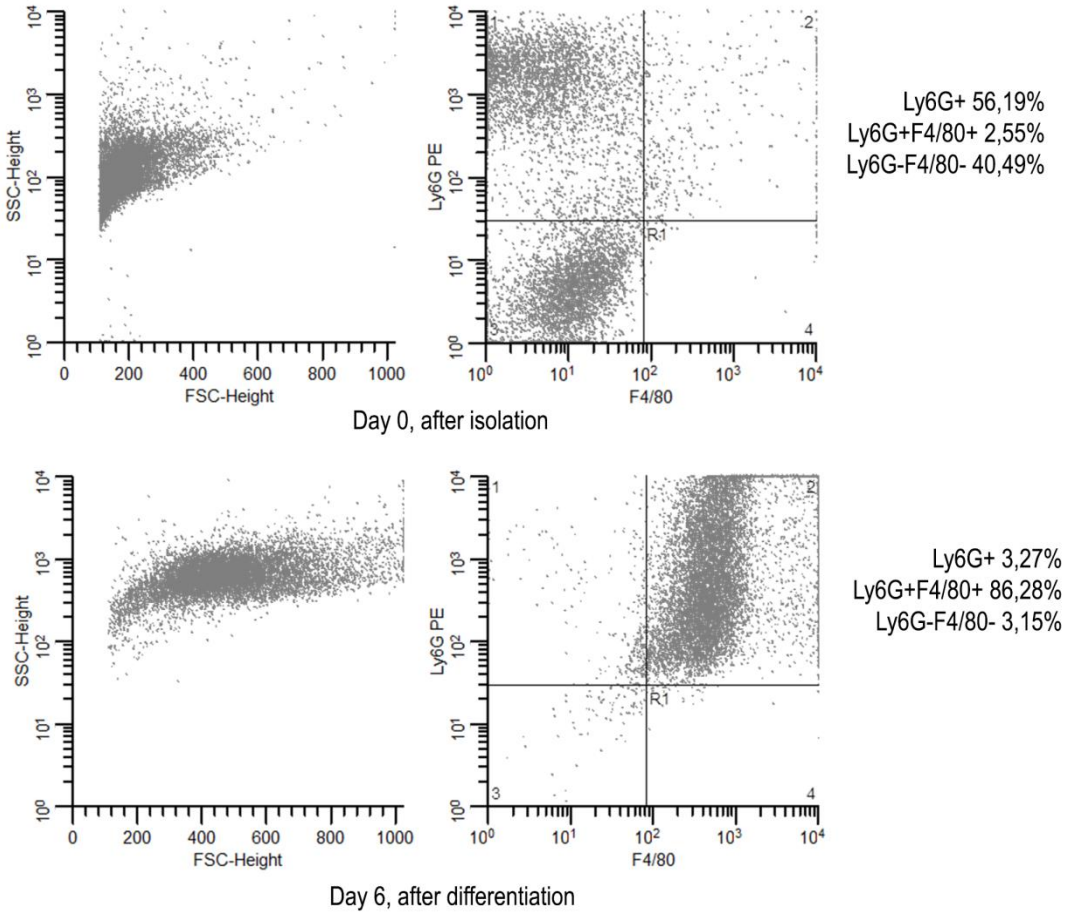

Figure 10: Characterization of BMDM cells by FACS analysis before and after differentiation

Furthermore, FACS analyses were used for the investigation of C18:0 mediated effects on THP-1 macrophage polarization. Percentage of M2 macrophages (alternatively activated, anti-inflammatory features) were measured with the help of the M2-marker CD209. As marker for macrophage activity, relative quantification of expression of the marker CD11b was used.

All FACS analyses were conducted in collaboration with Anna Sonnenburg (Charité Universitätsmedizin Berlin).

4.4.9. Immunofluorescence staining and phagocytosis assay

Phagocytosis activity of THP-1 macrophages, as well as M2-marker CD209 expression, were analyzed by immunohistochemistry. Therefore, THP-1 cells were seeded, differentiated and stimulated with E2 and BSA or C18:0, as described before.

For the phagocytosis assay, FITC-labeled beads (1:400) were added to the supernatant 2-3h prior to fixation of the cells. As next step, cells were washed once with PBS and for the phagocytosis assay additionally with Cell based Assay Buffer (provided in the kit from Cayman Chemicals), in order to wash away adsorbed beads, which were not internalized into the cells. Afterwards, cells were fixed with 3.7% formaldehyde solution for 10 min and washed with PBS for 5min under shaking. For CD209 staining, cells were incubated for 1h with PE-conjugated anti-human CD209 antibody (2.5µl per well). After three washing steps with PBS, nuclei were stained with DAPI (1:1000) for 7 min. Again, cells were washed three times with PBS and glass covers were mounted with mounting medium for analysis on microscope slides. Pictures from all samples were captured randomly with an all-in-one fluorescent microscope.

4.5. Statistical analysis

Statistical analysis was performed with GraphPad Prism Software. Statistical significance was assumed at $p<0.05$. For comparison of mean values between more than two groups data were evaluated by two-way ANOVA (analysis of variance) or two-way ANOVA with repeated measures, followed by Bonferroni posthoc test. Unpaired t-test was used in the case, that only two normally distributed groups are intended to be compared. All figure legends indicate the used test, the n-number and p-values. In the histograms deviation coefficients are displayed as standard error of the mean (SEM).

5. Results

The phenotype of atERαKO mice was investigated subjecting mice to a body weight dynamics-protocol, in order to elucidate the impact of adipose tissue-ERα on metabolism. The focus was laid on body weight gain and –loss.

5.1. Phenotyping of atERαKO mice

As described in the “Methods” section, three cohorts of atERαKO mice were characterized metabolically. The first two cohorts (6 weeks and 15 weeks old mice) were used for the baseline phenotyping in order to create an age matched control (adolescent and adult stage) group for the third cohort fed a HFD. Sex differences in regard to body weight gain, –loss and –regain as well as metabolism between WT female and male mice were already analyzed and published by our group (Benz et al., 2012). In this study the focus was laid on the differences between the genotypes WT and atERαKO, in order to outline the relevance of adipose tissue ERα in both sexes. Therefore, males and females are described separately in the following sections.

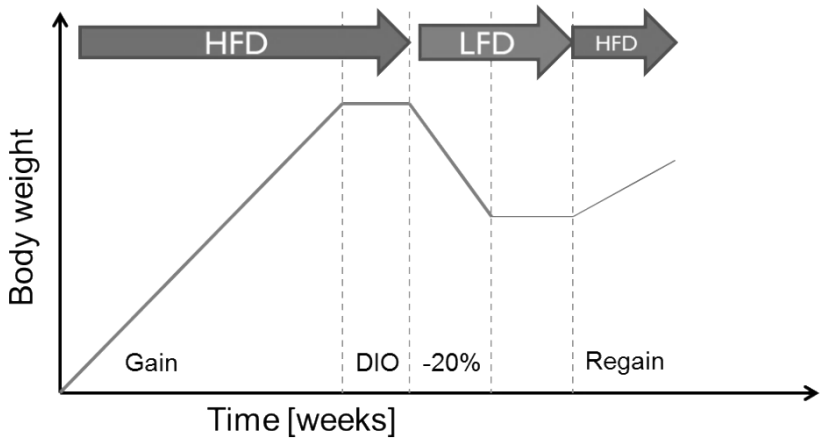

Figure 11: Established body weight cycling-model for characterization of body weight dynamics.

In the current study, the third cohort of atERαKO mice were subjected at the age of 6 weeks to HFD feeding (n=24 for females and n=17 for males for each genotype) to induce obesity. After 14 weeks, groups were randomized to a diet-induce obese (DIO) and to a caloric restriction (CR, -20%) subgroup. CR included a diet with 50% of calories of the mean daily intake in form of a low-fat diet (LFD). Caloric restriction was performed until mice lost respectively 20% of their DIO-weight. Maintenance of the reduced weight and regain due to ad-libitum HFD-feeding was not performed in this study, as body-weight gain and –loss are the metabolically more relevant stages.

5.1.1. Male mice

Metabolic characterization of males on CD

At the age of six weeks, atERαKO males displayed no differences in regard to body weight or energy expenditure (Fig. 12), when compared to control littermates (WT). As shown in Fig. 12A body composition also did not differ between the genotypes. However, the respiratory exchange ratio (RER) was lower for WT controls (0.91 ± 0.01 vs. 0.88 ± 0.01; n=4-5; p< 0.05), pointing towards more efficient lipid utilization, especially during the light-phase, when animals sleep and for usual do not consume food. Interestingly, at the age of 15 weeks, atERαKO mice were not significantly heavier than WT males, but showed a contrasting trend in body weight composition (Fig. 13A): they displayed lower lean mass (22.59 ± 0.5g vs. 22.92 ± 0.33g) and at the same time higher fat mass (3.55 ± 0.31g vs. 2.99 ± 0.26g). Even if these differences did not reach statistical relevance, relative lean mass (LM) differed significantly (75.44 ± 0.61% vs. 78.63 ± 1.00%; n=5; p<0.05), probably leading to the discrepancies between the genotypes in regard to energy expenditure normalized to lean mass. No differences occurred in locomotor activity, food intake or body temperature.

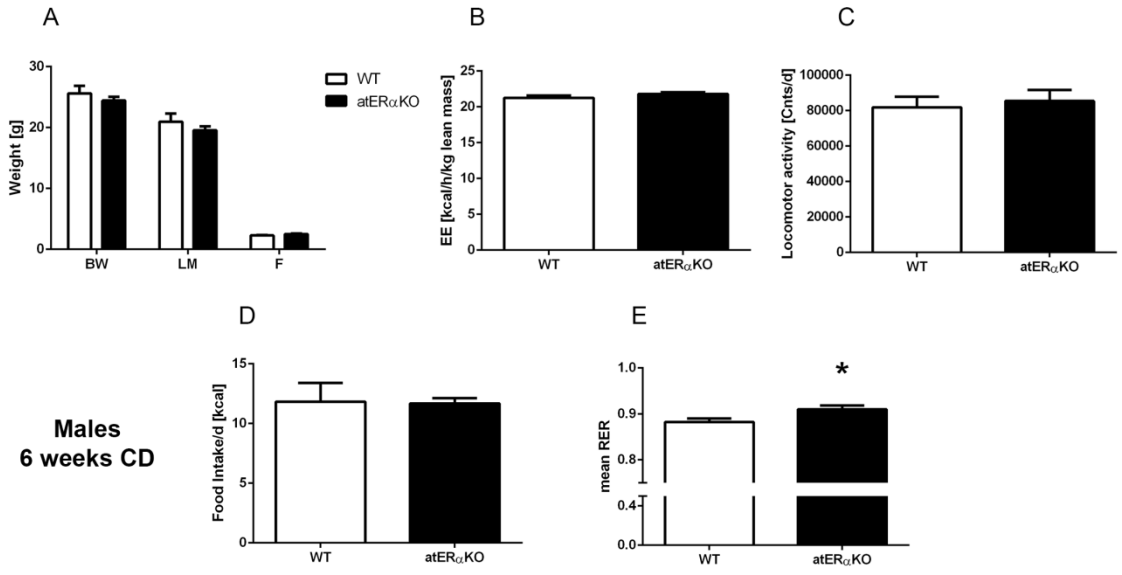

Figure 12: Metabolic baseline characterization of male atERαKO mice at the age of 6 weeks

(A) Body weight (BW), lean mass (LM) and fat mass (F) were assessed through MRI measurements of 5 mice per group. Mean energy expenditure (EE) normalized to lean mass **(B)**, total (23h) locomotor activity **(C)**, daily food intake calculated in calories **(D)** and mean respiratory exchange ratio (RER) **(E)** were measured in metabolic cages for 23 hours. n=5; unpaired t-Test; *P< 0.05 vs. WT.

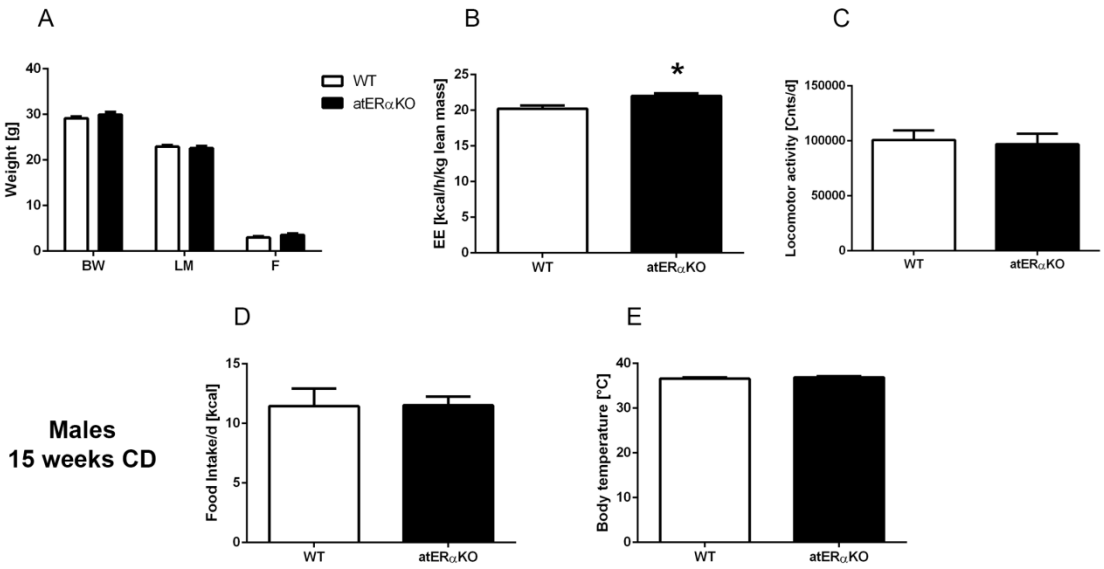

Figure 13: Metabolic baseline characterization of male atERαKO mice at the age of 15 weeks

(A) Body weight (BW), lean mass (LM) and fat mass (F) were assessed through MRI measurements of 5 mice per group. Mean energy expenditure (EE) normalized to lean mass **(B)**, total (23h) locomotor activity **(C)**, daily food intake calculated in calories **(D)** and mean respiratory exchange ratio (RER) **(E)** were measured in metabolic cages for 23 hours. n= 5; unpaired t-Test; *P< 0.05 vs. WT.

Metabolic characterization of males on HFD

The exposure to HFD corroborated the tendency of atERαKO males to be heavier than WT controls, leading to a significantly increased body weight gain throughout the 14 weeks of HFD-feeding (Fig. 14B). Already after four weeks of fat-enriched diet, a higher body weight could be recorded for the mutant mice (32.55 ± 0.61g vs 29.98 ± 0.59; n=17; p<0.01). Interestingly, at this time point no significant differences in body composition, energy expenditure, activity, body temperature or food intake occurred, however the fat mass was slightly increased (11.11 ± 0.94g vs. 8.53 ± 1.03g; P= 0.08; n=10). Body composition measurement after twelve weeks of HFD revealed besides the highly significant difference in body weight (48.34 ± 0.64g vs. 43.48 ± 0.99g) also discrepancies in lean mass (18.68 ± 0.31g vs. 17.21 ± 0.49g) as well as in fat mass (15.52 ± 0.33 vs. 13.42 ± 0.57g), as shown in Fig 14A. No differences in body temperature or energy expenditure could be recorded, but a lower locomotor activity (49414 ±3704cnts vs. 61173 ±4117cnts) and a tendency to a higher food intake (13.57 ± 0.81kcal/d vs. 12.43 ±1.11kcal/d) might be the reason for the increased body weight of male atERαKO during the DIO stage. Effects on the

glucose metabolism and insulin sensitivity were investigated through an intraperitoneal glucose tolerance- (GTT) and an insulin tolerance test (ITT). Both tests demonstrated that the knock-out of ERα in adipose tissue seems to not affect the whole body glucose metabolism in male mice (Fig. 15).

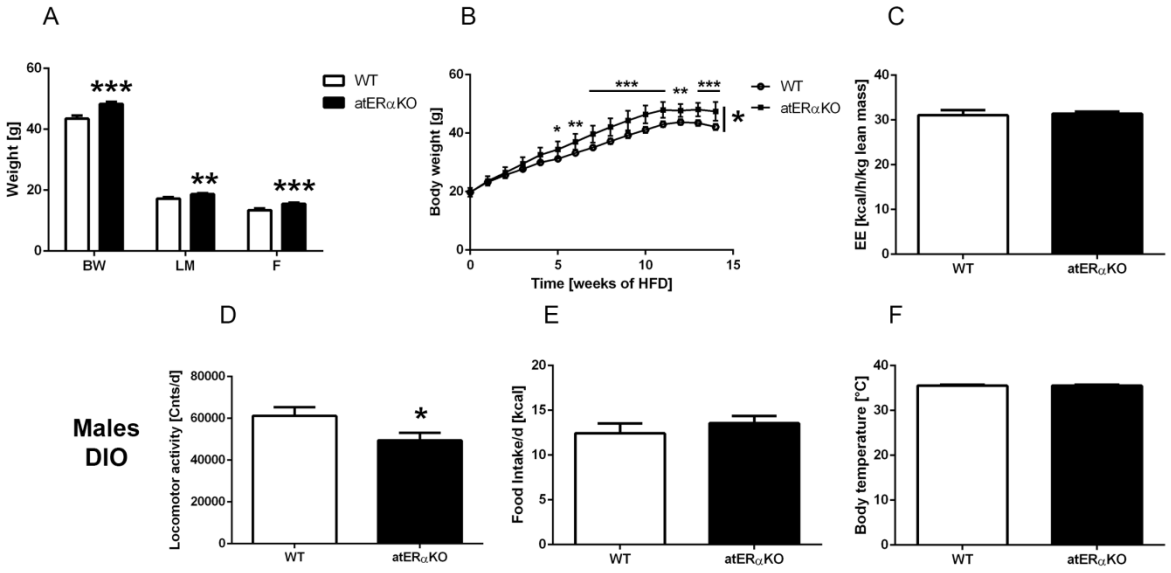

Figure 14: Metabolic characterization of diet-induced obese (DIO) male atERαKO mice (12weeks of HFD)

(A) Body composition of atERαKO and WT mice was measured by MRI. Significant differences in body weight (BW), lean mass (LM) and fat mass (F) could be registered. **(B)** Body weight development of male atERαKO and WT mice throughout HFD-feeding. atERαKO showed significantly higher BW after 5 weeks of HFD. While energy expenditure (EE) **(C)** and rectally measured body temperature **(F)** didn´t differ between the genotypes, food intake **(E)** was slightly increased for atERαKO mice and locomotor activity **(F)** was significantly decreased in respect to WT controls. n=17; unpaired t-Test and Two-way-ANOVA with repeated measures with Bonferroni posthoc test. *P<0.05; **P<0.01; ***P<0.001 vs. WT.

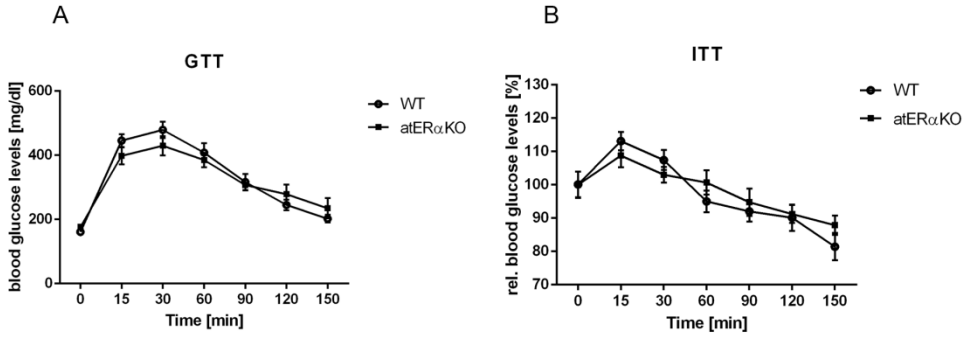

Figure 15: Glucose metabolism of diet-induced obese (DIO) male atERαKO mice (14weeks of HFD)

Intraperitoneal glucose tolerance **(A)** and insulin tolerance test **(B)** performed in male atERαKO and WT mice after 14 weeks of HFD-feeding. Blood glucose was measured before (time point 0), after 15 and 30 minutes after glucose/insulin injection. Afterwards, glucose levels were assessed every 30 min until 3 hours post-injection. No differences between the genotypes occurred in regard to insulin sensitivity and glucose tolerance. n=10; Two-way-ANOVA with repeated measures.

Metabolic characterization of males on CR

After stagnation of the increased body weight (DIO-stage), animals were subjected to caloric restriction (CR) as described in the “Methods” section. During this stage of the body weight-dynamics protocol, atERαKO mice maintained their increased body weight in comparison to WT mice throughout the whole period. Body composition measurements by MRI, revealed that the discrepancies between the genotypes are caused by the different amount of fat mass (13.32 ± 0.55g vs. 9.88 ± 1.06g). Metabolic cage analysis and GTT during CR could not elucidate any further effect of the knock-out of adipose tissue ERα on metabolism. Due to body weight loss, in both genotypes energy expenditure decreased when compared to DIO-stage, but no differences occurred between the genotypes (Fig 16D). However, the severe reduction of food intake led to a less effective weight loss in male atERαKO mice compared to WT males (Fig. 16C). Mutant mice needed two more days under caloric restriction to reach the targeted weight loss of 20% of their initial body weight (DIO-body weight). Interestingly, male atERαKO mice lost less fat mass when compared with WT mice. Even if the described effects might be expected for females rather than for males, it points towards the putative role of ERα in the context of lipolysis as previously shown in our group (Benz et al., 2012).

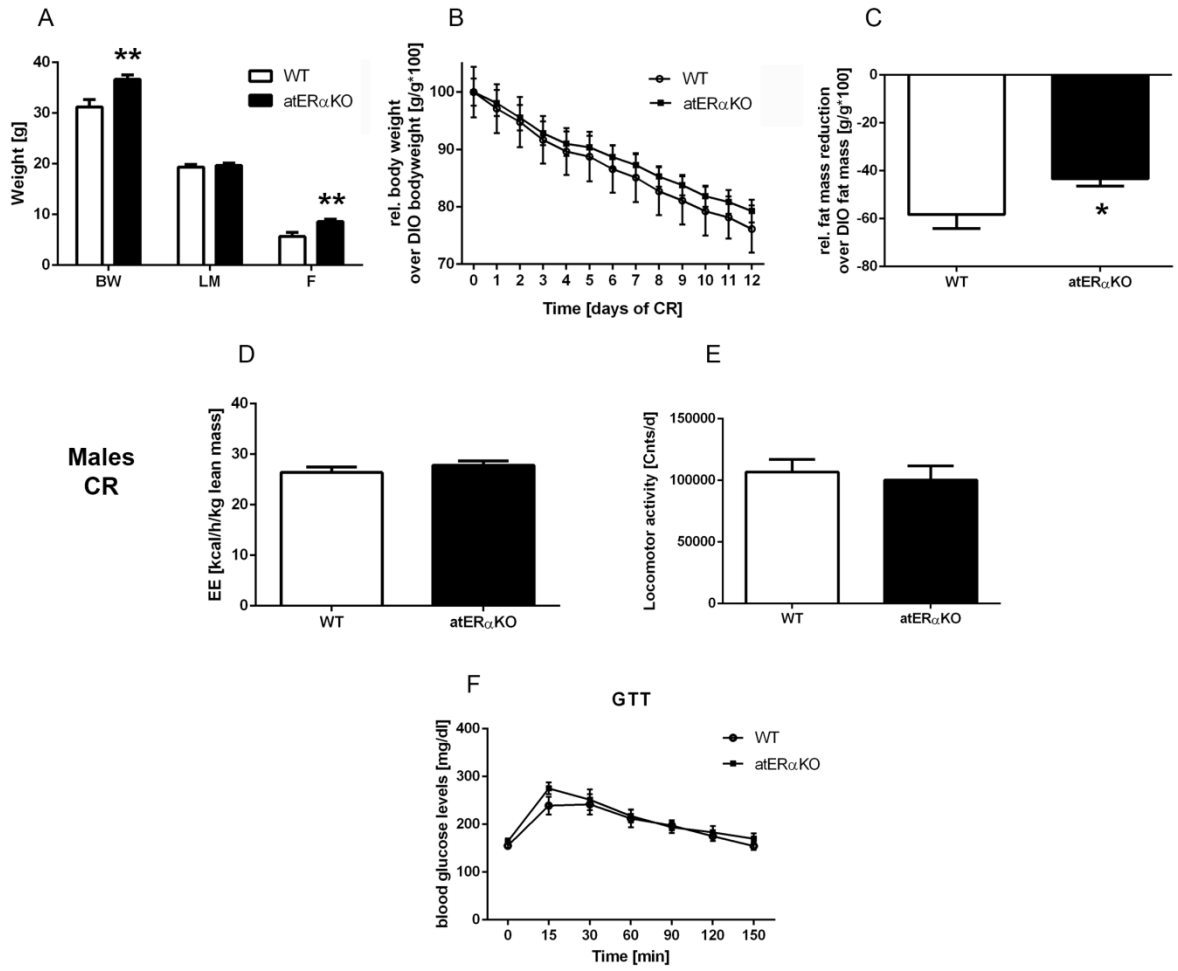

Figure 16: Metabolic characterization of caloric restricted (CR) male atERαKO mice

(A) Body composition of atERαKO and WT mice was measured by MRI. atERαKO males remained heavier than WT controls during caloric restriction (CR). Fat mass (F) differences could be registered, while lean mass (LM) was unchanged between genotypes. **(B)** Relative body weight loss of male atERαKO and WT mice throughout CR. atERαKO showed a slightly less effective BW loss, reaching the targeted BW of 80% (of DIO body weight) 2 days later than WT controls. **(C)** Relative fat mass reduction when compared with DIO state. Measurements of energy expenditure **(D)**, locomotor activity **(E)** and glucose tolerance test **(F)** didn´t elucidate other discrepancies between the genotypes. n=8; unpaired t-Test and Two-way-ANOVA with repeated measures with Bonferroni posthoc test. *P<0.05; **P<0.01; vs. WT.

Depletion of ERα not selective for adipose tissue

As recently described by Antonson and colleagues (Antonson et al., 2014), aP2-Cre mediated deletion of ERα occurs not only in adipose tissue, but also in the brain/hypothalamus. Analyses of ERα-expression on mRNA level, confirmed these findings, showing a significant decrease of the gene expression in white adipose tissue as well as in the hypothalamus of atERαKO mice. Control tissues as liver and skeletal muscle were not affected (Fig. 17).

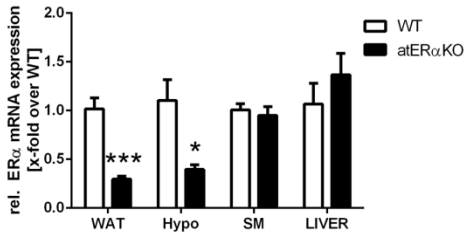

Figure 17: ERα expression analysis on mRNA level in different tissues of male atERαKO mice

ERα expression was significantly reduced in white adipose tissue (WAT) and also in the hypothalamus (Hypo). Control tissues as skeletal muscle (SM) and liver (LIVER) were as expected not affected by the knock-out. n= 4-5; *P<0.05; ***P<0.001.

In summary, metabolic changes in male atERαKO mice could be observed only after HFD-feeding. An increase in BW and a less propensity to lose fat mass in response to CR, points towards regulatory effects of ERα in this model. Whether the observed effects derive from the lack of adipose tissue ERα or is rather the result of the central depletion is unknown.

5.1.2. Female mice

Metabolic characterization of 6 weeks old females on CD

As expected, 6 weeks old female atERαKO mice compared to their control littermates (WT females) showed an increased BW and decreased EE, corroborating the hypothesis, that adipose tissue ERα might play a putative role in body weight homeostasis and whole body energy expenditure. Surprisingly, discrepancies in BW didn´t result from an enlarged fat depot (see table 2). Food intake and locomotor activity were not significantly regulated.

	WT	*atERαKO*
Body weight [g]	19.28± 0.55	22.80± 0.41***
Locomotor activity [cnts/d]	91477± 10009	81981± 7452
Food intake [kcal/d]	12.50± 1.38	12.11± 0.85
Energy expenditure [kcal/h/kg lean mass]	27.93± 0.81	23.79± 0.69**
Lean mass [g]	15.3± 0.47	17.94± 0.64*
Fat mass [g]	1.96± 0.11	2.03± 0.06

Table 2: Main metabolic parameters of 6 weeks old atERαKO compared to WT females (published in Ban et al., 2017 *Sci Reports*)

n =5. Two-tailed t-test *P<0.05; **P<0.01; ***P<0.01

Ablation of metabolic effects of adipocyte ERαKO in 15 weeks old females

Even more surprising were the findings in the second cohort of female animals characterized on CD. At the age of 15 weeks, neither differences in BW nor in EE could be recorded. Body temperature of female mice was as expected higher than of males, but no changes occurred between the genotypes (37.36°C± 0.10. vs. 37.26°C± 0.11). Interestingly, only LM reached significance (P=0.04), while the amount of fat mass was comparable between atERαKO and their control littermates. In this cohort, the genotype had no relevant impact on the parameters locomotor activity and food intake.

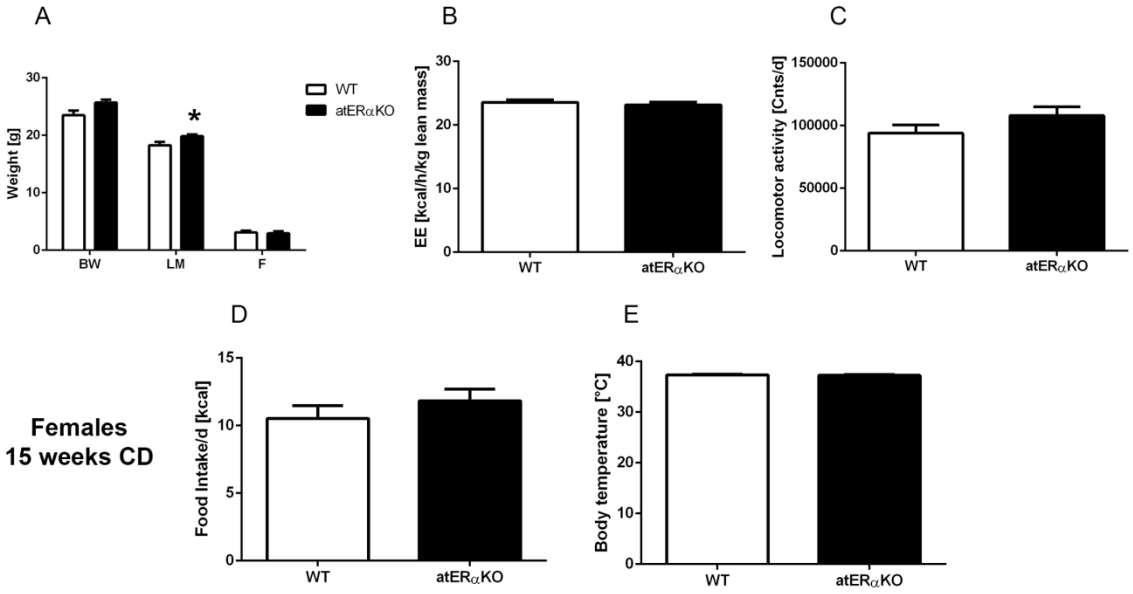

Figure 18: Metabolic baseline characterization of female atERαKO mice at the age of 15 weeks

(A) Body weight (BW), lean mass (LM) and fat mass (F) were assessed through MRI measurements of 5 mice per group. Mean energy expenditure (EE) normalized to lean mass **(B)**, total (23h) locomotor activity **(C)**, daily food intake calculated in calories **(D)** and mean respiratory exchange ratio (RER) **(E)** were measured in metabolic cages for 23 hours. n= 4-5; unpaired t-Test; *P< 0.05 vs. WT.

Females on HFD feeding

In line with the outcome of the analyses of the second cohort, female atERαKO did not differ from WT in regard to BW-gain during HFD-feeding (Fig. 19A+B). Even if during the first weeks of feeding atERαKO had an increased BW, these differences disappeared with the age of the animals, analogously to the observations made during CD-feeding (first and second cohort of animals). Energy expenditure, locomotor activity, body temperature, and food intake were not altered. Only lean mass was throughout all the measurements increased in mutant female mice. These data were very controversial to the findings of recent studies, which consolidate the role of ERα in the prevention of BW gain (Davis et al., 2013; Heine et al., 2000). As shown in Fig. 20 also glucose homeostasis (glucose tolerance and insulin sensitivity) was not affected by the knock-out of ERα.

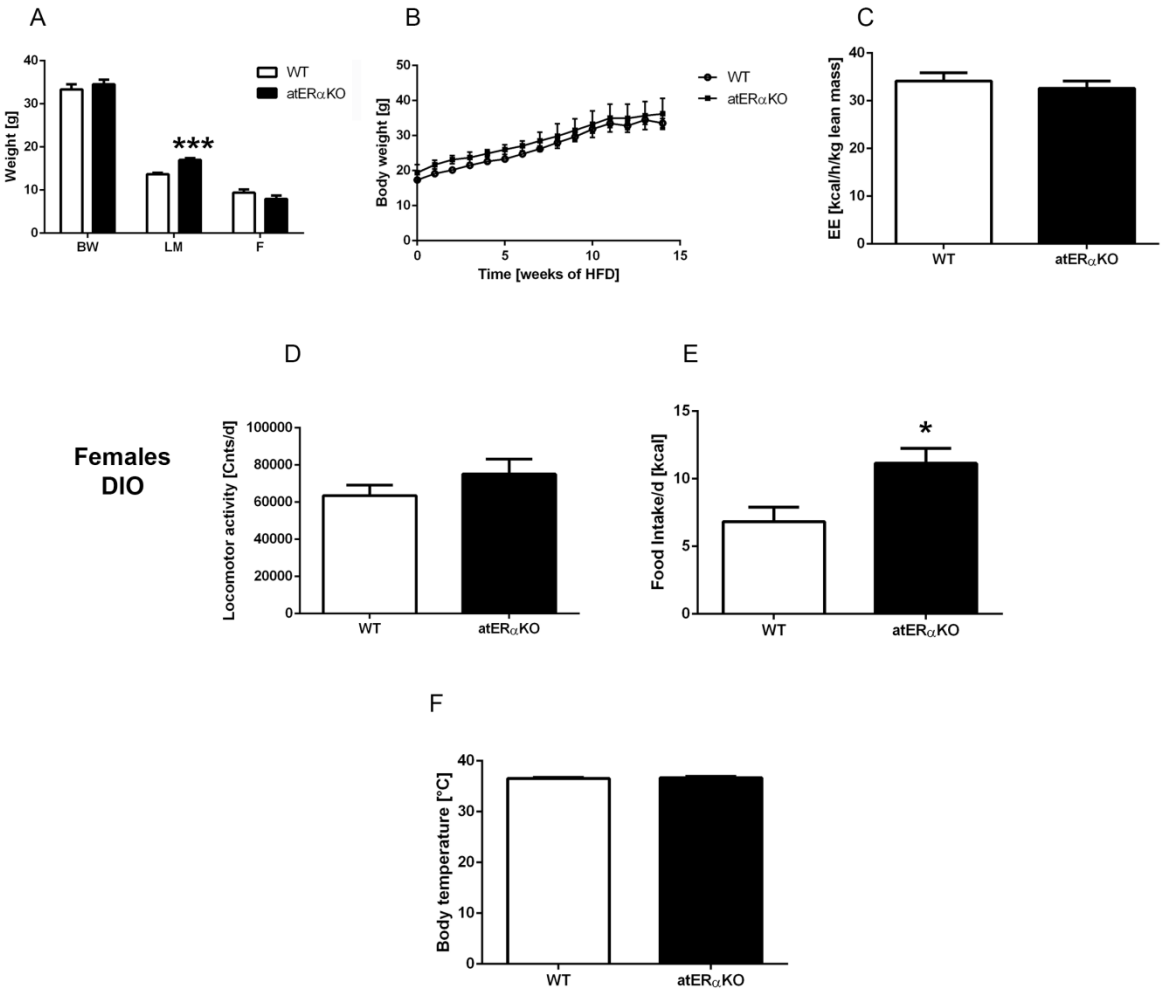

Figure 19: Metabolic characterization of diet-induced obese (DIO) female atERαKO mice (12weeks of HFD) (A-E published in Ban et al., 2017 *Sci Reports*)

(A) Body composition of atERαKO and WT mice was measured by MRI. Significant differences in body weight (BW) were abolished, only lean mass (LM) and not fat mass (F) differed between genotypes. **(B)** Body weight development of female atERαKO and WT mice. atERαKO showed higher BW during the first 4 weeks of HFD, but body weight gain throughout HFD-feeding wasn't significantly changed. While energy expenditure (EE) **(C)** and rectally measured body temperature **(F)** did not differ between the genotypes, food intake **(E)** was increased for atERαKO mice, similarly to male mice. Locomotor activity **(F)** was unchanged in respect to WT controls. n=17-20; unpaired t-Test and Two-way-ANOVA with repeated measures with Bonferroni posthoc test. *P<0.05; **P<0.01; ***P<0.001 vs. WT.

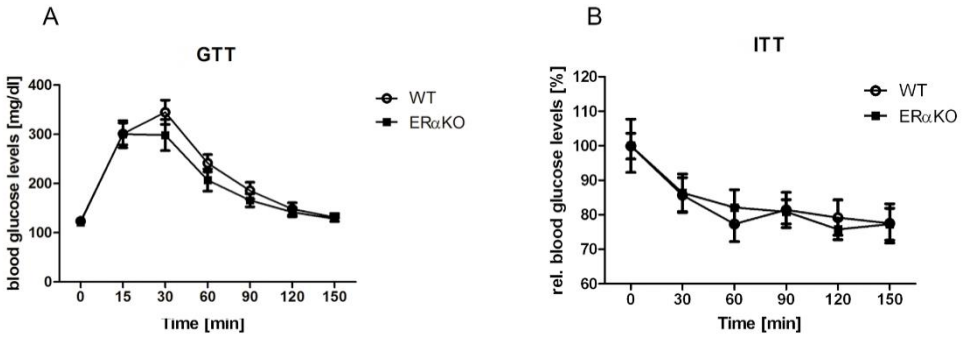

Figure 20: Glucose metabolism of diet-induced obese (DIO) female atERαKO mice (14weeks of HFD) (published in Ban et al., 2017 *Sci Reports*)

Intraperitoneal glucose tolerance **(A)** and insulin tolerance test **(B)** performed in female atERαKO and WT mice after 14 weeks of HFD-feeding. Blood glucose was measured before (time point 0), after 15 and 30 minutes after glucose/insulin injection. Afterwards, glucose levels were assessed every 30 min until 3 hours post-injection. No differences between the genotypes occurred in regard to insulin sensitivity and glucose tolerance. n=10; Two-way-ANOVA with repeated measures.

Caloric restriction

As described in the “Methods” section, after stagnation on a diet-induced-obese weight (DIO-weight, ca. after 14 weeks of HFD-feeding), effects of the knock-out model have been investigated on the ability of losing weight. As shown by Benz et al. (Benz et al., 2012), female mice used to reach the targeted weight (-20% of the initial, DIO-weight) more efficiently than males. This finding could be confirmed in the current study, even if the hypothesis, that atERαKO female mice would lose weight more slowly could not be supported by the present data. Mutant mice lost BW due to caloric restriction even faster than WT. Again, no differences in EE, activity, food intake or glucose tolerance could be outlined between the genotypes.

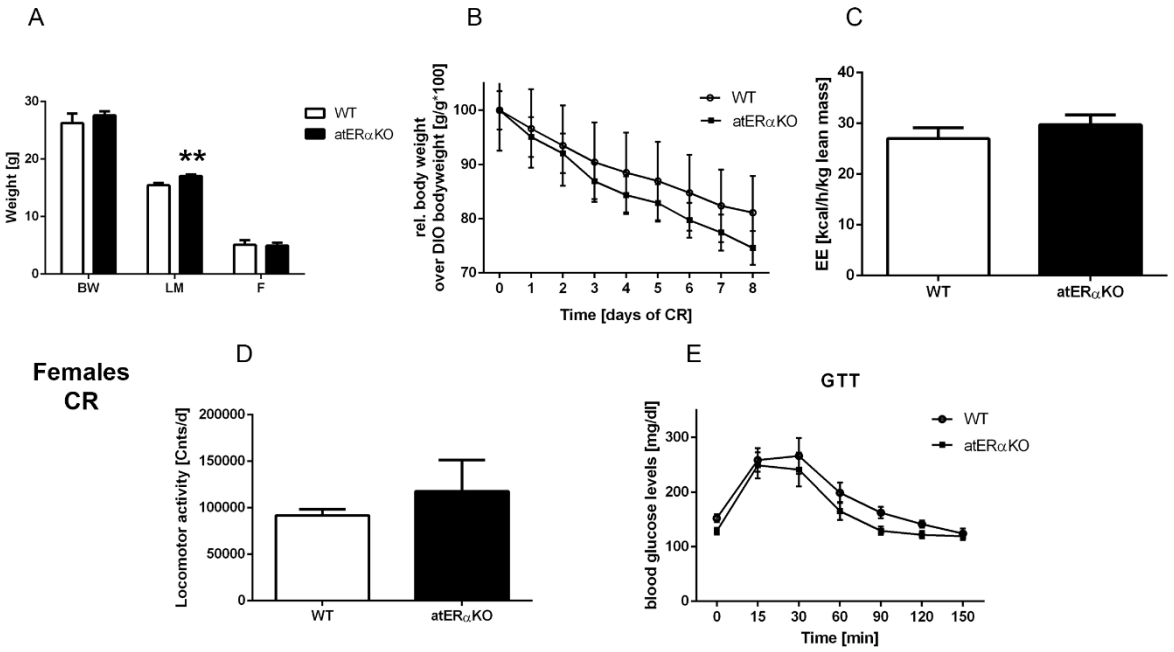

Figure 21: Metabolic characterization of caloric restricted (CR) female atERαKO mice

(A) Body composition of atERαKO and WT mice was measured by MRI. atERαKO females showed interestingly only an increased lean mass (LM). Fat mass (F) and whole body weight (BW) were unchanged between genotypes. **(B)** Relative body weight loss of female atERαKO and WT mice throughout CR. atERαKO showed surprisingly a slightly faster BW loss, reaching the targeted BW of 80% (of DIO body weight) already after 6 days of CR (WT reached the targeted BW after 8 days). Measurements of energy expenditure **(C)**, locomotor activity **(D)** and glucose tolerance test **(E)** did not elucidate other discrepancies between the genotypes. n=7-9; unpaired t-Test and Two-way-ANOVA with repeated measures with Bonferroni posthoc test. *P<0.05 vs. WT.

Reproductive phenotype of atERαKO

Besides being unfertile, already at the age of 6 weeks, atERαKO female mice displayed some reproductive tract abnormalities. As shown in the Fig. 22A, uteri were hyperplastic, fluid-filled and uterine walls seemed to be atrophic. Also ovaries were affected, looking hemorrhagic, pointing toward an overstimulation of follicles, which reach a mature stage (antral follicles) and fail to further develop due to lack of ovulation. Further microscopical analyses revealed morphological differences in the uterine structure of atERαKO mice, lacking of uterine glands and displaying flattened epithelial cells (Fig.22B). During HFD-feeding, some mice also showed abnormal accumulation of fat pads in the gonadal region. A similar phenotype was reported for central ERα-knock-out models (Xu et al., 2011).

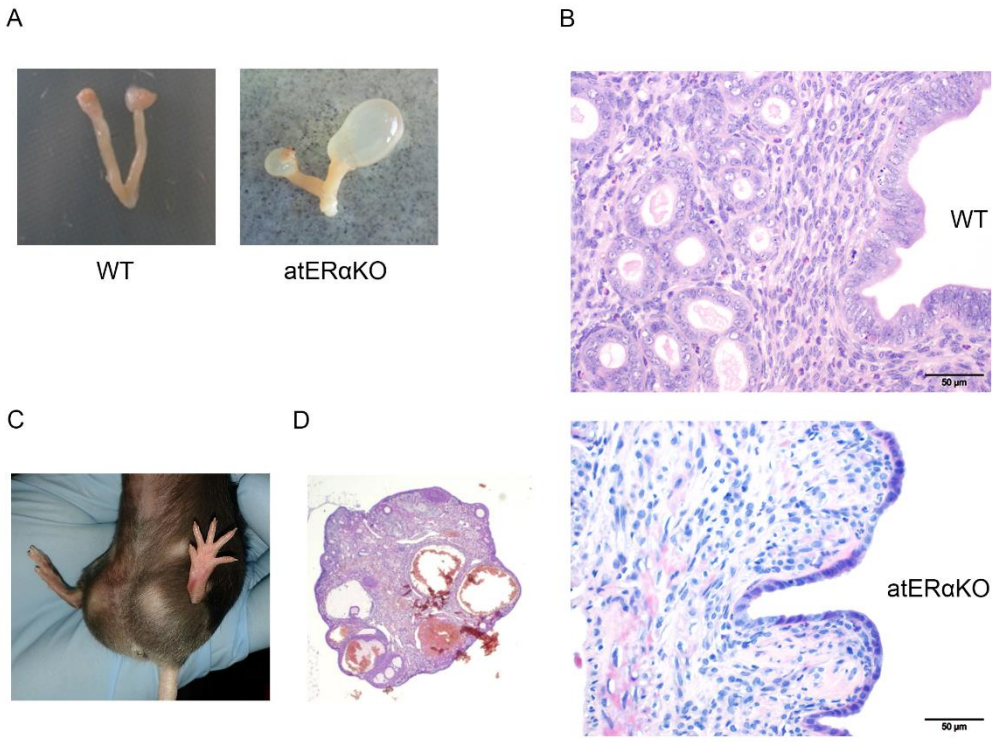

Figure 22: Reproductive phenotype of atERαKO female mice (CD) (published in Ban et al., 2017 *Sci Reports*)

(A) Picture of WT uterus compared to atERαKO uterus, which appears hyperplastic, massively fluid-filled and atrophic. **(B)** H&E staining of uteri of atERαKO, lacking in contrast to WT uteri of uterine glands and displaying flattened epithelial cells. **(C)** Gonadal region of atERαKO mice with accumulation of fat tissue. **(D)** Also ovaries were affected by abnormalities, containing many hemorrhagic antral follicles.

Depletion of ERα not selective for adipose tissue

As previously described, aP2-Cre mediated deletion of ERα occurred not only in adipose tissue, but also in the brain/hypothalamus. Analyses of ERα-expression on mRNA level in females, demonstrated a significant decrease of the gene expression in white adipose tissue and in the hypothalamus of atERαKO mice (Fig. 23A). As control tissue, uteri were additionally analyzed to skeletal muscle and liver as done for males.

As the regulation of hormone levels takes place in the hypothalamus (Beale et al., 2014), investigations of 17β-estradiol plasma levels (E2), revealed an impairment of the negative feedback-mechanism, by which the organism keeps hormone levels in physiological concentrations. In 6 weeks and 15 weeks old female atERαKO mice, as well as HFD-fed ones, E2 levels were markedly increased (Fig. 23B), confirming that

the hormonal homeostasis in these animals is affected by the (eventually partial) central knock-out of ERα.

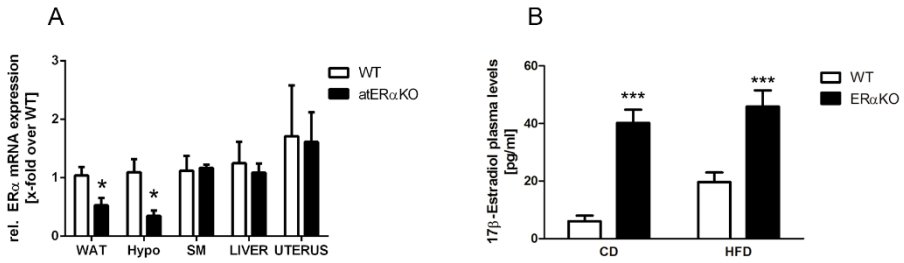

Figure 23: Ex-vivo characterization of the atERαKO model in females (B published in Ban et al., 2017 *Sci Reports*)

(A) ERα expression measurements of different tissues on mRNA level demonstrate an efficient depletion of ERα expression in white adipose tissue (WAT), but also in the hypothalamus (Hypo). Control tissues as skeletal muscle (SM), liver (LIVER) and uterus (UTERUS) were not affected by the knock-out. **(B)** 17β-estradiol levels analyzed in plasma of female mice, shows a highly increased hormone concentration of the estrogen in mutant mice, independently from the diet (CD=control diet; HFD= high-fat diet). n=5; unpaired t-Test; *P<0.05 and ***P<0.001 vs. WT.

In summary, the additional central *knock-out* of ERα in female mutant mice caused a disruption of the hormonal negative feedback, resulting in supraphysiological E2 plasma levels. Due to hormonal overstimulation of ERα-responsive tissues as the uterus, reproductive tract abnormalities could be identified in atERαKO female mice. The increase in BW and the lowered energy expenditure observed in the first cohort of atERαKO mice vanished in the second and third cohort independently from the administrated diet. The abrogated impact of the lack of ERα in those cohorts might be linked to elevated E2 levels after the onset of puberty.

5.2. High mortality due to uterine infections in female atERαKO mice during high-fat diet feeding

During the course of HFD-feeding, an alarming mortality rate for atERαKO mice on HFD could be observed in comparison to WT littermates but also compared to atERαKO fed a CD. Autopsies of these animals revealed severe inflammation processes taking place in the uteri, overwhelming also other organs and ending in a sepsis-like state. Pus-filled swelling of the uteri and microbiological analysis of the uterine fluid with the detection of commensal bacteria (like *E. coli* and *Enterococcus sp.*), pointed towards a severe bacterial infection. Approximately 1/3 of the HFD-fed atERαKO females, died or had to be prematurely sacrificed due to very severe illness. Pathological analyses of the other individuals revealed, that in all animals of

this group inflammation was ongoing, even if not in every case leading to visible illness.

Semi-quantitative analyses of the grade of inflammation demonstrated that indeed, HFD significantly increased the extent of the inflammation (Fig. 24C). Further investigations were done in histological sections of uteri, questioning the phenotype of the present immune cells involved in the inflammation process. Comparison of HFD-fed atERαKO versus CD-fed littermates demonstrated a huge difference in the number of neutrophils invading the lumen but also infiltrating through the uterine wall. Macrophages could be detected for a much lower content (Fig. 24D). WT animals were not appropriate as controls, as they did not show any inflammatory entity.

At this point, it was obvious, that the results from the investigations in HFD-fed atERαKO mice, could not lead to conclusions in regard to the influence of ERα on metabolism or body weight dynamics, as this group of mice was clearly not healthy and infectious diseases are a confounding factor in energy expenditure and balance.

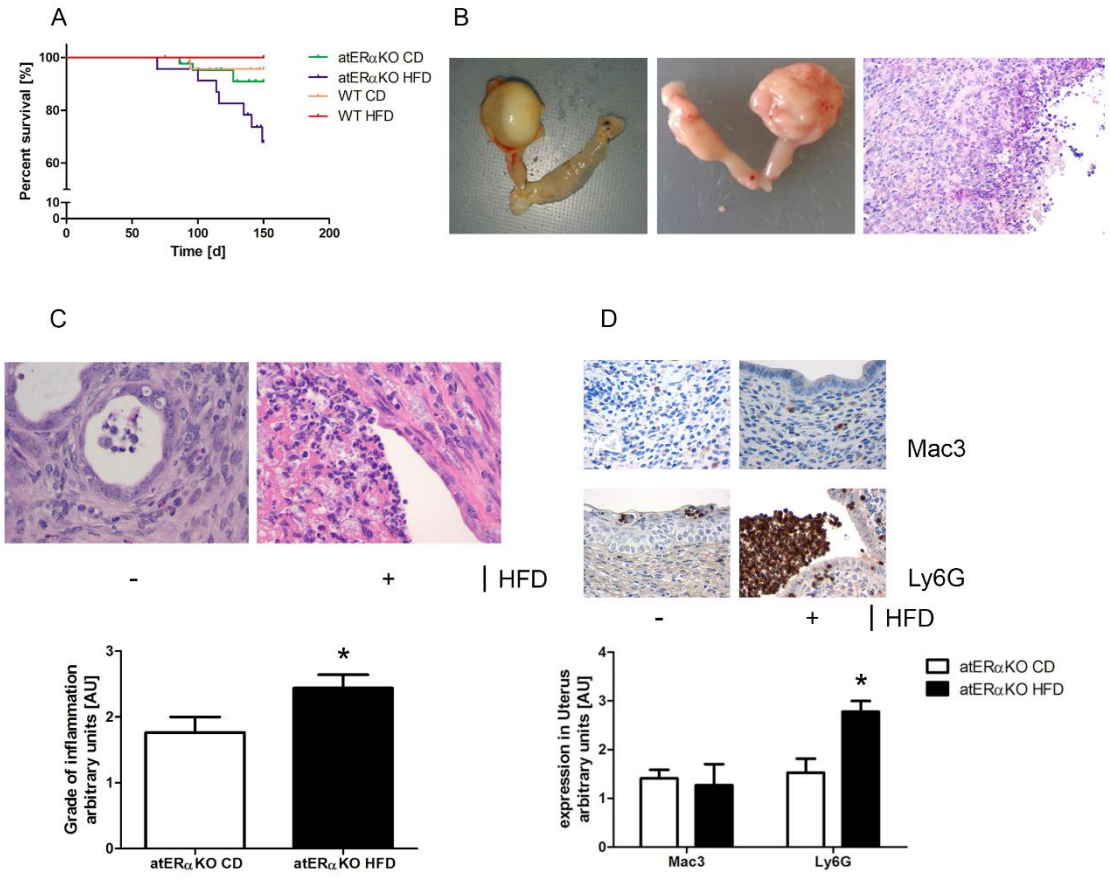

Figure 24: Severe bacterial infections of uterus of female atERαKO (published in Ban et al., 2017 *Sci Reports*)

(A) Survival curves of all 4 groups (WT and atERαKO, each fed CD or HFD) demonstrates high mortality rate in mutant mice fed a HFD. n= 17-23 **(B)** Pictures depicting macro- and microscopically inflammation taking place in uterus of atERαKO mice fed HFD. **(C)** Pathological analysis showing an aggravation of the severity of inflammatory process depending on the diet atERαKO mice were fed. **(D)** Mac3- (macrophage marker) and Ly6G- (neutrophil marker) staining elucidating the entity of immune cells involved in uterus inflammation, comparing CD-fed with HFD-fed atERαKO mice. n=9-17; unpaired t-Test or Two-way-ANOVA with Bonferroni posthoc-test; *P<0.05.

During the course of inflammatory processes, neutrophil granulocytes are recruited as potent mediators of host defense. Not only the recruitment, but also mechanisms organizing the resolution of inflammatory processes are crucial, in order to avoid damages of endogenous tissue. Neutrophil clearance is mainly orchestrated by neutrophils themselves and macrophages, more precisely by M2-macrophages (anti-inflammatory, alternatively activated) in a process called efferocytosis (Bratton and Henson, 2011). Therefore, damages of neutrophils- or macrophage signaling, might both affect the communication between these two cell types and lead to an impaired neutrophil clearance. To elucidate which cell population might be affected in our case, leading to an exaggeration of inflammation due to “simple ascending infections”, so called “Don´t eat me signals” of neutrophils were analyzed in the

uterine tissue of CD-fed atERαKO vs. HFD-fed atERαKO mice. These signals are proteins expressed on the cell membrane of neutrophils, in order to avoid depletion by M2-macrophages. Externalization of cytosolic phosphatidylserine (PS) would in contrary lead to phagocytosis and clearing of neutrophils (Bratton and Henson, 2011). Normalized to neutrophil content (expression of the neutrophil marker Ly6G was used as surrogate), no differences could be recorded in the expression of the "Don´t eat me-signals" PAI-1 and CD47 (Fig. 25A). On the other hand, measurement of the M1 marker iNOS (*Nos2*, inducible NO-synthase) and of Arginase1 (*Arg-1*,M2-marker) revealed a huge imbalance between those two macrophage subpopulations in HFD-fed atERαKO mice when compared to CD-fed ones. This finding pointed toward a repressive effect of the HFD in regard to M2-macrophages, causing indirectly an accumulation of neutrophils due to inefficient clearance.

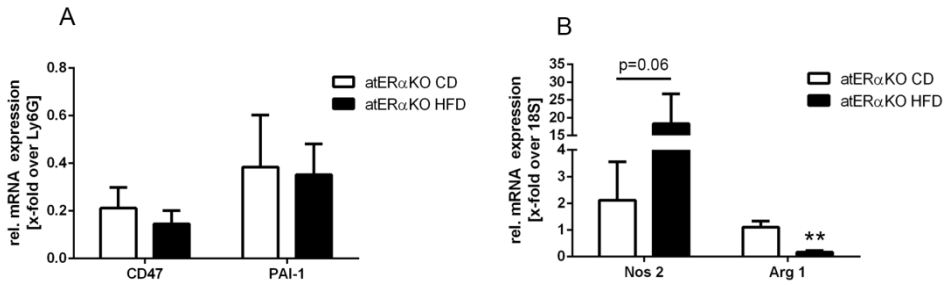

Figure 25: Immune cell markers in uteri of atERαKO mice (published in Ban et al., 2017 *Sci Reports*)

(A) Expression of "Don´t eat me signals" produced by neutrophils on mRNA level, measured in uteri of atERαKO mice fed HFD compared to mutant mice fed CD. Due to the difference of neutrophil content, expression was normalized to Ly6G-expression (neutrophil specific marker). **(B)** Discrepancies in expression of M1- (*Nos2*: inducible NO-synthase 2) and M2-marker (*Arg-1*: arginase 1) in HFD-fed group point towards a shift in macrophage polarization in the uteri of mutant mice due to HFD-feeding. n= 4-7; **P<0.01; unpaired t-test.

In conclusion, the high mortality rate of HFD-fed atERαKO female mice could be linked to severe inflammation of the uteri caused by infections with commensal bacteria as *E. coli. Ex-vivo* analyses of uterine tissues demonstrated that the inflammation is correlated with an accumulation of neutrophils likely damaging the host tissue. Simultaneously, a significant decrease in the presence of anti-inflammatory M2-macrophages could be observed.

5.3. High-fat diet induced effects on ERα signaling

As high E2 levels were registered in atERαKO in both diet-groups (see chapter 5.1.2) and as ERα is known to possess anti-inflammatory properties (Toniolo et al., 2015), the question rose up, whether HFD is able to influence ERα-signaling. A first hint was provided by the measurement of target genes in the E2-responsive-tissues spleen and uterus. As expected due to high systemic E2 levels, in CD-fed atERαKO female mice the target genes lactotransferrin (*Ltf*) in uterus and cathepsin D (*CTSD*) in the spleen, were significantly upregulated compared to control littermates. In the hypothalamus, the target gene *Wnt4* was not upregulated, as expected for an organ with decreased ERα-expression. The induction in uterus and spleen was interestingly abrogated, not reaching significance, in HFD-fed atERαKO mice, implicating an impairment of ERα-signaling due to HFD-feeding despite elevated E2-levels (Fig. 23B).

Therefore further investigations were needed to identify a potential mediator in the HFD, which is able to interfere in E2-ERα-signaling. For this purpose, lipid profiling of mouse plasma was performed to interrogate discrepancies in fatty acid composition between CD- and HFD-fed animals. Indeed, some fatty acid species were altered in HFD-treated atERαKO, among which C18:0 (stearic acid), C18:2n6 (linoleic acid), and C20:4n6 (arachidonic acid) were significantly upregulated, and only C18:1n9 (oleic acid) was downregulated (Fig.26B).

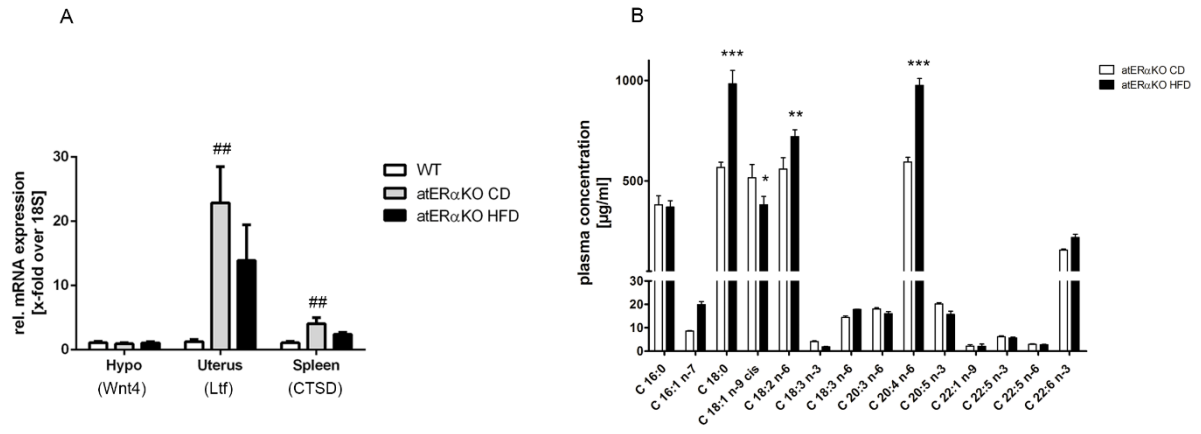

Figure 26: Ex-vivo analyses of atERαKO (published in Ban et al., 2017 *Sci Reports*)

(A) ERα target gene expression in hypothalamus (Hypo), uterus and spleen showing an induction of the respective genes (for each tissue measured gene is indicated below) in ERα- responsive tissues (uterus and spleen) for the atERαKo group fed CD. Increase of *Ltf*- and *CTSD*- expression in atERαKo group fed HFD didn´t reach statistical significance. n=5; ##P<0.01 vs. WT; One-way-ANOVA with Bonferroni posthoc test. **(B)** Lipid profiling of plasma of atERαKO female mice. Each sample was pooled out of three mice. n=3; *P<0.05; **P<0.01; ***P<0.001 vs. atERαKO CD. Two-way-ANOVA with Bonferroni posthoc test.

In summary, the HFD was observed to impact negatively the ERα-signaling and as well to influence the plasma lipid profile of atERαKO female mice.

5.4. Influence of stearic acid on macrophage polarization and function

Macrophage´s ability to polarize plays a crucial role during inflammation and wound healing processes, in order to overcome infections and at the same time reduce tissue damage and resolute inflammation. As mentioned before, M2 macrophages are indispensable for neutrophil clearance. As in atERαKO mice, M2-macrophage depletion was observed, the influence of C18:0 on macrophage polarization was investigated. Stearic acid was the most prominent fatty acid (FA) upregulated due to HFD in atERαKO animals. Furthermore, pro-inflammatory features on macrophages have been already described for this FA (Anderson et al., 2012).

C18:0 effects on polarization of THP-1 macrophages

To elucidate whether C18:0 is directly able to influence macrophage polarization, differentiated THP-1 cells were subjected to analyses of typical polarization markers on mRNA level. Expression of cluster of differentiation 206 (CD206; also known as mannose receptor C type 1 (MRC-1); M2-marker) and c-c chemokine receptor 7

(CCR7; M1-marker) were measured after stimulation with C18:0 ± LPS (mimicking a bacterial environment) on an E2-background. Indeed, C18:0 upregulated the expression of CCR7 to levels similar to LPS-stimulated samples and acted in a synergic manner when co-stimulated with LPS. Along this line, expression of CD206 was significantly and more powerfully downregulated by C18:0 than with LPS alone. Addition of LPS to C18:0 did not further lower the expression of CD206.

Analogously, another M2-marker (cluster of differentiation 209 (CD209)) was regulated in the same way by C18:0 as assessed by immunostaining and FACS-analyses (Fig. 27A+B+E). Staining of cluster of differentiation 11b (CD11b), an activation marker which is indispensable for cell adhesion and infiltration of macrophages, showed no significant regulation of this marker by C18:0 in FACS-analyses, but a slight tendency towards a repressive effect of C18:0 could be observed.

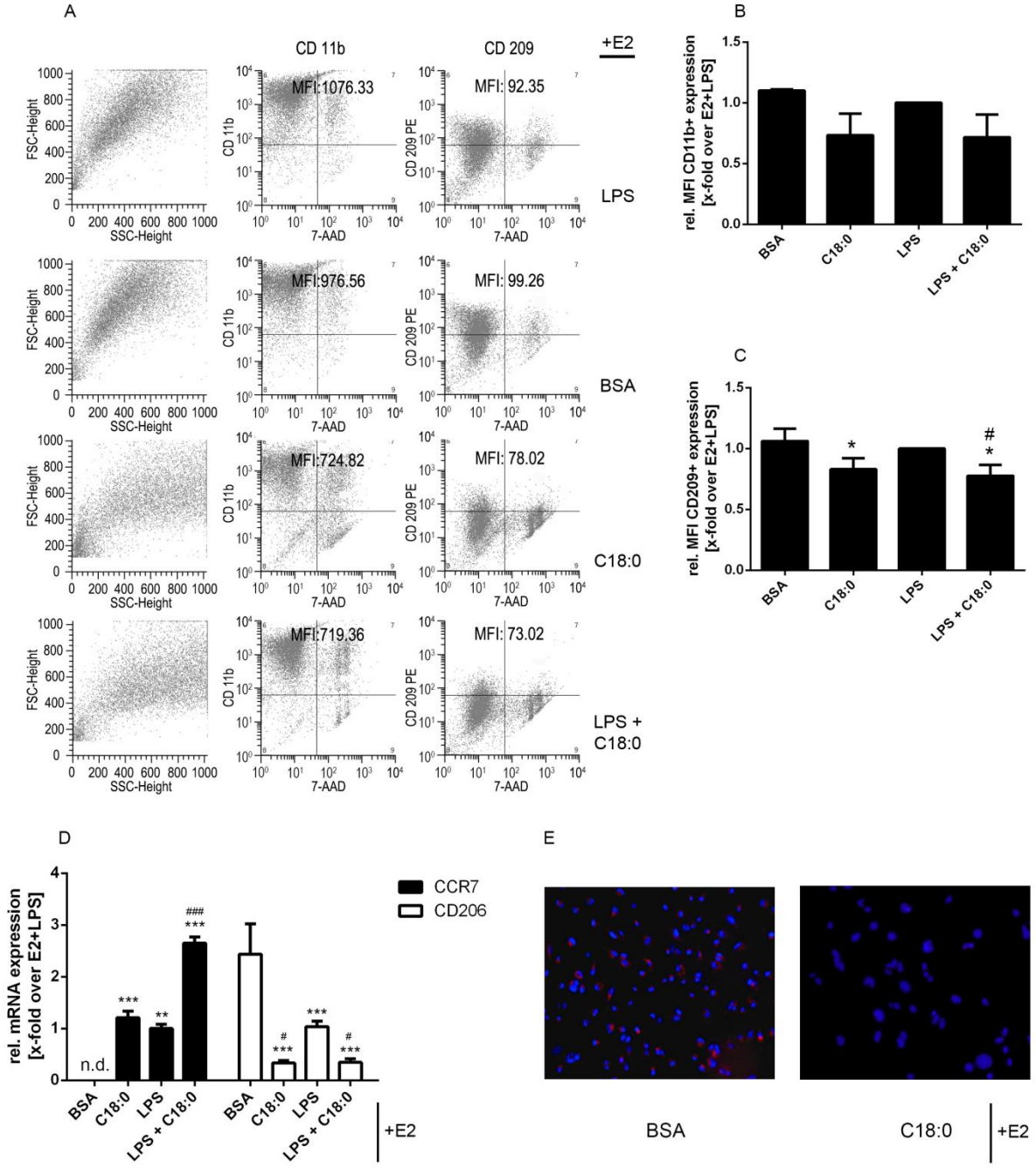

Figure 27: Effects of stearic acid on macrophage polarization in THP-1 cell model (published in Ban et al., 2017 *Sci Reports*)

(A) Representative FACS dot plots of THP-1 cells stimulated with estradiol (E2) and the fatty acid (C18:0) or control (BSA) with or without lipopolysaccharide of *E. coli* (LPS), mimicking a bacterial environment. First column of plots, represents FSC and SSC, while the second one depicts CD11b (activation marker) expression and the third one CD209 (M2-marker) expression. Absolute mean fluorescence intensity values (MFI) are calculated and displayed in the graphs. Relative MFI values normalized to the E2+LPS group are shown in **(B)** for CD11b and in **(C)** for CD209. **(D)** Expression of an M1-marker (CCR7) and of a M2-marker (CD206) were measured on mRNA level while the expression of another M2-marker (CD209) was assessed through immunostaining. Representative pictures are shown in **(E)**. Each experiment was repeated at least three times. **P<0.01, ***P<0.001 vs. E2+BSA; #P<0.05, ###P<0.001 vs. E2+LPS; One-way-ANOVA.

C18:0 effects on macrophage function in THP-1 cells

Even if CD11b was not significantly regulated by the FA, further investigations were needed to question the effects of C18:0 on the functionality of macrophages. Therefore, THP-1 macrophages were subjected to a test of their phagocytic activity. As Fig. 28 demonstrates, C18:0 treated cells were able to phagocyte fluorescent beads for a much lower extent than control-treated ones.

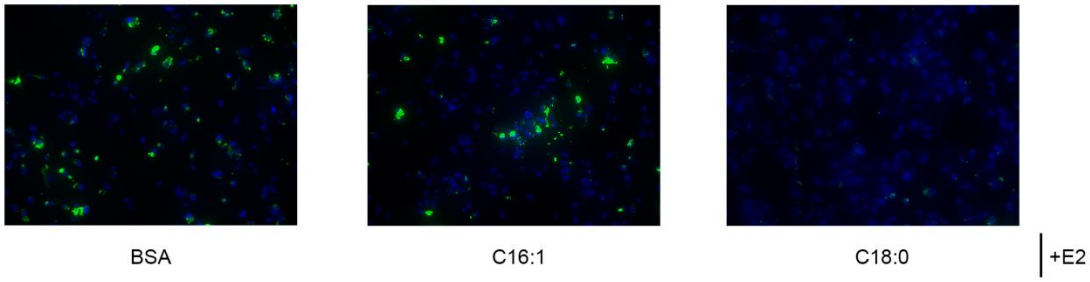

Figure 28: Phagocytosis assay in THP-1 cell model (published in Ban et al., 2017 *Sci Reports*)

Phagocytosis assay was performed to investigate effects of stearic acid on macrophage function, e.g. phagocytic ability. As additional control, to exclude physical interference of the FA with the beads, another FA, palmitoleic acid, was used (C16:1). Green fluorescence derives from internalized beads while nuclei of cells are stained with DAPI and are therefore blue. Representative pictures are depicted, chosen from three independent experiments with n=3.

In-vitro analyses with differentiated THP-1 cells, demonstrated that C18:0 induces pro-inflammatory effects in macrophages despite the presence of E2, which is rather known to induce M2-polarization. Furthermore the fatty acid impaired the phagocytic ability of THP-1 macrophages.

5.5. Stearic acid as a “non-classical” modulator of ERα

The observed impact of HFD on ERα-signaling and in parallel the negative influence of C18:0 on M2-polarization led to the question whether C18:0 is possibly the mediator of E2 repressive effects. Therefore, actions of the FA were investigated on the expression of a known ERα-target gene, which is (at least partly) involved in the E2 mediated M2-polarization: interleukin 4-receptor (IL-4r). The corresponding cytokine, interleukin 4 (IL-4) is one of the most potent anti-inflammatory triggers for macrophages (Zhu et al., 2015) and is used in cell culture as a mediator for M2-programming *in-vitro* (Vogel et al., 2014). In BMDM, C18:0 was able to repress the expression of IL-4-receptor despite E2 co-stimulation, as shown in Fig. 29A.

The finding that C18:0 is decreasing the expression of an ERα-target gene in macrophages, led to the next question, e.g. whether stearic acid is directly influencing the transcriptional activity of ERα. For this purpose, luciferase gene-reporter assay experiments were conducted in THP-1 macrophages, assessing the E2-induced transcriptional activity of ERα depending on the co-administration of C18:0. Indeed, as shown in Fig. 29B, the FA was able to highly repress transcriptional activity of ERα in macrophages.

Next, expression of ERα in dependence of C18:0 co-stimulation was assessed by WB, in order to question whether the FA might influence transcriptional activity through downregulation of the nuclear receptor. Analyses of 6, 12 and 24 hours of stimulation of BMDM revealed no regulation of ERα expression on protein levels (Fig. 29D). Though, 24h stimulation with stearic acid seemed to reduce overall protein expression in primary macrophages, pointing towards a higher susceptibility of this cell type in-vitro towards the FA.

As subjected in chapter 1.5.1, FAs are more than just nutrients supplying energy, but important modulators in cell function. For palmitic acid (C16:0), La Rosa and colleagues (La Rosa et al., 2012) already demonstrated the ability of FAs to bind to ERα and to modulate its transcriptional function by acylation at the residue C447. The mutation of this binding site resulted in the present study in attenuation of C18:0 mediated inhibition of transcriptional activity (Fig. 29C), demonstrating that this specific cysteine residue is at least one of the possible targets of the fatty acid. To assess whether C18:0 itself is able to bind to ERα, immunoprecipitation (IP) experiments were conducted in HeLa cells overexpressing ERα after co-stimulation of E2 and stearic acid versus E2 and BSA, as control. After the IP, protein-beads complexes were subjected to analysis by LC/MS in order to identify fatty acids possibly binding to the protein of interest. Indeed, few fatty acids could be found in the ERα-precipitates and were quantified. Mainly three FAs were present in considerable amount: palmitic acid (C16:0), oleic acid (C18:1n9) and linoleic acid (C18:2n6). Only C18:1n9 was significantly induced by C18:0 stimulation, suggesting desaturation of C18:0 after incorporation into the cells. Oleic acid is indeed the main metabolite of C18:0 and C18:0 was itself not detectable in the IPs.

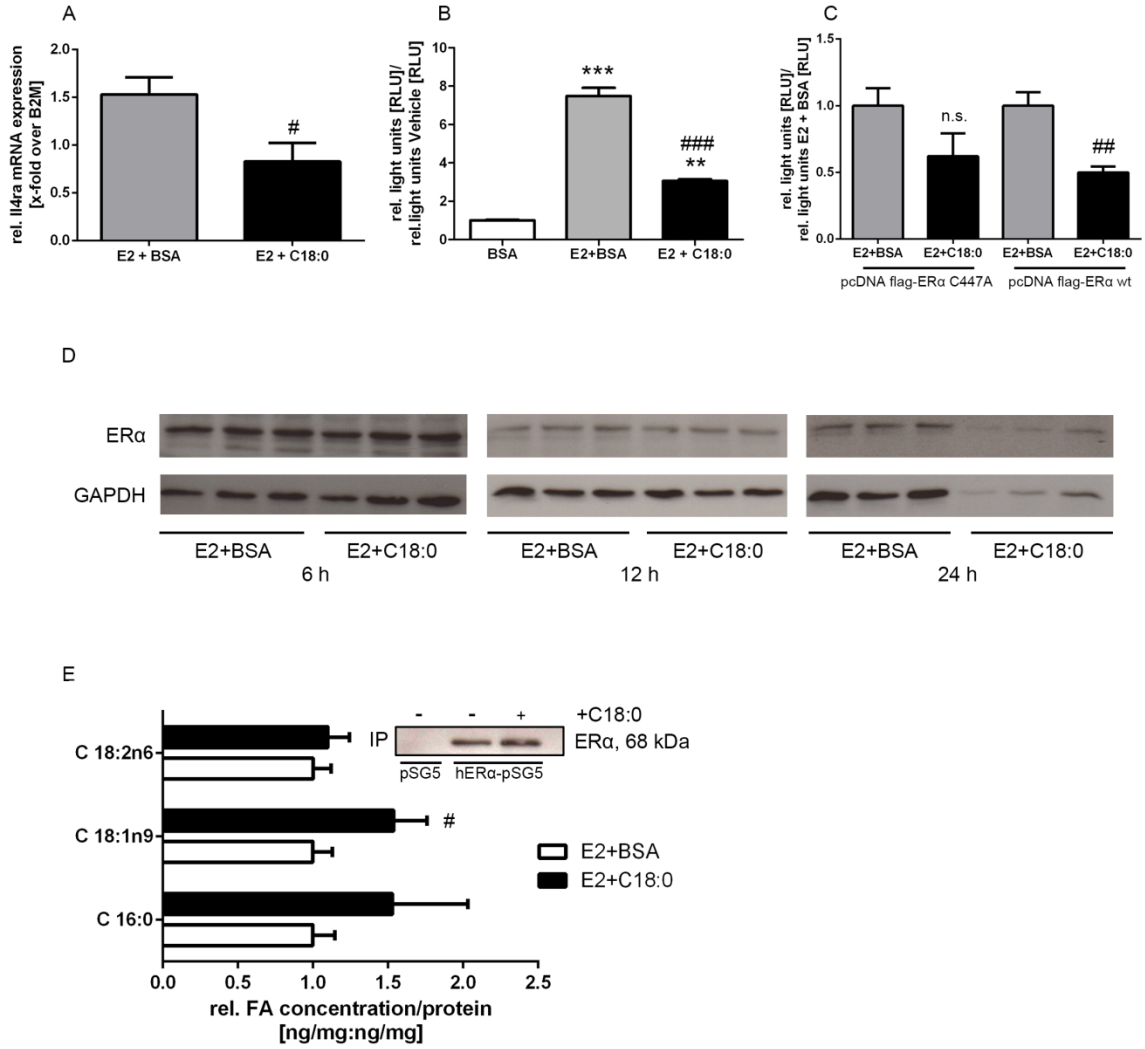

Figure 29: Effects of stearic acid on ERα-signaling (A-C and E published in Ban et al., 2017 *Sci Reports*)

(A) IL-4 receptor (target gene of ERα in macrophages) expression on mRNA level in bone marrow derived macrophages (BMDM) after stimulation with estradiol (E2) and BSA or C18:0 (n=7-9). **(B)** Luciferase gene reporter assay in THP-1 cells with wild-type ERα and **(C)** with mutant ERα (C447A-ERα), showing an inhibitory effect of C18:0 on ERE-activity and attenuation of this effect in cells transfected with mutant ERα (n=3-8). **(D)** ERα-expression analysis by Western Blot after co-stimulation with E2 and stearic acid (or BSA as control) in BMDM. Duration of stimulation is indicated below each blot. GAPDH was used as loading control. **(E)** Fatty acid analysis of protein precipitates by LC/MS assay after immunoprecipitation of ERα from HeLa cells (n=3). Inlay: control of immuno-precipitates by Western Blot. Experiments were repeated at least three times. n.s.= not significant vs. E2+BSA; ***P<0.001 vs. BSA; #P<0.05, ##P<0.01 and ###P<0.001 vs. E2+BSA (one-way-ANOVA or unpaired t-test).

In conclusion, these results point towards a previously unknown interaction between ERα and dietary fatty acids, modulating the transcriptional activity of this nuclear receptor and therefore influencing negatively macrophage function and immune

response. In the present multifactorial context, the proposed negative interference resulted likely in the exaggeration of uterine bacterial infections in atERαKO females.

6. Discussion

In the present study, we aimed to outline the impact of adipose tissue ERα on whole body metabolism and adipose tissue biology. However, the used ERα$^{flox/flox}$ /aP2-Cre$^{+/-}$ model lacked of specificity for adipose tissue. Most importantly, hypothalamic depletion of ERα induced high E2 levels due to the disruption of the negative feedback mechanism regulating circulating hormone levels. Notably, HFD-feeding in female atERαKO mice resulted in fatal bacterial infections of the uterus. Taking into account that severe infections limit the interpretation of metabolic data, we focused on the etiology of the inflammation process taking place in these animals. The current study demonstrates that HFD triggers and sustains inflammatory processes at predilection sites, disturbing the physiological mechanisms underlying resolution of inflammation. In the present investigation, exposure to HFD led to an exaggerated response to commensal bacteria and host tissue damage with markedly increased number of infiltrating neutrophils in female atERαKO mice. The abundant infiltration of neutrophils in the damaged uterine tissue was accompanied by depletion of anti-inflammatory macrophages (M2). Since HFD was the obvious trigger for inflammation, analysis of plasma fatty acid composition was performed. It revealed induction of few fatty acids in HFD-fed atERαKO mice when compared to CD-fed controls. Among these, stearic acid was significantly elevated by HFD-consumption. Additional analyses in differentiated THP-1 cells evidenced the involvement of stearic acid in the depletion of anti-inflammatory M2 macrophage. Despite high E2 concentration, which promotes anti-inflammatory features in macrophages, stearic acid inhibited *in-vitro* polarization towards the M2 phenotype. Further experiments outlined a previously unknown interaction between stearic acid and ERα. This study demonstrates that stearic acid is able to inhibit estrogen receptor alpha transcriptional activity in macrophages. Finally, a novel mechanism, likely involving the acylation of ERα by the main metabolite of stearic acid (oleic acid) is proposed.

Estrogen receptor alpha and adipose tissue biology

ERα impacts adipose tissue biology and whole body metabolism (Heine et al., 2000; Hevener et al., 2015). In previous studies partly conducted by our group, it has been demonstrated that BW regulation is affected by sexual dimorphism. In a rodent

model, Benz et al accurately investigated differences between male and female WT mice in an analogous feeding protocol as done in this study (Benz et al., 2012). It has been shown that due to caloric restriction, female mice are prone to lose weight in a faster and more effective fashion. This trend was sustained by higher lipolytic activity of female adipose tissue, as assessed in an *ex-vivo* lipolysis assay. The hypothesis of ERα being involved in increased fatty acid utilization was corroborated by the attenuation of lipolytic activity in global ERα knock-out mice (Benz et al., 2012). Females presented lower RER values and the induction of the expression of the lipases HSL and ATGL could be correlated to ERα action. However, these results needed to be confirmed in an adipose tissue-specific model in order to outline peripheral effects of ERα *in-vivo*. Therefore, the aP2-Cre mediated ERαKO model was chosen and generated as an adipose tissue-specific mouse model.

The aP2-Cre and other Cre-lines mediated knock-out models

In the present study, we investigated the aP2-Cre$^{+/-}$/ ERα model, whereas the group of D. Clegg chose previously a similar approach characterizing ERα deletion in adipocytes mediated by an adiponectin promoter driven-Cre (Davis et al., 2013). Davis and colleagues demonstrated that lack of ERα in adipose tissue leads in males to increased adipocyte size, local fibrosis and inflammation (Davis et al., 2013). On the other hand, females displayed increased BW (differences arising after 12 weeks of age), enlargement of adipocyte size and visceral fat accumulation (Davis et al., 2013). Moreover, selective deletion of adipocyte ERα in those animals resulted in altered whole body glucose metabolism, i.e. glucose intolerance (Davis et al., 2013). Interestingly, this effect characterized only male mice, suggesting that females might be protected through compensatory mechanisms or simply due to higher E2 levels. Conversely to our investigations, the experiments of this study were conducted only under normal feeding conditions. However, the major difference between the study designs was the utilized Cre-line to generate the knock-out model. The first and mostly used adipose-specific Cre-line is the aP2-Cre. The majority of the studies were conducted in two different strains, one generated in the lab of Evans (aP2^{Salk}) and one from Kahn´s lab (aP2^{Bl}) (Kang et al., 2014). They present discrepancies in gene deletion efficiency and tissue selectivity, as demonstrated by Jeffery and colleagues (Jeffery et al., 2014). While the recombination in the animals generated in

the Evans lab addresses 50-80% of white adipocytes and similar percentage of brown adipocytes, the aP2^{Bl} –Cre line affects mainly brown adipocytes and adipose tissue endothelial cells (Jeffery et al., 2014). One of the main concerns about both lines is the lack of specificity, demonstrated by the expression of Cre-recombinase in non-adipose tissues as brain and to negligible extent in skeletal muscle, liver and heart (Lee et al., 2013; Mullican et al., 2013). Moreover, other studies identified the expression of aP2 in lymphatic tissue/ macrophages (Ferrell et al., 2008; Fu et al., 2002; Makowski et al., 2001) elucidating the possible affection of macrophages, which are pivotal regulators of adipose tissue homeostasis. However, a depletion of the targeted gene in macrophages of aP2-Cre^{Salk} line has not been confirmed (Mayoral et al., 2015). Davis et al. investigated the impact of an adiponectin (Adipoq)-Cre mediated ERα deletion. Compared to aP2-Cre lines, Adipoq-Cre models have been described as highly specific for adipocytes (Lee et al., 2013; Mullican et al., 2013). However, late onset of recombination restricts the evaluation of the relevance of the targeted gene during adipogenesis. *In-vitro*, adiponectin expression is induced only on Day 4 of adipocyte differentiation (Kang et al., 2014). On the other hand, moderate recombination, i.e. only 50% reduction of ERα expression in isolated mature adipocytes (Davis et al., 2013) and loss of efficiency throughout the breeding of these animals (D. Clegg, personal communications) are additional limitations of the Adipoq-Cre line generated by the lab of P. Scherer. Variations in efficiency of recombination depend not only on the copy number and the location of the gene encoding the Cre, but also on the location of the floxed alleles and the distance in between them (Kang et al., 2014). In our case, utilizing the aP2-Cre ^{Salk} line and the ERα floxed mouse generated by the Gustafsson lab (Antonson et al., 2012), we obtained a robust deletion of the targeted gene in adipose tissue. However, measurement of ERα gene expression was assessed in whole adipose tissue rather than in isolated mature adipocytes as done in the study of Davis and colleagues (Davis et al., 2013). In our model, skeletal muscle and liver were not affected, while a significant reduction of ERα expression was assessed in the hypothalamus.

Alternative Cre-lines have been developed, in order to manipulate temporally the onset of the knock-out. In some cases, as for aP2-driven Hdac3 or Dicer knock-out, the targeted gene is essential for the development of the organism and deletion of this gene caused unexpected lethality (Kang et al., 2014). To circumvent developmental issues in such models, investigators developed inducible Cre-lines, in

order to control the temporal onset of recombination. However, inducible Cre-lines available for adipose tissue require the application of tamoxifen. Besides the lower efficiency of the available tamoxifen-inducible Cre-line aP2-CreERT (Lee et al., 2013), the exposure of exogenous estrogens are inconvenient in studies on ERα or ERβ action. Further novel models are the resistin (Retn)-driven recombination developed in the lab of M. Lazar and the Pdgfrα-mediated Cre line. Similarly to aP2-Cre lines, the Retn-Cre was shown to cause targeted deletion also in the brain (Wintermantel et al., 2006), while Pdgfrα is more suitable for deletion in adipocyte precursor cells (Jeffery et al., 2014). Another Adipoq-Cre line was generated by the Rosen lab (Adipoq-Cre^{R}). In this context, it is worth to mention, that these mice are bacterial artificial chromosome (BAC) transgenic and that passenger genes present on BAC might influence the mouse´s phenotype (Eguchi et al., 2011; Kang et al., 2014). In conclusion, all available strategies for targeted deletion or ERα in adipocytes *in-vivo* have confounders that have to be taken into account.

Induction of BW gain and less efficiency of caloric restriction in male atERαKO

In line with investigations done by the group of D. Clegg, male atERαKO fed a chow diet displayed similar BW as their control littermates. Davis and colleagues showed that altered body weight affected only female mutant mice lacking ERα in adipose tissue (Davis et al., 2013). On the other hand, in the publication by Xu et al, deletion of ERα in POMC neurons and in the VMH regions, does not lead to increased BW, conversely to whole CNS knock-out, mediated by the Nestin-Cre (Xu et al., 2011). Male ERα$^{flox/flox}$/Nestin-Cre mice were heavier compared to their control littermates already at the age of 6 weeks. These findings suggest that in males, other regions than the VMH and the arcuate nucleus might be responsible for the phenotype observed in the Nestin-Cre driven deletion of ERα. Notably, this leads to the assumption, that the aP2-Cre mediated deletion of ERα in the CNS could affect the VMH and/or the ARC without resulting in increased BW while CD feeding. In our study, differences in terms of BW but not body composition were induced in atERαKO by HFD-feeding. Interestingly, mutant mice gained not only more fat, but also lean mass. During caloric restriction (CR), atERαKO male mice lost weight less rapidly than WT controls and CR was not as effective in mutant mice in terms of losing the excessive fat, mice accumulated previously during HFD-feeding. In

previous studies done by our group, ERα was demonstrated to be critical for the lipolytic activity of adipose tissue and was correlated to higher expression of adipose triglyceride lipase (ATGL) (Benz et al., 2012). However, these findings were restricted to females, emphasizing sexual dimorphism in regard to lipolysis (Benz et al., 2012). Additionally, the described effects in male atERαKO mice, might be the result either of the deletion of ERα in adipose tissue and in regulatory brain regions responsible for energy homeostasis. To investigate the origin of modulation through ERα, a different and more specific model should be chosen. A proof of concept would be the exposure of ERα$^{flox/flox}$/Adipoq-Cre, used in the study of Davis and colleagues, and of other brain-specific ERα knock-out models to the same feeding protocol, as done for atERαKO mice. However, deletion of ERα in the VMH can be probably excluded, as SF-1 Cre mediated deletion of ERα in HFD-fed male mice did not result in increased body weight (Xu et al., 2011). In summary, it appears difficult to discriminate the origin of the metabolic changes observed in male HFD-fed atERαKO. However, the impaired ability of the mutant mice to downsize their body fat during caloric restriction underlines a pivotal role of ERα in lipolysis. This confirms our initial hypothesis and is in line with the observations made in female mice in previous studies by our group (Benz et al., 2012).

Reproductive phenotype due to high E2 levels in atERαKO female mice

As previously described by Antonson and colleagues, female atERαKO mice are characterized by elevated circulating E2 levels and by reproductive abnormalities as grossly fluid-filled uteri, atrophic uterine wall, absence of uterine glandular structures and over-stimulated ovaries (Antonson et al., 2014). Furthermore histology of the ovaries of the mutant mice, showed several antral follicles, while no corpora lutea could be observed (Antonson et al., 2014). Taken together, it becomes obvious, that these animals were infertile and displayed an acyclic or arrested estrous cycle. In accordance to different brain-specific ERα knock-out models, which presented elevated circulating E2 levels and reproductive abnormalities as well (Wintermantel et al., 2006), the negative feedback mechanism regulating E2 plasma concentrations seemed to be affected in atERαKO mice. The reproductive phenotype was similar to the abnormalities observed in the neuron-specific deletion of ERα, mediated by the CamKIIa-Cre (Wintermantel et al., 2006). Analogously to the animals with POMC

neuron-specific deletion of ERα, simultaneous knock-out of ERα and elevated E2 levels, create a model which is difficult to interpret (Xu et al., 2011). In those investigations for example, higher estrogen plasma concentrations act on other central regions, likely impacting positively energy expenditure and sympathetic outflow (Xu et al., 2011). For those cases, adjustment of the E2 levels of the control littermates could be an attempt to eliminate the confounder of diverging estrogen levels. However, not only the additional ERα depletion in the hypothalamus and elevated E2 levels, but also the high mortality observed in HFD-fed female atERαKO mice, are major limitations of interpreting our metabolic data. The initial assessment of the metabolic phenotype of mutant female mice at the age of 6 weeks, demonstrated increased BW and a reduction in energy expenditure. Surprisingly, the discrepancies between the genotypes were not caused by higher fat mass, but rather by increased lean mass of the mutants. However, these differences vanished with the onset of puberty, likely due to elevated estrogen plasma levels. High E2 concentrations might have masked the expected effects caused by depletion of ERα in an adipose tissue-specific knock-out. This might be the reason for the discrepancies between the present study and the investigations performed by Davis and colleagues (Davis et al., 2013). Again, the difficulties of interpreting the metabolic data in female atERαKO mice are linked to the lack of specificity of the utilized model. High E2 levels might compensate the depletion of ERα expression and surely overstimulate organs non-affected by the knock-out. This creates a complex model of partial ERα depletion and simultaneous high E2 action.

HFD induces lethal phenotype in female atERαKO

The current study, however, reports for the first time high mortality in an ERα knock-out model exposed to HFD. Approximately one third of female atERαKO mice died prematurely or had to be euthanized following severe bacterial infections in the uterine tract. Mice lacking hypothalamic ERα (Wintermantel et al., 2006; Xu et al., 2011), or only in POMC (Xu et al., 2011) neurons have been shown to have an interrupted negative feedback mechanism, which induces the production of gonadotropin hormones and enhances the estrogen production in the ovaries. Unfortunately, in the current study it was not possible to measure luteinizing hormone (LH) and follicle stimulating hormone (FSH) plasma levels, as the assessment of E2

concentration required the majority of the obtained plasma from sacrificed mice. Conventional ELISA methods for measurement of those hormones require at least 50-100 µl plasma or serum. However, disruption of hypothalamic ERα signaling resulted in elevated E2 levels, which clearly affected uterine development and the ovaries (Wintermantel et al., 2006). Importantly, in none of the reported models, severe infections have been reported. Antonson et al, utilizing the same animal model as done in the present study, observed analogously reproductive abnormalities, but no remarkable infections (Antonson et al., 2014). The obvious difference between the two studies is the exposure of female atERαKO to HFD-feeding. HFD has been often linked to adipose tissue inflammation (Masoodi et al., 2015; Weisberg et al., 2003) and increased circulating inflammation markers as TNFα or IL6 (Kratz et al., 2014). However, several models have been exposed to HFD to induce obesity and, for our knowledge, none of these models displayed similar complications following high dietary fat consumption. The fact that atERαKO mice fed a HFD developed the same type of bacterial infection points toward a clear predilection site: the uterus. Anatomical abnormalities in the reproductive tract were observed in those mice already during CD-feeding. Female atERαKO displayed loss of glandular structures, atrophy of the vaginal muscular layer, grossly enlarged uteri, filled with watery fluid. Antonson et al demonstrated that the vaginal opening of these animals presented abnormal accumulation of squamous cornified epithelial cells (Antonson et al., 2014). They suggested that obstruction due to exaggerated keratosis might be the reason for the development of hydrometra. However, accumulation of cornified epithelial cells is not exclusive to atERαKO females and, in normal cycling mice, does not lead to the observed changes (Antonson et al., 2014). Thus, the etiology of the described reproductive phenotype remains unclarified and one can speculate that it might result from the overstimulation of the uterus by elevated E2 levels. Additionally, altered progesterone (P4) levels might have contributed to the changes seen in the uteri of atERαKO female mice. High P4 plasma concentrations have been shown in rodents to cause thinning of the vaginal epithelial layer (Marx et al., 1996) as observed in our model. However, it might be suggested, that the changes in vaginal opening and mostly the hydrometra, created a convenient environment for commensal bacteria. Furthermore, it has been demonstrated, that alterations in the hormonal levels influence the susceptibility of the female reproductive tract to infections. Immune cells present in the female

reproductive tract are challenged by keeping a balance between efficient protection from pathogens and maintenance of a milieu allowing successful implantation and pregnancy (Wira et al., 2015). Thus it is not surprising that depending on the menstrual cycle and E2 and P4 levels, the immune system is modulated in order to create optimal conditions for fertilization. Notably, these conditions are correlated to higher vulnerability to infectious diseases (Wira et al., 2015). In this context, *in-vitro* studies showed that E2 inhibits the expression of the “pattern of recognition receptors” toll-like receptor (TLR) 4 in uterine fibroblasts and TLR2 and TLR6 in vaginal epithelial cells (Wagner and Johnson, 2012). Furthermore, E2 impacts and limits the secretion of macrophage migration inhibitory factor (MIF), IL6, IL8 and TNF (Fahey et al., 2008; Schaefer et al., 2005). As mechanism responsible for some of these effects, it has been demonstrated that E2 antagonizes nuclear factor 'kappa-light-chain-enhancer' of activated B-cells (NFκB). E2 regulates the translocation of the pro-inflammatory transcription factor into the nucleus and prevents the degradation of associated proteins, keeping NFκB in the inactive form (NFκB inhibitors) (Ghisletti et al., 2005; Murphy et al., 2010). Importantly, the described anti-inflammatory features of E2 suggest that high E2 levels are linked to higher pathogen tolerance which might facilitate infections. Thus, high E2 levels in atERαKO females might cause higher susceptibility to commensal bacterial infections not only due to anatomical changes, but also disabling proper recognition by the epithelial barrier. Moreover, it is known that sex hormones physiologically modulate the presence of different immune cell populations within the uterus (Wira et al., 2015). The most abundant subset of immune cells present in the female reproductive tract are T cells (CD3+), followed by macrophages (CD68+), granulocytes (CD66+) and natural killer cells (NK cells). For macrophages it is known that they increase in number during menstruation and after a decline at the end of menstruation stay stable throughout the proliferative phase (Berbic et al., 2009). Conversely, NK cells are most abundant during the secretory phase (King and Critchley, 2010). Interestingly, in atERαKO female uteri CD3+ cells where barely present. Additionally to the limitation in terms of animal tissue, the unexpected onset of severe infections did not allow the establishment of an alternative method to immunostaining in order to further characterize the phenotype of immune cells present in the uteri. An approach by FACS analysis would have been helpful to investigate eventual differences in immune cell distribution between CD- and HFD-fed atERαKO uteri. Importantly,

immunostaining allowed the identification of a striking increase in neutrophil granulocytes (Ly6G+) in HFD-fed mutant mice. In summary, altered levels of sexual hormones, especially E2, seemed to impact the uterine epithelial barrier and immune defense of atERαKO, facilitating the survival of commensal bacteria in the uterus. However, some components of the HFD clearly triggered the development of the observed infections leading to exaggeration of the inflammatory processes.

Uterine infections characterized by lack of M2 macrophages

Usually, infections with commensal bacteria, as *E. coli* and *Enterococcus sp*., as recognized in the uterine tissue of these animals, do not represent huge challenges for the immune system. As discussed above, hormonal changes and anatomical abnormalities in atERαKO rendered the uteri of these animals a predilection site for infections. Interestingly, infected uterine tissue of HFD-fed atERαKO mice was characterized by massive neutrophil transmural infiltration, damaging the epithelial barrier. As already discussed, the clearance of neutrophils among resolution of the inflammatory process, is linked to mechanisms orchestrated by neutrophils themselves and anti-inflammatory macrophages. Thus, the lack of M2 macrophages in infected tissue pointed toward a disturbed recruitment of and/or communication with macrophages. Defects in neutrophil clearance have been previously linked to severe inflammatory diseases including sepsis, auto-immune diseases cardiovascular disorders and cancer (McCracken and Allen, 2014). More specifically, impaired neutrophil clearance can result in secondary infections, due to damages of host tissue structures (Amulic et al., 2012; Fullerton et al., 2013). In this study, both M1/M2 ratio and neutrophil signals inhibiting efferocytosis were assessed based on the mRNA expression of typical markers in the uterine tissue. A further approach leading to more precise results would have been the isolation of those immune cell populations by FACS sorting and assessment of the marker expression on protein levels/ mean fluorescence intensity (FACS). Again, limited time for the establishment of the assay and limited tissue availability were technical obstacles. As alternative, *in-vitro* co-cultures would have been valuable experiments to investigate interactions between macrophages and neutrophils. Protocols for the isolation of neutrophils from blood have been established for both human and mouse samples (Boxio et al., 2004). However, extraction from mouse blood delivers low quantity, due to limited

blood volume and to lower percentage of neutrophils in mouse when compared to human blood (30% versus 70% of total leukocytes) (Amulic et al., 2012). Moreover, a further technical limitation is provided by the short life of isolated neutrophils *in-vivo* and in culture (Amulic et al., 2012; Boxio et al., 2004). Importantly, mRNA analyses of relevant markers, displayed imbalance of M1/M2 polarized macrophages, rather than upregulation of “don´t eat me signals” leading to inhibition of efferocytosis. Therefore, the focus in the next experiments was laid on the mechanism influencing macrophage polarization. Notably, several studies demonstrated that ERα promotes M2 polarization (Ribas et al., 2011; Toniolo et al., 2015). The possible depletion of macrophage ERα due to the utilization of the aP2-Cre line (Mao et al., 2009; Urs et al., 2006) might be a plausible reason for the observed shift to M1 polarization. However, the aP2-Cre line used in the present study was demonstrated by Mayoral and colleagues to not affect macrophage expression of the targeted gene (Mayoral et al., 2015). The direct proof by measurement of ERα in isolated macrophages, or alternatively in bone marrow-derived macrophages (BMDM), was not possible. The isolation protocol for BMDMs was established at the end of the *in-vivo* experiments and the animal breeding had to be terminated due to regulations on severe phenotypes (in accordance to regulation imposed by LaGeSo, Berlin). Moreover, in atERαKO female mice cathepsin D (CTSD), which is highly expressed in macrophages and an ERα target gene, was significantly upregulated in the spleen when compared to WT. This result corroborates the recent finding of Mayoral et al. and renders the depletion of ERα in macrophages unlikely. Notably, measurement of the expression of target genes in ERα responsive tissues pointed towards an impairment of ERα signaling in HFD-fed atERαKO mice. Despite analogously high circulating E2 levels as in the CD-fed cohort, the expression of those target genes was not significantly upregulated when compared to WT, as observed in CD-fed atERαKO. In order to outline the differences between the diets and possible pathogenic mediators of HFD-feeding, analysis of the fatty acid plasma composition of female atERαKO mice was performed. Two polyunsaturated FAs (linoleic and arachidonic acid) and only the saturated FA stearic acid were upregulated. Investigations regarding the impact of the identified FAs were conducted only for stearic acid. Stearic acid was demonstrated in previous studies to inhibit E2 action by downregulating ERα expression in the hypothalamus (Morselli et al., 2014). Furthermore, pro-inflammatory effects on macrophages have been observed by the

treatment with stearic acid (Anderson et al., 2012; Shi et al., 2006). Stearic acid was shown to upregulate IL6 expression in RAW264.7 macrophage cell line and to induce endoplasmic reticulum stress (Anderson et al., 2012). Saturated fatty acids have been demonstrated to induce inflammation through mimicking the effects of the endotoxin LPS, stimulating TLR2 and TLR4 (Fritsche, 2015), while polyunsaturated FAs suppress the pro-inflammatory actions of saturated FAs (Liu et al., 2013). However, further controls, as mixture of different FAs as done in the study by Foryst-Ludwig and colleagues (Foryst-Ludwig et al., 2015) and the examination of the two other upregulated FAs in regard to macrophage polarization, would have provided further evidence of the specificity of the effects of stearic acid in the studied model.

Stearic acid inhibits M2 polarization of macrophages despite high E2

atERαKO mice presented high E2 levels. Despite anti-inflammatory action of ERα on macrophages, polarization towards an anti-inflammatory phenotype was ablated in HFD-fed mice. The identification of stearic acid as the mostly upregulated FA following HFD-feeding, led to the hypothesis that stearic acid might interfere with ERα-signaling. Therefore, experiments were carried out to investigate stearic acid´s repressive action on ERα. In this context, the group of D. Clegg demonstrated that stearic acid downregulates ERα expression in hypothalamic tissues (Morselli et al., 2014). However, measurement of ERα protein levels in BMDMs did not confirm the findings made in CNS regions, suggesting that the FA-mediated inhibition of ERα-action relies on a different mechanism. Experiments performed in differentiated THP-1 cells, as a more robust model for macrophages than BMDMs, underlined the pro-inflammatory priming through C18:0. mRNA analysis of M1 and M2 markers, as c-c chemokine receptor 7 (CCR7, M1 marker) (Lee et al., 2009) and mannose receptor C type 1 (MRC1/CD206, M2 marker) (Stout and Suttles, 2004) demonstrated suppression of the M2 phenotype and simultaneous induction of the M1 marker. This finding was supported by additional immunostaining experiments analyzing the expression of a second M2 marker, cluster of differentiation 209 (CD209/ DC-SIGN) (Mercalli et al., 2013). Unfortunately, for both immunostaining and FACS analysis the quality of the antibody for CCR7 and CD206 was not sufficient to perform the analysis under the desired conditions. However, CD209 staining and FACS analysis confirmed the previous findings in terms of mRNA

expression patterns. Moreover, assessment of the phagocytosis ability of macrophages indicated impaired internalization of fluorescent particles by macrophages treated with stearic acid. In line with the study of Ribas and colleagues, demonstrating decreased ability of phagocytosis of myeloid cells lacking ERα (Ribas et al., 2011), this finding corroborates the hypothesis that C18:0 might interrupt E2-ERα-signaling. Furthermore, stearic acid exposure was observed to downregulate the expression of IL4-receptor, which is required for M2-induction. IL4 is one of the most prominent stimuli that induce M2 reprogramming (Stout and Suttles, 2004). ERα activation in macrophages is known to induce the expression of IL4 receptor (IL4r) (Ribas et al., 2011), priming the cell for anti-inflammatory signals. Despite E2 co-administration, differentiated BMDMs significantly downregulated IL4r mRNA expression due to stearic acid. This finding was in line with the assumption that stearic acid is able to interfere with ERα-signaling. The direct analysis of the impact of stearic acid on ERα transcriptional activity revealed a previously unknown interaction between the fatty acid and nuclear hormone action.

Modulation of ERα through stearic acid by esterification

To elucidate the mechanism underlying the modulation of ERα by stearic acid, immunoprecipitation of ERα was performed after stimulation with the FA and E2. After isolation of the targeted protein, a HPLC/MS approach was used to identify and quantify fatty acid(s) in the protein lysate. Notably, few fatty acids were found to bind to the receptor. Among them, only oleic acid was significantly induced by the treatment of stearic acid. Recently, an inverted approach was established by Senyilmaz et al, who synthesized C18:0 derivates with alkyne and azide-functionalities in order to allow binding to the beads and precipitate the FA with the bound proteins (Senyilmaz et al., 2015). Thus, they reported the binding of stearic acid in the process of acylation, or more precisely “stearoylation” (Senyilmaz et al., 2015). In this study, they demonstrated protein function modulation of the human transferrin receptor 1 by covalent binding of the FA. However, the process of S-acylation of different proteins has been identified as a post-translational modification, more than ten years ago. Often it is referred to as “palmitoylation”, as the most frequent fatty acid acylating proteins is palmitic acid (C16:0) (Bijlmakers and Marsh, 2003). However, besides palmitoylation of peripheral and integral membrane

proteins, further modifications of structure and function of proteins by lipids have been recognized. (N)-terminal myristoylation of cytosolic proteins; isoprenylation at the C-terminus of cytoplasmic proteins and the binding of glycophosphatidyl-inositol to plasma membrane proteins are analogous modifications (Bijlmakers and Marsh, 2003). Already at that time, it was identified, that not only palmitic acid could be esterified at cysteine residues, but also other saturated FAs as stearic or myristic acid as well as unsaturated FAs as oleic acid (Resh, 1999). Until now, only the acylation of ERα by palmitic acid has been observed to modulate estrogen receptor function. Palmitoylation of ERα has been investigated by the group of M. Marino, who proved esterification at the cysteine residue C447 (Acconcia et al., 2004). They demonstrated that modification of the ERα facilitates membrane localization and activation of extracellular regulated kinase (ERK) (Acconcia et al., 2004). Furthermore, the same group investigated the impact of palmitoylation on transcriptional activity and degradation by the proteasome following ubiquitination of the receptor. In this study they claimed necessity of palmitoylation for protecting ERα from fast degradation (La Rosa et al., 2012). Additionally, they indicated that esterification at C447 is required for phosphorylation of the receptor at the S118 residue. This modification is known to regulate transcriptional activity of ERα, even if its role is not fully understood (La Rosa et al., 2012). Moreover, mutation of the C447 residue was shown to repress transcriptional activity in Hek293 transfected cells (La Rosa et al., 2012). These findings were controversial to the results from the present study, demonstrating stearic acid inhibiting transcriptional activity of ERα. However, in the study of La Rosa et al., the reduction of transcriptional activity was assessed by overexpression of the mutant variant of ERα and compared with the WT receptor. This methodology can lead to differences in the expression of ERα, as they previously showed that the mutant form is more prone to proteasome degradation (La Rosa et al., 2012). The discrepancy in transcriptional activity might therefore be related to differences in ERα abundancy instead of inhibition of the transcriptional machinery. The analogous experimental design to our investigations, i.e. supplementation of C16:0, has not been performed. Nevertheless, different fatty acid species might modulate the same protein in divergent manner. Palmitoylation of ERα is linked to higher membrane localization of the steroid receptor. Therefore, a useful model to study the impact of this modification might be the novel “MOER” (membrane-only estrogen receptor alpha) mice (Pedram et al., 2009). In the current

study, it has been demonstrated that stimulation with stearic acid induces the binding of oleic acid to ERα. Oleic acid is a monounsaturated FA and more importantly the main metabolite of stearic acid after transformation through stearoyl-CoA desaturase 1 (SCD-1) (Sampath and Ntambi, 2005). Esterification with a monounsaturated FA rather than with a saturated one might cause an alternative conformational modification of ERα. Furthermore, the mutation of the C447 residue is likely involved in the modulation of the sex steroid receptor observed in the present study. However, the tendency of C18:0 to reduce the ERE activity also in the mutant variant of ERα suggests concomitant residues or mechanisms by which the fatty acid(s) influence transcriptional activity of ERα. FAs are essential components of phospholipids constituting the cellular membrane, influencing physical properties of the membrane as for example fluidity. Fluidity is a major parameter impacting the ability of phagocytosis in macrophages (Schumann, 2016). Several studies demonstrated that administration of unsaturated FAs correlated with higher phagocytosis rate, independently from the used pathogens (Calder et al., 1990; Lecchi et al., 2011). On the other hand, supplementation with C16:0 caused the opposite effect as observed for unsaturated FAs (Calder et al., 1990). Summarizing the previous findings, Calder postulated that the higher the ratio unsaturated to saturated of FAs, the more efficient phagocytosis ability of immune cells (Calder, 2008). In this context, the work done by different groups evidenced the relevance of lipid rafts in several functions of macrophages, including adhesion, pathogen engulfment, migration and cell signaling (Kannan et al., 2008; Lee et al., 2007). Supplementation of macrophages with unsaturated FAs was demonstrated by Schumann et al to lead to enrichment of lipid rafts, which in response altered the functionality of membrane domains (Schumann et al., 2011). This is supposed to affect macrophage function, as lipid rafts were identified as important regulators and pivotal structures for the correct assembling of cell-surface domains with their co-receptors (Schumann et al., 2011; Wong et al., 2009). In order to analyze the impact of the HFD and C18:0 increase in plasma levels on macrophage membrane composition, a cell fractioning approach would have been helpful. After isolation of the cell membrane from further cellular components as mitochondria, nucleus and cytosolic proteins, a HPLC/MS analysis would have elucidated possible differences in membrane composition of atERαKO mice. However, isolation of macrophages from HFD- vs. CD-fed atERαKO mice could not be performed as mentioned before due to technical and animal related limitations.

This would have been helpful, to identify possible abnormalities in the processing of FAs. Studies related to functional uptake of FAs in macrophages, demonstrated that the exaggerated accumulation of FAs is limited by angiopoietin-like protein 4 (Angptl4), modulating the activity of lipoprotein lipase (LPL) (Yoshida et al., 2002). In the work done by Lichtenstein and colleagues knock-out of this gene induced in HFD-fed mutant mice severe ascites and fibrinopurulent peritonitis. Similarly to the female atERαKO model, exposure to HFD was sufficient to induce a lethal phenotype (Lichtenstein et al., 2010). Furthermore, they demonstrated that Angptl4 inhibits foam cell formation of mesenteric lymph node-resident macrophages and prevents macrophage endoplasmic reticulum stress (Lichtenstein et al., 2010). The fact that saturated FAs induce endoplasmic reticulum stress engaging one of the three major pathway branches, i.e. activation of inositol requiring enzyme 1-alpha (IRE1α), is in line with the findings of other groups (Anderson et al., 2012; Lichtenstein et al., 2010; Robblee et al., 2016). In the context of obesity induced adipose tissue macrophage activation, Robblee and colleagues demonstrated that saturated FAs can activate the NOD-Like Receptor family, Pyrin domain containing 3 (NLRP3)-inflammasome. The activation of the NLRP3-inflammasome enables the caspase 1 (Cas1) to convert pro-interleukin 1β to the active form IL1β, which is released by macrophages to induce pro-inflammatory signals (Robblee et al., 2016). In the study performed by Anderson et al, the effects of stearic acid on induction of endoplasmic reticulum stress were further characterized. They demonstrated that accumulation of C18:0 induced the expression of target genes of NFκB and phosphorylation of c-Jun N-terminal kinase (JNK) (Anderson et al., 2012). Moreover, they showed that induction of inflammation and endoplasmic reticulum stress is independent from TLR2- and TLR4-signaling, performing analogous experiments in macrophages isolated from TLR2- and TLR4-knock-out mice. However, results demonstrating endoplasmic reticulum stress, inflammation and apoptosis, were achieved by artificially induced accumulation of intracellular stearic acid. Triacsin, a long-chain acyl-CoA synthetases-inhibitor was added as co-treatment to the fatty acid. Stearic acid treatment on its own did not provoke the same effects (Anderson et al., 2012). Thus, it is doubtful, whether the induced lipotoxicity and the resulting apoptosis are relevant under physiological conditions. However, the mechanism beyond endoplasmic reticulum stress has been already confirmed for saturated FAs by other studies. Stearic acid is the most abundant dietary FAs correlated to Western diet consumption (Spady et al., 1993).

However, it is obtained not exclusively by dietary lipid consumption, but it can be synthesized by the organism through elongation of palmitate as well (Sampath and Ntambi, 2005). In conditions of energy demand, C18:0 can be translocated to the mitochondria by the palmitoyl transferase-1 and be oxidized for ATP production (Foster, 2004). In the contrary case of positive energy balance, stearate can be esterified and stored in form of triglyceride. However, before storage, stearate is rapidly converted to oleate (C18:1n-9), which is the preferable FA for lipid synthesis (Ntambi and Miyazaki, 2004). Therefore, it is unclear, whether stearic acid´s impact on macrophages can be encompassed under the effects of saturated fatty acids. After uptake into the cell, desaturation of C18:0 is a predominant process and greater than for other saturated FAs (Bruce and Salter, 1996). Interestingly, investigations in stearoyl-CoA desaturase (SCD-1) knock-out mice, lacking the rate-limiting enzyme transforming C18:0 to oleic acid (Bruce and Salter, 1996), showed less hepatic triglyceride accumulation (Ntambi and Miyazaki, 2004). Moreover, these mice had increased lipid oxidation rates and were protected from insulin resistance and HFD-induced obesity. This suggests that the process of converting stearic acid to oleic acid protects the mutant mice from metabolic disorders following less adipose tissue inflammation (Ntambi et al., 2002; Rahman et al., 2003). Nevertheless, independently whether stearic or oleic acid are responsible for increased inflammatory signals in macrophages of HFD-fed atERαKO, there is a clear causality between higher FA concentrations and inflammation. Similarly to stearic acid in the study by Anderson et al., ERβ has been shown to cause apoptosis and inflammasome activation with following IL1β secretion (Han et al., 2015). This finding might be of interest for our model, as atERαKO mice are exposed to high E2 levels. In the study concerning endometriosis, the authors demonstrated a correlation between endometriosis and high ERβ expression in affected endometrial cells in humans (Han et al., 2012). Through non-genomic action, ERβ induced inflammation, interacting with the inflammasome machinery and leading to enhanced lesion survival (Han et al., 2015). In previous studies, ERβ has been linked to vascular inflammation (Novella et al., 2012). On the other hand, there are several studies demonstrating positive, i.e. anti-inflammatory, effects of ERβ. For example ERβ activation ameliorated the survival rates in a rodent pneumonia-induced sepsis model (Christaki et al., 2010). Thus the role of ERβ has been conversely discussed and remains elusive concerning the general influence on inflammation processes. However, the fact that ERβ might

enhance inflammation and apoptosis in macrophages might be an additive effect in the complex setting of the infections affecting atERαKO. It might be suggested, that due to inhibition of ERα action through stearic/oleic acid, high E2 concentrations activated mostly ERβ creating an imbalance between ERα and ERβ-signaling. However, further experiments would be needed in order to proof these suggestions and to investigate the effects of modulation by stearic acid in relation to ERβ function. In summary, the present study proposes a novel interaction between ERα-function and stearic/oleic acid, likely involving stearoylation of the nuclear receptor and leading to impaired ERα-signaling in macrophages. In the female atERαKO mice, the identified interaction potentially affected the physiological immune response of these animals, likely promoting bacterial infection.

Clinical relevance of modulation of ERα

Today, the consumption of fat-rich food and the prevalence of obesity in women are increasing (Ogden et al., 2012). At the same time the incidence of endometrial and breast cancer is raising and is correlated to obesity/ a higher BMI, especially in postmenopausal women (Ligibel and Strickler, 2013; Shaw et al., 2016). Mechanistically, not only adipokines (e.g. insulin-like growth factor 1) and insulin are discussed as potential triggers, but also high estrogen plasma levels are linked to the development of breast cancer (Ligibel and Strickler, 2013). Analogously to the mutant mouse model of the present study, postmenopausal obese women have high levels of circulating fatty acids and, due to the increased production of estrogens in expanded adipose tissue, of estrogens (Ligibel and Strickler, 2013). The interaction between ERα and HFD-induced fatty acids might be therefore a critical factor influencing the risk for cancer and inflammatory diseases in obese women. Furthermore, the proposed mechanism is supported by the finding, that disruption of ERα-signaling might be the main cause for higher susceptibility to pyometra. In the experiments done by Kendziorski et al, the authors exposed C57B6/J mice to the endocrine disruptor chemical bisphenol A (BPA), which induced the development of pyometra (Kendziorski et al., 2012). However, they showed strain specific effects of BPA, demonstrating that C57B6/J mice are more affected than CD1 mice (Kendziorski et al., 2012). Nevertheless, the present study might be relevant not only for rodent species. Further animal species are more likely to suffer from inflammatory

disorders in the female reproductive tract. In female dogs and cows, pyometra is a serious and very common disease (Brodzki et al., 2014; Smith, 2006). In bitches, the pathogenesis has been correlated to dysregulation of sexual hormones with enhanced progesterone stimulation and high estradiol levels (Smith, 2006). Moreover, the present findings might also be relevant for uterine infections in humans. Sexually transmitted infections are the primary cause for reproductive failure and gynecological cancers (Wira et al., 2015). These disorders are major challenges for the mucosal immune system, which is required for pathogen protection and, at the same time, which should allow successful reproduction. As discussed above, the mucosal immune system is regulated by sex hormones and therefore affected by menstrual cycle-dependent remodeling of the mucosal tissue (Wira et al., 2015). Disruption of hormonal regulation and simultaneous consumption of dietary lipids might similarly lead in humans to higher susceptibility for sexually transmitted infections. The utilization of hormonal agents as birth control, combined with the higher incidence of obesity related exposure to excessive lipids might create a condition of higher risk. Obesity and inflammation have been already correlated to an increase in cancer incidence (Park et al., 2014). However, the long-term impact of the pharmacological application of birth control has not yet been evaluated and is a major field that should be explored in more detail in the next decades. On the other hand, the present study opens new perspectives for the modulation of ERα function and possible utilization in combination with SERMs, e.g. in the treatment of breast cancer. The modification of the ERα conformation by different fatty acids should be therefore studied in order to evaluate the impact of E2 and SERMs on the activation of the receptor. One might also speculate that a lipid-based co-therapy could ameliorate or even avoid some side effects induced by SERMs.

7. Conclusion and Outlook

The main aim of the current study was to characterize *in-vivo* adipose tissue-specific effects of ERα on adipose tissue biology. However, the focus had to be redesignated. Due to the unexpected and fatal phenotype encompassing uterine bacterial infections in female HFD-fed atERαKO mice, the metabolic impact of the knock-out was limited. Moreover, the unspecificity of the knock-out model for adipose tissue was an additional limitation to discriminate peripheral from central ERα effects. However, the present study encompasses the identification of a previously unknown interaction, between dietary fatty acids and estrogen receptor alpha. It demonstrates that dietary fatty acids are able to modulate ERα-function, impairing transcriptional activity of the nuclear receptor in macrophages. Modulation of ERα in those immune cells might have led to the observed phenotype in female atERαKO mice. We suggested that the proposed mechanism, likely involving acylation of the receptor, might enhance inflammation in a complex and multi-factorial process.

The exact pathogenesis of the occurring phenotype is however still elusive and requires further investigations. More importantly, the interference in E2-ERα-signaling through dietary fatty acids might be relevant for the etiology of sexually transmitted infections. The mechanism and the impact of fatty acids on the immune response should be studied in further detail. Today, fatty acids are recognized to represent important regulators in cell signaling, rather than being simple fuels for the organism. In obesity, the excess of lipids represents one of the major changes which are related to inflammatory processes. Therefore, the recognition of regulatory effects through FAs is of main interest. Modulation by acylation of proteins is a mechanism that should be further elucidated. The understanding of the fate of dietary lipids within the organism and possible modulation of fatty acid composition in obese individuals, might unmask new pharmacological targets. These targets might at least prevent higher susceptibility to inflammation and related metabolic disorders or even cancer.

8. References

Acconcia, F., Ascenzi, P., Fabozzi, G., Visca, P., and Marino, M. (2004). S-palmitoylation modulates human estrogen receptor-alpha functions. Biochem Biophys Res Commun *316*, 878-883.

Amulic, B., Cazalet, C., Hayes, G.L., Metzler, K.D., and Zychlinsky, A. (2012). Neutrophil function: from mechanisms to disease. Annu Rev Immunol *30*, 459-489.

Anderson, E.K., Hill, A.A., and Hasty, A.H. (2012). Stearic acid accumulation in macrophages induces toll-like receptor 4/2-independent inflammation leading to endoplasmic reticulum stress-mediated apoptosis. Arterioscler Thromb Vasc Biol *32*, 1687-1695.

Antonson, P., Matic, M., Portwood, N., Kuiper, R.V., Bryzgalova, G., Gao, H., Windahl, S.H., Humire, P., Ohlsson, C., Berggren, P.O.*, et al.* (2014). aP2-Cre-mediated inactivation of estrogen receptor alpha causes hydrometra. PLoS One *9*, e85581.

Antonson, P., Omoto, Y., Humire, P., and Gustafsson, J.A. (2012). Generation of ERalpha-floxed and knockout mice using the Cre/LoxP system. Biochem Biophys Res Commun *424*, 710-716.

Baulieu, E.E., Binart, N., Cadepond, F., Catelli, M.G., Chambraud, B., Garnier, J., Gasc, J.M., Groyer-Schweizer, G., Oblin, M.E., Radanyi, C.*, et al.* (1990). Receptor-associated nuclear proteins and steroid/antisteroid action. Ann N Y Acad Sci *595*, 300-315.

Beale, K.E., Kinsey-Jones, J.S., Gardiner, J.V., Harrison, E.K., Thompson, E.L., Hu, M.H., Sleeth, M.L., Sam, A.H., Greenwood, H.C., McGavigan, A.K.*, et al.* (2014). The physiological role of arcuate kisspeptin neurons in the control of reproductive function in female rats. Endocrinology *155*, 1091-1098.

Bennett, P.A., Lindell, K., Wilson, C., Carlsson, L.M., Carlsson, B., and Robinson, I.C. (1999). Cyclical variations in the abundance of leptin receptors, but not in circulating leptin, correlate with NPY expression during the oestrous cycle. Neuroendocrinology *69*, 417-423.

Benz, V., Bloch, M., Wardat, S., Bohm, C., Maurer, L., Mahmoodzadeh, S., Wiedmer, P., Spranger, J., Foryst-Ludwig, A., and Kintscher, U.

(2012). Sexual dimorphic regulation of body weight dynamics and adipose tissue lipolysis. PLoS One *7*, e37794.

Berbic, M., Schulke, L., Markham, R., Tokushige, N., Russell, P., and Fraser, I.S. (2009). Macrophage expression in endometrium of women with and without endometriosis. Hum Reprod *24*, 325-332.

Berthois, Y., Katzenellenbogen, J.A., and Katzenellenbogen, B.S. (1986). Phenol red in tissue culture media is a weak estrogen: implications concerning the study of estrogen-responsive cells in culture. Proc Natl Acad Sci U S A *83*, 2496-2500.

Bijlmakers, M.J., and Marsh, M. (2003). The on-off story of protein palmitoylation. Trends Cell Biol *13*, 32-42.

Bjorntorp, P. (1992). Hormonal effects on fat distribution and its relationship to health risk factors. Acta Paediatr Suppl *383*, 59-60; discussion 61.

Borregaard, N. (2010). Neutrophils, from marrow to microbes. Immunity *33*, 657-670.

Bouchard, C., Depres, J.P., and Tremblay, A. (1993a). Exercise and obesity. Obes Res *1*, 133-147.

Bouchard, C., Despres, J.P., and Mauriege, P. (1993b). Genetic and nongenetic determinants of regional fat distribution. Endocr Rev *14*, 72-93.

Boxio, R., Bossenmeyer-Pourie, C., Steinckwich, N., Dournon, C., and Nusse, O. (2004). Mouse bone marrow contains large numbers of functionally competent neutrophils. J Leukoc Biol *75*, 604-611.

Bratton, D.L., and Henson, P.M. (2011). Neutrophil clearance: when the party is over, clean-up begins. Trends Immunol *32*, 350-357.

Brinkmann, V., Reichard, U., Goosmann, C., Fauler, B., Uhlemann, Y., Weiss, D.S., Weinrauch, Y., and Zychlinsky, A. (2004). Neutrophil extracellular traps kill bacteria. Science *303*, 1532-1535.

Brodzki, P., Kostro, K., Brodzki, A., Niemczuk, K., and Lisiecka, U. (2014). Cytometric analysis of surface molecules of leucocytes and phagocytic activity of granulocytes and monocytes/macrophages in cows with pyometra. Reprod Domest Anim *49*, 858-864.

Bruce, J.S., and Salter, A.M. (1996). Metabolic fate of oleic acid, palmitic acid and stearic acid in cultured hamster hepatocytes. Biochem J *316 (Pt 3)*, 847-852.

Calder, P.C. (2008). The relationship between the fatty acid composition of immune cells and their function. Prostaglandins Leukot Essent Fatty Acids *79*, 101-108.

Calder, P.C., Bond, J.A., Harvey, D.J., Gordon, S., and Newsholme, E.A. (1990). Uptake and incorporation of saturated and unsaturated fatty acids into macrophage lipids and their effect upon macrophage adhesion and phagocytosis. Biochem J *269*, 807-814.

Caligioni, C.S. (2009). Assessing reproductive status/stages in mice. Curr Protoc Neurosci *Appendix 4*, Appendix 4I.

Calippe, B., Douin-Echinard, V., Delpy, L., Laffargue, M., Lelu, K., Krust, A., Pipy, B., Bayard, F., Arnal, J.F., Guery, J.C.*, et al.* (2010). 17Beta-estradiol promotes TLR4-triggered proinflammatory mediator production through direct estrogen receptor alpha signaling in macrophages in vivo. J Immunol *185*, 1169-1176.

Calle, E.E., and Kaaks, R. (2004). Overweight, obesity and cancer: epidemiological evidence and proposed mechanisms. Nat Rev Cancer *4*, 579-591.

Cannon, B., and Nedergaard, J. (2004). Brown adipose tissue: function and physiological significance. Physiol Rev *84*, 277-359.

Cao, H., Gerhold, K., Mayers, J.R., Wiest, M.M., Watkins, S.M., and Hotamisligil, G.S. (2008). Identification of a lipokine, a lipid hormone linking adipose tissue to systemic metabolism. Cell *134*, 933-944.

Chawla, A., Nguyen, K.D., and Goh, Y.P. (2011). Macrophage-mediated inflammation in metabolic disease. Nat Rev Immunol *11*, 738-749.

Chen, M., Wolfe, A., Wang, X., Chang, C., Yeh, S., and Radovick, S. (2009). Generation and characterization of a complete null estrogen receptor alpha mouse using Cre/LoxP technology. Mol Cell Biochem *321*, 145-153.

Christaki, E., Opal, S.M., Keith, J.C., Jr., Kessinian, N., Palardy, J.E., Parejo, N.A., Lavallie, E., Racie, L., Mounts, W., Malamas, M.S.*, et al.* (2010). Estrogen receptor beta agonism increases survival in

experimentally induced sepsis and ameliorates the genomic sepsis signature: a pharmacogenomic study. J Infect Dis *201*, 1250-1257.

Cinti, S., Mitchell, G., Barbatelli, G., Murano, I., Ceresi, E., Faloia, E., Wang, S., Fortier, M., Greenberg, A.S., and Obin, M.S. (2005). Adipocyte death defines macrophage localization and function in adipose tissue of obese mice and humans. J Lipid Res *46*, 2347-2355.

Clegg, D.J., Brown, L.M., Woods, S.C., and Benoit, S.C. (2006). Gonadal hormones determine sensitivity to central leptin and insulin. Diabetes *55*, 978-987.

Cole, M.P., Jones, C.T., and Todd, I.D. (1971). A new anti-oestrogenic agent in late breast cancer. An early clinical appraisal of ICI46474. Br J Cancer *25*, 270-275.

Coleman, D.L. (2010). A historical perspective on leptin. Nat Med *16*, 1097-1099.

Considine, R.V., Sinha, M.K., Heiman, M.L., Kriauciunas, A., Stephens, T.W., Nyce, M.R., Ohannesian, J.P., Marco, C.C., McKee, L.J., Bauer, T.L.*, et al.* (1996). Serum immunoreactive-leptin concentrations in normal-weight and obese humans. N Engl J Med *334*, 292-295.

Cora, M.C., Kooistra, L., and Travlos, G. (2015). Vaginal Cytology of the Laboratory Rat and Mouse: Review and Criteria for the Staging of the Estrous Cycle Using Stained Vaginal Smears. Toxicol Pathol *43*, 776-793.

Couse, J.F., Bunch, D.O., Lindzey, J., Schomberg, D.W., and Korach, K.S. (1999). Prevention of the polycystic ovarian phenotype and characterization of ovulatory capacity in the estrogen receptor-alpha knockout mouse. Endocrinology *140*, 5855-5865.

Couse, J.F., Curtis, S.W., Washburn, T.F., Lindzey, J., Golding, T.S., Lubahn, D.B., Smithies, O., and Korach, K.S. (1995). Analysis of transcription and estrogen insensitivity in the female mouse after targeted disruption of the estrogen receptor gene. Mol Endocrinol *9*, 1441-1454.

Critchley, H.O., Brenner, R.M., Henderson, T.A., Williams, K., Nayak, N.R., Slayden, O.D., Millar, M.R., and Saunders, P.T. (2001). Estrogen receptor beta, but not estrogen receptor alpha, is present in the vascular endothelium of the human and nonhuman primate endometrium. J Clin Endocrinol Metab *86*, 1370-1378.

Critchley, H.O., and Saunders, P.T. (2009). Hormone receptor dynamics in a receptive human endometrium. Reprod Sci *16*, 191-199.
Cunningham, J.W., and Wiviott, S.D. (2014). Modern obesity pharmacotherapy: weighing cardiovascular risk and benefit. Clin Cardiol *37*, 693-699.

Dagdeviren, S., Jung, D.Y., Lee, E., Friedline, R.H., Noh, H.L., Kim, J.H., Patel, P.R., Tsitsilianos, N., Tsitsilianos, A.V., Tran, D.A.*, et al.* (2016). Altered Interleukin-10 Signaling in Skeletal Muscle Regulates Obesity-Mediated Inflammation and Insulin Resistance. Mol Cell Biol *36*, 2956-2966.

Danielsen, M., Hinck, L., and Ringold, G.M. (1989). Mutational analysis of the mouse glucocorticoid receptor. Cancer Res *49*, 2286s-2291s.

Davis, K.E., M, D.N., Sun, K., W, M.S., J, D.B., J, A.Z., Zeve, D., L, D.H., D, W.C., L, M.G.*, et al.* (2013). The sexually dimorphic role of adipose and adipocyte estrogen receptors in modulating adipose tissue expansion, inflammation, and fibrosis. Mol Metab *2*, 227-242.

de Souza, C.O., Teixeira, A.A.S., Biondo, L.A., Lima Junior, E.A., Batatinha, H.A.P., and Rosa Neto, J.C. (2017). Palmitoleic Acid Improves Metabolic Functions in Fatty Liver by PPARalpha-Dependent AMPK Activation. J Cell Physiol *232*, 2168-2177.

Dela, F., Ploug, T., Handberg, A., Petersen, L.N., Larsen, J.J., Mikines, K.J., and Galbo, H. (1994). Physical training increases muscle GLUT4 protein and mRNA in patients with NIDDM. Diabetes *43*, 862-865.

Eguchi, J., Wang, X., Yu, S., Kershaw, E.E., Chiu, P.C., Dushay, J., Estall, J.L., Klein, U., Maratos-Flier, E., and Rosen, E.D. (2011).

Transcriptional control of adipose lipid handling by IRF4. Cell Metab *13*, 249-259.

El Kasmi, K.C., and Stenmark, K.R. (2015). Contribution of metabolic reprogramming to macrophage plasticity and function. Semin Immunol *27*, 267-275.

Elliott, M.R., and Ravichandran, K.S. (2010). Clearance of apoptotic cells: implications in health and disease. J Cell Biol *189*, 1059-1070.

Ettinger, B., Black, D.M., Mitlak, B.H., Knickerbocker, R.K., Nickelsen, T., Genant, H.K., Christiansen, C., Delmas, P.D., Zanchetta, J.R., Stakkestad, J.*, et al.* (1999). Reduction of vertebral fracture risk in postmenopausal women with osteoporosis treated with raloxifene: results from a 3-year randomized clinical trial. Multiple Outcomes of Raloxifene Evaluation (MORE) Investigators. JAMA *282*, 637-645.
Exley, M.A., Hand, L., O'Shea, D., and Lynch, L. (2014). Interplay between the immune system and adipose tissue in obesity. J Endocrinol *223*, R41-48.

Fahey, J.V., Wright, J.A., Shen, L., Smith, J.M., Ghosh, M., Rossoll, R.M., and Wira, C.R. (2008). Estradiol selectively regulates innate immune function by polarized human uterine epithelial cells in culture. Mucosal Immunol *1*, 317-325.

Faulds, M.H., Zhao, C., Dahlman-Wright, K., and Gustafsson, J.A. (2012). The diversity of sex steroid action: regulation of metabolism by estrogen signaling. J Endocrinol *212*, 3-12.

Feil, R., Wagner, J., Metzger, D., and Chambon, P. (1997). Regulation of Cre recombinase activity by mutated estrogen receptor ligand-binding domains. Biochem Biophys Res Commun *237*, 752-757.

Fenzl, A., and Kiefer, F.W. (2014). Brown adipose tissue and thermogenesis. Horm Mol Biol Clin Investig *19*, 25-37.

Ferrell, R.E., Kimak, M.A., Lawrence, E.C., and Finegold, D.N. (2008). Candidate gene analysis in primary lymphedema. Lymphat Res Biol *6*, 69-76.

Finan, B., Yang, B., Ottaway, N., Stemmer, K., Muller, T.D., Yi, C.X., Habegger, K., Schriever, S.C., Garcia-Caceres, C., Kabra, D.G.*, et al.* (2012). Targeted estrogen delivery reverses the metabolic syndrome. Nat Med *18*, 1847-1856.

Flegal, K.M., Carroll, M.D., Kit, B.K., and Ogden, C.L. (2012). Prevalence of obesity and trends in the distribution of body mass index among US adults, 1999-2010. JAMA *307*, 491-497.

Foryst-Ludwig, A., Clemenz, M., Hohmann, S., Hartge, M., Sprang, C., Frost, N., Krikov, M., Bhanot, S., Barros, R., Morani, A.*, et al.* (2008).

Metabolic actions of estrogen receptor beta (ERbeta) are mediated by a negative cross-talk with PPARgamma. PLoS Genet *4*, e1000108.

Foryst-Ludwig, A., Kreissl, M.C., Benz, V., Brix, S., Smeir, E., Ban, Z., Januszewicz, E., Salatzki, J., Grune, J., Schwanstecher, A.K.*, et al.* (2015). Adipose Tissue Lipolysis Promotes Exercise-Induced Cardiac Hypertrophy Involving the Lipokine C16:1n7-Palmitoleate. J Biol Chem.

Foster, D.W. (2004). The role of the carnitine system in human metabolism. Ann N Y Acad Sci *1033*, 1-16.

Friedman, J.M., and Halaas, J.L. (1998). Leptin and the regulation of body weight in mammals. Nature *395*, 763-770.

Fritsche, K.L. (2015). The science of fatty acids and inflammation. Adv Nutr *6*, 293S-301S.

Fu, M.H., Maher, A.C., Hamadeh, M.J., Ye, C., and Tarnopolsky, M.A. (2009). Exercise, sex, menstrual cycle phase, and 17beta-estradiol influence metabolism-related genes in human skeletal muscle. Physiol Genomics *40*, 34-47.

Fu, Y., Luo, N., Lopes-Virella, M.F., and Garvey, W.T. (2002). The adipocyte lipid binding protein (ALBP/aP2) gene facilitates foam cell formation in human THP-1 macrophages. Atherosclerosis *165*, 259-269.
Fullerton, J.N., O'Brien, A.J., and Gilroy, D.W. (2013). Pathways mediating resolution of inflammation: when enough is too much. J Pathol *231*, 8-20.

Galvan-Pena, S., and O'Neill, L.A. (2014). Metabolic reprograming in macrophage polarization. Front Immunol *5*, 420.

Gambacciani, M., Ciaponi, M., Cappagli, B., Piaggesi, L., De Simone, L., Orlandi, R., and Genazzani, A.R. (1997). Body weight, body fat distribution, and hormonal replacement therapy in early postmenopausal women. J Clin Endocrinol Metab *82*, 414-417.

Geary, N., Asarian, L., Korach, K.S., Pfaff, D.W., and Ogawa, S. (2001). Deficits in E2-Dependent Control of Feeding, Weight Gain, and Cholecystokinin Satiation in ER-alpha Null Mice. Endocrinology *142*, 4751-4757.

Ghisletti, S., Meda, C., Maggi, A., and Vegeto, E. (2005). 17beta-estradiol inhibits inflammatory gene expression by controlling NF-kappaB intracellular localization. Mol Cell Biol *25*, 2957-2968.

Greenblatt, R.B., Roy, S., and Mahesh, V.B. (1962). Induction of ovulation. Am J Obstet Gynecol *84*, 900-912.

Gruber, C.J., Gruber, D.M., Gruber, I.M., Wieser, F., and Huber, J.C. (2004). Anatomy of the estrogen response element. Trends Endocrinol Metab *15*, 73-78.

Haarbo, J., Marslew, U., Gotfredsen, A., and Christiansen, C. (1991). Postmenopausal hormone replacement therapy prevents central distribution of body fat after menopause. Metabolism *40*, 1323-1326.

Hall, J.M., McDonnell, D.P., and Korach, K.S. (2002). Allosteric regulation of estrogen receptor structure, function, and coactivator recruitment by different estrogen response elements. Mol Endocrinol *16*, 469-486.

Han, S.J., Hawkins, S.M., Begum, K., Jung, S.Y., Kovanci, E., Qin, J., Lydon, J.P., DeMayo, F.J., and O'Malley, B.W. (2012). A new isoform of steroid receptor coactivator-1 is crucial for pathogenic progression of endometriosis. Nat Med *18*, 1102-1111.

Han, S.J., Jung, S.Y., Wu, S.P., Hawkins, S.M., Park, M.J., Kyo, S., Qin, J., Lydon, J.P., Tsai, S.Y., Tsai, M.J.*, et al.* (2015). Estrogen Receptor beta Modulates Apoptosis Complexes and the Inflammasome to Drive the Pathogenesis of Endometriosis. Cell *163*, 960-974.

Heery, D.M., Kalkhoven, E., Hoare, S., and Parker, M.G. (1997). A signature motif in transcriptional co-activators mediates binding to nuclear receptors. Nature *387*, 733-736.

Heine, P.A., Taylor, J.A., Iwamoto, G.A., Lubahn, D.B., and Cooke, P.S. (2000). Increased adipose tissue in male and female estrogen receptor-alpha knockout mice. Proc Natl Acad Sci U S A *97*, 12729-12734.

Henderson, T.A., Saunders, P.T., Moffett-King, A., Groome, N.P., and Critchley, H.O. (2003). Steroid receptor expression in uterine natural killer cells. J Clin Endocrinol Metab *88*, 440-449.

Hevener, A.L., Clegg, D.J., and Mauvais-Jarvis, F. (2015). Impaired estrogen receptor action in the pathogenesis of the metabolic syndrome. Mol Cell Endocrinol *418 Pt 3*, 306-321.

Hillier, S.G., Whitelaw, P.F., and Smyth, C.D. (1994). Follicular oestrogen synthesis: the 'two-cell, two-gonadotrophin' model revisited. Mol Cell Endocrinol *100*, 51-54.

Hoffmann, B., Hoveler, R., Hasan, S.H., and Failing, K. (1992). Ovarian and pituitary function in dogs after hysterectomy. J Reprod Fertil *96*, 837-845.

Horne, A.W., King, A.E., Shaw, E., McDonald, S.E., Williams, A.R., Saunders, P.T., and Critchley, H.O. (2009). Attenuated sex steroid receptor expression in fallopian tube of women with ectopic pregnancy. J Clin Endocrinol Metab *94*, 5146-5154.

Jacq, X., Brou, C., Lutz, Y., Davidson, I., Chambon, P., and Tora, L. (1994). Human TAFII30 is present in a distinct TFIID complex and is required for transcriptional activation by the estrogen receptor. Cell *79*, 107-117.

Jeffery, E., Berry, R., Church, C.D., Yu, S., Shook, B.A., Horsley, V., Rosen, E.D., and Rodeheffer, M.S. (2014). Characterization of Cre recombinase models for the study of adipose tissue. Adipocyte *3*, 206-211.

Jensen, E.V. (1962). On the mechanism of estrogen action. Perspect Biol Med *6*, 47-59.

Jones, B.J., and Bloom, S.R. (2015). The New Era of Drug Therapy for Obesity: The Evidence and the Expectations. Drugs *75*, 935-945.
Jordan, V.C. (1988). Chemosuppression of breast cancer with tamoxifen: laboratory evidence and future clinical investigations. Cancer Invest *6*, 589-595.

Jordan, V.C., Phelps, E., and Lindgren, J.U. (1987). Effects of anti-estrogens on bone in castrated and intact female rats. Breast Cancer Res Treat *10*, 31-35.

Kamat, A., Hinshelwood, M.M., Murry, B.A., and Mendelson, C.R. (2002). Mechanisms in tissue-specific regulation of estrogen biosynthesis in humans. Trends Endocrinol Metab *13*, 122-128.

Kambara, K., Ohashi, W., Tomita, K., Takashina, M., Fujisaka, S., Hayashi, R., Mori, H., Tobe, K., and Hattori, Y. (2015). In vivo depletion of CD206+ M2 macrophages exaggerates lung injury in endotoxemic mice. Am J Pathol *185*, 162-171.

Kanda, H., Tateya, S., Tamori, Y., Kotani, K., Hiasa, K., Kitazawa, R., Kitazawa, S., Miyachi, H., Maeda, S., Egashira, K.*, et al.* (2006). MCP-1 contributes to macrophage infiltration into adipose tissue, insulin resistance, and hepatic steatosis in obesity. J Clin Invest *116*, 1494-1505.

Kang, S., Kong, X., and Rosen, E.D. (2014). Adipocyte-specific transgenic and knockout models. Methods Enzymol *537*, 1-16.
Kannan, S., Audet, A., Huang, H., Chen, L.J., and Wu, M. (2008). Cholesterol-rich membrane rafts and Lyn are involved in phagocytosis during Pseudomonas aeruginosa infection. J Immunol *180*, 2396-2408.

Kendziorski, J.A., Kendig, E.L., Gear, R.B., and Belcher, S.M. (2012). Strain specific induction of pyometra and differences in immune responsiveness in mice exposed to 17alpha-ethinyl estradiol or the endocrine disrupting chemical bisphenol A. Reprod Toxicol *34*, 22-30.

Kennedy, A.D., and DeLeo, F.R. (2009). Neutrophil apoptosis and the resolution of infection. Immunol Res *43*, 25-61.

Kim, M.S., Rossi, M., Abusnana, S., Sunter, D., Morgan, D.G., Small, C.J., Edwards, C.M., Heath, M.M., Stanley, S.A., Seal, L.J.*, et al.* (2000). Hypothalamic localization of the feeding effect of agouti-related peptide and alpha-melanocyte-stimulating hormone. Diabetes *49*, 177-182.
King, A.E., and Critchley, H.O. (2010). Oestrogen and progesterone regulation of inflammatory processes in the human endometrium. J Steroid Biochem Mol Biol *120*, 116-126.

Kissler, H.J., and Settmacher, U. (2013). Bariatric surgery to treat obesity. Semin Nephrol *33*, 75-89.

Klinge, C.M. (2001). Estrogen receptor interaction with estrogen response elements. Nucleic Acids Res *29*, 2905-2919.

Klinge, C.M., Bodenner, D.L., Desai, D., Niles, R.M., and Traish, A.M. (1997). Binding of type II nuclear receptors and estrogen receptor to full and half-site estrogen response elements in vitro. Nucleic Acids Res *25*, 1903-1912.

Kopelman, P.G. (2000). Obesity as a medical problem. Nature *404*, 635-643.

Kratz, M., Coats, B.R., Hisert, K.B., Hagman, D., Mutskov, V., Peris, E., Schoenfelt, K.Q., Kuzma, J.N., Larson, I., Billing, P.S.*, et al.* (2014). Metabolic dysfunction drives a mechanistically distinct proinflammatory phenotype in adipose tissue macrophages. Cell Metab *20*, 614-625.

Krysko, O., Vandenabeele, P., Krysko, D.V., and Bachert, C. (2010). Impairment of phagocytosis of apoptotic cells and its role in chronic airway diseases. Apoptosis *15*, 1137-1146.

Kuiper, G.G., Enmark, E., Pelto-Huikko, M., Nilsson, S., and Gustafsson, J.A. (1996). Cloning of a novel receptor expressed in rat prostate and ovary. Proc Natl Acad Sci U S A *93*, 5925-5930.

Kumada, M., Kihara, S., Ouchi, N., Kobayashi, H., Okamoto, Y., Ohashi, K., Maeda, K., Nagaretani, H., Kishida, K., Maeda, N.*, et al.* (2004). Adiponectin specifically increased tissue inhibitor of metalloproteinase-1 through interleukin-10 expression in human macrophages. Circulation *109*, 2046-2049.

La Rosa, P., Pesiri, V., Leclercq, G., Marino, M., and Acconcia, F. (2012). Palmitoylation regulates 17beta-estradiol-induced estrogen receptor-alpha degradation and transcriptional activity. Mol Endocrinol *26*, 762-774.

Lavin, Y., Mortha, A., Rahman, A., and Merad, M. (2015). Regulation of macrophage development and function in peripheral tissues. Nat Rev Immunol *15*, 731-744.

Lecchi, C., Invernizzi, G., Agazzi, A., Ferroni, M., Pisani, L.F., Savoini, G., and Ceciliani, F. (2011). In vitro modulation of caprine monocyte immune functions by omega-3 polyunsaturated fatty acids. Vet J *189*, 353-355.

Lee, H.S., Park, J.H., Kang, J.H., Kawada, T., Yu, R., and Han, I.S. (2009). Chemokine and chemokine receptor gene expression in the mesenteric adipose tissue of KKAy mice. Cytokine *46*, 160-165.

Lee, K.Y., Russell, S.J., Ussar, S., Boucher, J., Vernochet, C., Mori, M.A., Smyth, G., Rourk, M., Cederquist, C., Rosen, E.D.*, et al.* (2013). Lessons on conditional gene targeting in mouse adipose tissue. Diabetes *62*, 864-874.

Lee, W.L., Mason, D., Schreiber, A.D., and Grinstein, S. (2007). Quantitative analysis of membrane remodeling at the phagocytic cup. Mol Biol Cell *18*, 2883-2892.

Lefevre, L., Gales, A., Olagnier, D., Bernad, J., Perez, L., Burcelin, R., Valentin, A., Auwerx, J., Pipy, B., and Coste, A. (2010). PPARgamma ligands switched high fat diet-induced macrophage M2b polarization toward M2a thereby improving intestinal Candida elimination. PLoS One *5*, e12828.

Levin, E.R. (2009a). G protein-coupled receptor 30: estrogen receptor or collaborator? Endocrinology *150*, 1563-1565.

Levin, E.R. (2009b). Plasma membrane estrogen receptors. Trends Endocrinol Metab *20*, 477-482.

Ley, K. (2002). Integration of inflammatory signals by rolling neutrophils. Immunol Rev *186*, 8-18.

Li, Y., Erzurumlu, R.S., Chen, C., Jhaveri, S., and Tonegawa, S. (1994). Whisker-related neuronal patterns fail to develop in the trigeminal brainstem nuclei of NMDAR1 knockout mice. Cell *76*, 427-437.

Lichtenstein, L., Mattijssen, F., de Wit, N.J., Georgiadi, A., Hooiveld, G.J., van der Meer, R., He, Y., Qi, L., Koster, A., Tamsma, J.T.*, et al.* (2010). Angptl4 protects against severe proinflammatory effects of saturated fat by inhibiting fatty acid uptake into mesenteric lymph node macrophages. Cell Metab *12*, 580-592.

Ligibel, J.A., and Strickler, H.D. (2013). Obesity and its impact on breast cancer: tumor incidence, recurrence, survival, and possible interventions. Am Soc Clin Oncol Educ Book, 52-59.

Liu, H.Q., Qiu, Y., Mu, Y., Zhang, X.J., Liu, L., Hou, X.H., Zhang, L., Xu, X.N., Ji, A.L., Cao, R.*, et al.* (2013). A high ratio of dietary n-3/n-6 polyunsaturated fatty acids improves obesity-linked inflammation and insulin resistance through suppressing activation of TLR4 in SD rats. Nutr Res *33*, 849-858.

Lopez, M., and Tena-Sempere, M. (2015). Estrogens and the control of energy homeostasis: a brain perspective. Trends Endocrinol Metab *26*, 411-421.

Lottenberg, A.M., Afonso Mda, S., Lavrador, M.S., Machado, R.M., and Nakandakare, E.R. (2012). The role of dietary fatty acids in the pathology of metabolic syndrome. J Nutr Biochem *23*, 1027-1040.

Louis-Sylvestre, J. (1980). Neuroendocrinology of hyperphagias and obesities. Reprod Nutr Dev *20*, 1545-1562.

Mader, S., Kumar, V., de Verneuil, H., and Chambon, P. (1989). Three amino acids of the oestrogen receptor are essential to its ability to distinguish an oestrogen from a glucocorticoid-responsive element. Nature *338*, 271-274.

Maehre, H.K., Jensen, I.J., Elvevoll, E.O., and Eilertsen, K.E. (2015). omega-3 Fatty Acids and Cardiovascular Diseases: Effects, Mechanisms and Dietary Relevance. Int J Mol Sci *16*, 22636-22661.

Makowski, L., Boord, J.B., Maeda, K., Babaev, V.R., Uysal, K.T., Morgan, M.A., Parker, R.A., Suttles, J., Fazio, S., Hotamisligil, G.S.*, et al.* (2001). Lack of macrophage fatty-acid-binding protein aP2 protects mice deficient in apolipoprotein E against atherosclerosis. Nat Med *7*, 699-705.

Mao, J., Yang, T., Gu, Z., Heird, W.C., Finegold, M.J., Lee, B., and Wakil, S.J. (2009). aP2-Cre-mediated inactivation of acetyl-CoA carboxylase 1 causes growth retardation and reduced lipid accumulation in adipose tissues. Proc Natl Acad Sci U S A *106*, 17576-17581.

Marx, P.A., Spira, A.I., Gettie, A., Dailey, P.J., Veazey, R.S., Lackner, A.A., Mahoney, C.J., Miller, C.J., Claypool, L.E., Ho, D.D.*, et al.* (1996). Progesterone implants enhance SIV vaginal transmission and early virus load. Nat Med *2*, 1084-1089.

Masoodi, M., Kuda, O., Rossmeisl, M., Flachs, P., and Kopecky, J. (2015). Lipid signaling in adipose tissue: Connecting inflammation & metabolism. Biochim Biophys Acta *1851*, 503-518.

Maximov, P.Y., Lee, T.M., and Jordan, V.C. (2013). The discovery and development of selective estrogen receptor modulators (SERMs) for clinical practice. Curr Clin Pharmacol *8*, 135-155.

Mayoral, R., Osborn, O., McNelis, J., Johnson, A.M., Oh da, Y., Izquierdo, C.L., Chung, H., Li, P., Traves, P.G., Bandyopadhyay, G.*, et al.* (2015). Adipocyte SIRT1 knockout promotes PPARgamma activity, adipogenesis and insulin sensitivity in chronic-HFD and obesity. Mol Metab *4*, 378-391.

Mazidi, M., and Kengne, A.P. (2017). Nutrient patterns and their relationship with general and central obesity in US adults. Eur J Clin Invest.

McCracken, J.M., and Allen, L.A. (2014). Regulation of human neutrophil apoptosis and lifespan in health and disease. J Cell Death *7*, 15-23.

McKenna, N.J., Lanz, R.B., and O'Malley, B.W. (1999). Nuclear receptor coregulators: cellular and molecular biology. Endocr Rev *20*, 321-344.
Mercalli, A., Calavita, I., Dugnani, E., Citro, A., Cantarelli, E., Nano, R., Melzi, R., Maffi, P., Secchi, A., Sordi, V.*, et al.* (2013). Rapamycin unbalances the polarization of human macrophages to M1. Immunology *140*, 179-190.

Miller, J.R., Siripurkpong, P., Hawes, J., Majdalawieh, A., Ro, H.S., and McLeod, R.S. (2008). The trans-10, cis-12 isomer of conjugated linoleic acid decreases adiponectin assembly by PPARgamma-dependent and PPARgamma-independent mechanisms. J Lipid Res *49*, 550-562.

Morentin, B., and Audicana, C. (2011). Population-based study of out-of-hospital sudden cardiovascular death: incidence and causes of death in middle-aged adults. Rev Esp Cardiol *64*, 28-34.

Morselli, E., Fuente-Martin, E., Finan, B., Kim, M., Frank, A., Garcia-Caceres, C., Navas, C.R., Gordillo, R., Neinast, M., Kalainayakan, S.P.*, et al.* (2014). Hypothalamic PGC-1alpha protects against high-fat diet exposure by regulating ERalpha. Cell Rep *9*, 633-645.
Mosselman, S., Polman, J., and Dijkema, R. (1996). ER beta: identification and characterization of a novel human estrogen receptor. FEBS Lett *392*, 49-53.

Mosser, D.M., and Edwards, J.P. (2008). Exploring the full spectrum of macrophage activation. Nat Rev Immunol *8*, 958-969.

Mukwevho, E., and Joseph, J.S. (2014). Calmodulin dependent protein kinase II activation by exercise regulates saturated & unsaturated fatty acids and improves some metabolic syndrome markers. Life Sci *111*, 53-61.

Mullican, S.E., Tomaru, T., Gaddis, C.A., Peed, L.C., Sundaram, A., and Lazar, M.A. (2013). A novel adipose-specific gene deletion model demonstrates potential pitfalls of existing methods. Mol Endocrinol *27*, 127-134.

Munoz, L.E., Lauber, K., Schiller, M., Manfredi, A.A., and Herrmann, M. (2010). The role of defective clearance of apoptotic cells in systemic autoimmunity. Nat Rev Rheumatol *6*, 280-289.

Murphy, A.J., Guyre, P.M., and Pioli, P.A. (2010). Estradiol suppresses NF-kappa B activation through coordinated regulation of let-7a and miR-125b in primary human macrophages. J Immunol *184*, 5029-5037.

Murray, P.J., Allen, J.E., Biswas, S.K., Fisher, E.A., Gilroy, D.W., Goerdt, S., Gordon, S., Hamilton, J.A., Ivashkiv, L.B., Lawrence, T.*, et al.* (2014). Macrophage activation and polarization: nomenclature and experimental guidelines. Immunity *41*, 14-20.

Murray, P.J., and Wynn, T.A. (2011). Protective and pathogenic functions of macrophage subsets. Nat Rev Immunol *11*, 723-737.
Myers, M.G., Cowley, M.A., and Munzberg, H. (2008). Mechanisms of leptin action and leptin resistance. Annu Rev Physiol *70*, 537-556.

Novella, S., Heras, M., Hermenegildo, C., and Dantas, A.P. (2012). Effects of estrogen on vascular inflammation: a matter of timing. Arterioscler Thromb Vasc Biol *32*, 2035-2042.

Ntambi, J.M., and Miyazaki, M. (2004). Regulation of stearoyl-CoA desaturases and role in metabolism. Prog Lipid Res *43*, 91-104.
Ntambi, J.M., Miyazaki, M., Stoehr, J.P., Lan, H., Kendziorski, C.M., Yandell, B.S., Song, Y., Cohen, P., Friedman, J.M., and Attie, A.D. (2002). Loss of stearoyl-CoA desaturase-1 function protects mice against adiposity. Proc Natl Acad Sci U S A *99*, 11482-11486.

Ogawa, S., Chan, J., Chester, A.E., Gustafsson, J.A., Korach, K.S., and Pfaff, D.W. (1999). Survival of reproductive behaviors in estrogen receptor beta gene-deficient (betaERKO) male and female mice. Proc Natl Acad Sci U S A *96*, 12887-12892.

Ogden, C.L., Carroll, M.D., Kit, B.K., and Flegal, K.M. (2012). Prevalence of obesity in the United States, 2009-2010. NCHS Data Brief, 1-8.
Ogden, C.L., Carroll, M.D., Kit, B.K., and Flegal, K.M. (2014). Prevalence of childhood and adult obesity in the United States, 2011-2012. JAMA *311*, 806-814.

Olefsky, J.M., and Glass, C.K. (2010). Macrophages, inflammation, and insulin resistance. Annu Rev Physiol *72*, 219-246.

Ordonez, P., Moreno, M., Alonso, A., Llaneza, P., Diaz, F., and Gonzalez, C. (2008). 17beta-Estradiol and/or progesterone protect from insulin resistance in STZ-induced diabetic rats. J Steroid Biochem Mol Biol *111*, 287-294.

Park, J., Morley, T.S., Kim, M., Clegg, D.J., and Scherer, P.E. (2014). Obesity and cancer--mechanisms underlying tumour progression and recurrence. Nat Rev Endocrinol *10*, 455-465.

Pedram, A., Razandi, M., Kim, J.K., O'Mahony, F., Lee, E.Y., Luderer, U., and Levin, E.R. (2009). Developmental phenotype of a membrane only estrogen receptor alpha (MOER) mouse. J Biol Chem *284*, 3488-3495.

Pratt, W.B. (1993). The role of heat shock proteins in regulating the function, folding, and trafficking of the glucocorticoid receptor. J Biol Chem *268*, 21455-21458.

Rahman, S.M., Dobrzyn, A., Dobrzyn, P., Lee, S.H., Miyazaki, M., and Ntambi, J.M. (2003). Stearoyl-CoA desaturase 1 deficiency elevates insulin-signaling components and down-regulates protein-tyrosine phosphatase 1B in muscle. Proc Natl Acad Sci U S A *100*, 11110-11115.

Regitz-Zagrosek, V., and Kararigas, G. (2017). Mechanistic Pathways of Sex Differences in Cardiovascular Disease. Physiol Rev *97*, 1-37.

Resh, M.D. (1999). Fatty acylation of proteins: new insights into membrane targeting of myristoylated and palmitoylated proteins. Biochim Biophys Acta *1451*, 1-16.

Riant, E., Waget, A., Cogo, H., Arnal, J.F., Burcelin, R., and Gourdy, P. (2009). Estrogens protect against high-fat diet-induced insulin resistance and glucose intolerance in mice. Endocrinology *150*, 2109-2117.

Ribas, V., Drew, B.G., Le, J.A., Soleymani, T., Daraei, P., Sitz, D., Mohammad, L., Henstridge, D.C., Febbraio, M.A., Hewitt, S.C.*, et al.* (2011). Myeloid-specific estrogen receptor alpha deficiency impairs metabolic homeostasis and accelerates atherosclerotic lesion development. Proc Natl Acad Sci U S A *108*, 16457-16462.

Ribas, V., Drew, B.G., Zhou, Z., Phun, J., Kalajian, N.Y., Soleymani, T., Daraei, P., Widjaja, K., Wanagat, J., de Aguiar Vallim, T.Q., *et al.* (2016). Skeletal muscle action of estrogen receptor alpha is critical for the maintenance of mitochondrial function and metabolic homeostasis in females. Sci Transl Med *8*, 334ra354.

Ribas, V., Nguyen, M.T., Henstridge, D.C., Nguyen, A.K., Beaven, S.W., Watt, M.J., and Hevener, A.L. (2010). Impaired oxidative metabolism and inflammation are associated with insulin resistance in ERalpha-deficient mice. Am J Physiol Endocrinol Metab *298*, E304-319.

Rincon-Cervera, M.A., Valenzuela, R., Hernandez-Rodas, M.C., Marambio, M., Espinosa, A., Mayer, S., Romero, N., Barrera, M.S.C., Valenzuela, A., and Videla, L.A. (2016). Supplementation with antioxidant-rich extra virgin olive oil prevents hepatic oxidative stress and reduction of desaturation capacity in mice fed a high-fat diet: Effects on fatty acid composition in liver and extrahepatic tissues. Nutrition *32*, 1254-1267.

Robblee, M.M., Kim, C.C., Porter Abate, J., Valdearcos, M., Sandlund, K.L., Shenoy, M.K., Volmer, R., Iwawaki, T., and Koliwad, S.K. (2016). Saturated Fatty Acids Engage an IRE1alpha-Dependent Pathway to Activate the NLRP3 Inflammasome in Myeloid Cells. Cell Rep *14*, 2611-2623.

Robert-Koch-Institute (2012). GEDA Study.

Robertson, K.M., O'Donnell, L., Simpson, E.R., and Jones, M.E. (2002). The phenotype of the aromatase knockout mouse reveals dietary phytoestrogens impact significantly on testis function. Endocrinology *143*, 2913-2921.

Ruffell, B., Affara, N.I., and Coussens, L.M. (2012). Differential macrophage programming in the tumor microenvironment. Trends Immunol *33*, 119-126.

Sadovsky, Y., Webb, P., Lopez, G., Baxter, J.D., Fitzpatrick, P.M., Gizang-Ginsberg, E., Cavailles, V., Parker, M.G., and Kushner, P.J. (1995). Transcriptional activators differ in their responses to overexpression of TATA-box-binding protein. Mol Cell Biol *15*, 1554-1563.

Sainz, N., Gonzalez-Navarro, C.J., Martinez, J.A., and Moreno-Aliaga, M.J. (2015). Leptin signaling as a therapeutic target of obesity. Expert Opin Ther Targets *19*, 893-909.

Sampath, H., and Ntambi, J.M. (2005). The fate and intermediary metabolism of stearic acid. Lipids *40*, 1187-1191.

Schaefer, T.M., Wright, J.A., Pioli, P.A., and Wira, C.R. (2005). IL-1beta-mediated proinflammatory responses are inhibited by estradiol via down-regulation of IL-1 receptor type I in uterine epithelial cells. J Immunol *175*, 6509-6516.

Schiwon, M., Weisheit, C., Franken, L., Gutweiler, S., Dixit, A., Meyer-Schwesinger, C., Pohl, J.M., Maurice, N.J., Thiebes, S., Lorenz, K.*, et al.* (2014). Crosstalk between sentinel and helper macrophages permits neutrophil migration into infected uroepithelium. Cell *156*, 456-468.
Schumann, J. (2016). It is all about fluidity: Fatty acids and macrophage phagocytosis. Eur J Pharmacol *785*, 18-23.

Schumann, J., Leichtle, A., Thiery, J., and Fuhrmann, H. (2011). Fatty acid and peptide profiles in plasma membrane and membrane rafts of PUFA supplemented RAW264.7 macrophages. PLoS One *6*, e24066.
Schwartz, M.W., Peskind, E., Raskind, M., Boyko, E.J., and Porte, D., Jr. (1996). Cerebrospinal fluid leptin levels: relationship to plasma levels and to adiposity in humans. Nat Med *2*, 589-593.

Senyilmaz, D., Virtue, S., Xu, X., Tan, C.Y., Griffin, J.L., Miller, A.K., Vidal-Puig, A., and Teleman, A.A. (2015). Regulation of mitochondrial morphology and function by stearoylation of TFR1. Nature *525*, 124-128.
Serhan, C.N., Krishnamoorthy, S., Recchiuti, A., and Chiang, N. (2011). Novel anti-inflammatory--pro-resolving mediators and their receptors. Curr Top Med Chem *11*, 629-647.

Shalova, I.N., Lim, J.Y., Chittezhath, M., Zinkernagel, A.S., Beasley, F., Hernandez-Jimenez, E., Toledano, V., Cubillos-Zapata, C., Rapisarda, A., Chen, J.*, et al.* (2015). Human monocytes undergo functional re-programming during sepsis mediated by hypoxia-inducible factor-1alpha. Immunity *42*, 484-498.

Shaw, E., Farris, M., McNeil, J., and Friedenreich, C. (2016). Obesity and Endometrial Cancer. Recent Results Cancer Res *208*, 107-136.
Shi, H., Kokoeva, M.V., Inouye, K., Tzameli, I., Yin, H., and Flier, J.S. (2006). TLR4 links innate immunity and fatty acid-induced insulin resistance. J Clin Invest *116*, 3015-3025.

Shiau, A.K., Barstad, D., Loria, P.M., Cheng, L., Kushner, P.J., Agard, D.A., and Greene, G.L. (1998). The structural basis of estrogen receptor/coactivator recognition and the antagonism of this interaction by tamoxifen. Cell *95*, 927-937.

Smith, F.O. (2006). Canine pyometra. Theriogenology *66*, 610-612.
Smith, G.P. (2000). The controls of eating: a shift from nutritional homeostasis to behavioral neuroscience. Nutrition *16*, 814-820.

Spady, D.K., Woollett, L.A., and Dietschy, J.M. (1993). Regulation of plasma LDL-cholesterol levels by dietary cholesterol and fatty acids. Annu Rev Nutr *13*, 355-381.

Stanford, K.I., Middelbeek, R.J., and Goodyear, L.J. (2015). Exercise Effects on White Adipose Tissue: Beiging and Metabolic Adaptations. Diabetes *64*, 2361-2368.

Stout, R.D., and Suttles, J. (2004). Functional plasticity of macrophages: reversible adaptation to changing microenvironments. J Leukoc Biol *76*, 509-513.

Stricklett, P.K., Nelson, R.D., and Kohan, D.E. (1999). The Cre/loxP system and gene targeting in the kidney. Am J Physiol *276*, F651-657.
Sun, K., Kusminski, C.M., and Scherer, P.E. (2011). Adipose tissue remodeling and obesity. J Clin Invest *121*, 2094-2101.

Swift, D.L., Johannsen, N.M., Lavie, C.J., Earnest, C.P., and Church, T.S. (2014). The role of exercise and physical activity in weight loss and maintenance. Prog Cardiovasc Dis *56*, 441-447.

Takemura, Y., Ouchi, N., Shibata, R., Aprahamian, T., Kirber, M.T., Summer, R.S., Kihara, S., and Walsh, K. (2007). Adiponectin modulates inflammatory reactions via calreticulin receptor-dependent clearance of early apoptotic bodies. J Clin Invest *117*, 375-386.

Toniolo, A., Fadini, G.P., Tedesco, S., Cappellari, R., Vegeto, E., Maggi, A., Avogaro, A., Bolego, C., and Cignarella, A. (2015). Alternative activation of human macrophages is rescued by estrogen treatment in vitro and impaired by menopausal status. J Clin Endocrinol Metab *100*, E50-58.

Umesono, K., and Evans, R.M. (1989). Determinants of target gene specificity for steroid/thyroid hormone receptors. Cell *57*, 1139-1146.

Urs, S., Harrington, A., Liaw, L., and Small, D. (2006). Selective expression of an aP2/Fatty Acid Binding Protein 4-Cre transgene in non-adipogenic tissues during embryonic development. Transgenic research *15*, 647-653.

van der Klaauw, A.A., and Farooqi, I.S. (2015). The hunger genes: pathways to obesity. Cell *161*, 119-132.

Vogel, D.Y., Glim, J.E., Stavenuiter, A.W., Breur, M., Heijnen, P., Amor, S., Dijkstra, C.D., and Beelen, R.H. (2014). Human macrophage polarization in vitro: maturation and activation methods compared. Immunobiology *219*, 695-703.

Wagner, R.D., and Johnson, S.J. (2012). Probiotic lactobacillus and estrogen effects on vaginal epithelial gene expression responses to Candida albicans. J Biomed Sci *19*, 58.

Wajchenberg, B.L. (2000). Subcutaneous and visceral adipose tissue: their relation to the metabolic syndrome. Endocr Rev *21*, 697-738.

Weisberg, S.P., McCann, D., Desai, M., Rosenbaum, M., Leibel, R.L., and Ferrante, A.W., Jr. (2003). Obesity is associated with macrophage accumulation in adipose tissue. J Clin Invest *112*, 1796-1808.

Weischenfeldt, J., and Porse, B. (2008). Bone Marrow-Derived Macrophages (BMM): Isolation and Applications. CSH Protoc *2008*, pdb prot5080.

Wintermantel, T.M., Campbell, R.E., Porteous, R., Bock, D., Grone, H.J., Todman, M.G., Korach, K.S., Greiner, E., Perez, C.A., Schutz, G.*, et al.* (2006). Definition of estrogen receptor pathway critical for estrogen positive feedback to gonadotropin-releasing hormone neurons and fertility. Neuron *52*, 271-280.

Wira, C.R., Rodriguez-Garcia, M., and Patel, M.V. (2015). The role of sex hormones in immune protection of the female reproductive tract. Nat Rev Immunol *15*, 217-230.

Witko-Sarsat, V., Mocek, J., Bouayad, D., Tamassia, N., Ribeil, J.A., Candalh, C., Davezac, N., Reuter, N., Mouthon, L., Hermine, O.*, et al.* (2010). Proliferating cell nuclear antigen acts as a cytoplasmic platform controlling human neutrophil survival. J Exp Med *207*, 2631-2645.

Wong, C.H., Heit, B., and Kubes, P. (2010). Molecular regulators of leucocyte chemotaxis during inflammation. Cardiovasc Res *86*, 183-191.

Wong, S.W., Kwon, M.J., Choi, A.M., Kim, H.P., Nakahira, K., and Hwang, D.H. (2009). Fatty acids modulate Toll-like receptor 4 activation through regulation of receptor dimerization and recruitment into lipid rafts in a reactive oxygen species-dependent manner. J Biol Chem *284*, 27384-27392.

Wu, D., Molofsky, A.B., Liang, H.E., Ricardo-Gonzalez, R.R., Jouihan, H.A., Bando, J.K., Chawla, A., and Locksley, R.M. (2011). Eosinophils sustain adipose alternatively activated macrophages associated with glucose homeostasis. Science *332*, 243-247.

Xu, Y., Nedungadi, T.P., Zhu, L., Sobhani, N., Irani, B.G., Davis, K.E., Zhang, X., Zou, F., Gent, L.M., Hahner, L.D*., et al.* (2011). Distinct hypothalamic neurons mediate estrogenic effects on energy homeostasis and reproduction. Cell Metab *14*, 453-465.

Yang, Z.H., Inoue, S., Taniguchi, Y., Miyahara, H., Iwasaki, Y., Takeo, J., Sakaue, H., and Nakaya, Y. (2015). Long-term dietary supplementation with saury oil attenuates metabolic abnormalities in mice fed a high-fat diet: combined beneficial effect of omega-3 fatty acids and long-chain monounsaturated fatty acids. Lipids Health Dis *14*, 155.

Yao, Y., Hong, S., Zhou, H., Yuan, T., Zeng, R., and Liao, K. (2009). The differential protein and lipid compositions of noncaveolar lipid microdomains and caveolae. Cell Res *19*, 497-506.

Yore, M.M., Syed, I., Moraes-Vieira, P.M., Zhang, T., Herman, M.A., Homan, E.A., Patel, R.T., Lee, J., Chen, S., Peroni, O.D*., et al.* (2014). Discovery of a class of endogenous mammalian lipids with anti-diabetic and anti-inflammatory effects. Cell *159*, 318-332.

Yoshida, K., Shimizugawa, T., Ono, M., and Furukawa, H. (2002). Angiopoietin-like protein 4 is a potent hyperlipidemia-inducing factor in mice and inhibitor of lipoprotein lipase. J Lipid Res *43*, 1770-1772.

Zhu, L., Zhao, Q., Yang, T., Ding, W., and Zhao, Y. (2015). Cellular metabolism and macrophage functional polarization. Int Rev Immunol *34*, 82-100.

Curriculum vitae

Der Lebenslauf ist in der Online-Version aus Gründen des Datenschutzes nicht enthalten.

Publication list and conferences

Publications:

- Foryst-Ludwig A, Kreissl MC, Benz V, Brix S, Smeir E, Ban Z, Januszewicz E, Salatzki J, Grune J, Schwanstecher AK, Blumrich A, Schirbel A, Klopfleisch R, Rothe M, Blume K, Halle M, Wolfarth B, Kershaw EE, Kintscher U.
  Adipose Tissue Lipolysis Promotes Exercise-induced Cardiac Hypertrophy Involving the Lipokine C16:1n7-Palmitoleate. (J Biol Chem, 2015)

- Ban Z, Maurischat P, Benz V, Brix S, Sonnenburg A, Schuler G, Klopfleisch R, Rothe M, Gustafsson JÅ, Foryst-Ludwig A, Kintscher U.
  High-Fat Diet Induces Unexpected Fatal Uterine Infections in Mice with aP2-Cre-mediated Deletion of Estrogen Receptor Alpha. (Sci Rep, 2017)

- Brix S, Beyhoff N, Blumrich A, Betz I, Grune J, Salatzki J, Ban Z, Ott C, Grune T, Klopfleisch R, Kintscher U, Foryst-Ludwig A.
  Pharmacological Inhibition of HDAC6 Reduces Mal-Adaptive Cardiac Hypertrophy. (in preparation)

- Salatzki J, Foryst-Ludwig A, Bentele K, Blumrich A, Smeir E, Ban Z, Brix S, Grune J, Klopfleisch R, Surma MA, Klose C, Rothe M, Heinzel FR, Krannich A, Kershaw EE, Beule D, Marx N, Kintscher U.
  Adipose Tissue Lipolysis Modifies the Cardiac Lipidome in Pressure-Overload-Induced Left Ventricular Failure. (in preparation)

Scientific conferences with poster presentation:

2014	**DPhG Doktorandentagung 2014**, Wuppertal (Germany)
2014	**EMBO|EMBL Symposium: Translating Diabetes**, Heidelberg (Germany)
2015	**DDG (Deutsche Diabetes Gesellschaft) 2015**, Berlin (Germany)
2016	**Keystone Symposium: Obesity and Adipose Tissue Biology**, Banff (Canada)
2016	**DDG 2016**, Berlin (Germany) *Travel grant award

Danksagung

Die Danksagung ist in der Online-Version aus Gründen des Datenschutzes nicht enthalten.

Die Danksagung ist in der Online-Version aus Gründen des Datenschutzes nicht enthalten.